

Amino acid residues constituting the agonist binding site of the human
P2X3 receptor and subunit stoichiometry of heteromeric P2X2/3 and
P2X2/6 receptors

Dissertation
zur Erlangung des akademischen Grades
Dr. rer. med.

an der Medizinischen Fakultät
der Universität Leipzig

Engereicht von: Prof. Dr. med. Haihong Wang
Geboren am 18.10.1962 in Jiang Su, China

Angefertigt am: Rudolf-Boehm-Institut für Pharmakologie und Toxikologie
der Universität Leipzig

Betreuer: Prof. Dr. med Peter Illes

Beschluss über die Verleihung des Doktorgrades vom: 23.04.2013

Index of contents

Index of contents	I
Introductory remarks	II
„Wissenschaftlicher Anteil des Promovenden an der Publikation“	III
„Bibliographische Beschreibung“	IV
I. Introduction	1
Pain as a sensory quality	1
Neuronal circuitry for pain processing and sensation in the PNS and CNS	2
Transformation of thermal, mechanical and chemical stimuli into electrical activity by nociceptors; nociceptor-targeted therapeutic approaches	4
Release mechanisms for nucleotides and their fate in the extracellular space	6
Nucleotide receptor-types	7
ATP-sensitive P2 receptors and pain-sensation	8
References	11
II. Scientific background and aims of my thesis	16
ATP binding-sites of P2X3 receptors; subunit composition of P2X2/3 and P2X2/6 heteromeric receptors	16
The aims of the present work	17
III. Publications	18
IV. Summary and conclusions	43
Amino acid residues constituting the agonist binding site of the human P2X3 receptor	43
ATP binding site mutagenesis reveals different subunit stoichiometry of functional P2X2/3 and P2X2/6 receptors	45
„Eigenständigkeitserklärung“	48
Curriculum vitae	49
Acknowledgements	51

Introductory remarks

I have chosen for the presentation of my results a cumulative PhD Thesis. Two publications are discussed thereby; in one of them I have a shared co-authorship with Dr. rer. nat. Mandy Bodnar, and in the second one I am the fourth author.

These publications are the following:

Bodnar M*, **Wang H***, Riedel T, Hintze S, Kato E, Fallah G, Gröger-Arndt H, Giniatullin R, Grohmann M, Hausmann R, Schmalzing G, Illes P, Rubini P (2011) Amino acid residues constituting the agonist binding site of the human P2X3 receptor. J Biol Chem 286:2739-2749 (*Both authors contributed equally to this work).

Hausmann R, Bodnar M, Woltersdorf R, **Wang H**, Fuchs M, Messemer N, Qin Y, Gunther J, Riedel T, Grohmann M, Nieber K, Schmalzing G, Rubini P, Illes P (2012) ATP binding site mutagenesis reveals different subunit stoichiometry of functional P2X2/3 and P2X2/6 receptors. J Biol Chem 287:13930-13943.

Erklärung über den wissenschaftlichen Anteil des Promovenden zur Publikation

Die beiden Publikationen, die meiner Doktorarbeit als Grundlage dienen, sind im Zuge meines einjährigen Aufenthaltes am Rudolf-Boehm-Institut für Pharmakologie und Toxikologie der Universität Leipzig entstanden. Beide Arbeiten beschäftigen sich mit dem rekombinanten humanen P2X3-Rezeptor und seinen Bindungsstellen-Mutanten, die zwecks funktioneller Untersuchungen in HEK293-Zellen und Oocyten exprimiert wurden. Es handelt sich um eine Multiautoren-Arbeit, die komplexe methodische Ansätze beinhaltet. Es wurden Patch-Clamp-Ableitungen an HEK293-Zellen mit der Ca^{2+} -Mikrofluorimetrie, dem Zwei-Elektroden-Spannungsklemm-Verfahren (an Oocyten), der Protein-Aufreinigung und Affinitäts-Chromatographie sowie der Homologiemodellierung der Rezeptorstruktur und der kinetischen Modellierung von P2X3-Rezeptorströmen kombiniert. Mein Beitrag beschränkte sich auf die Patch-Clamp-Ableitungen aus den HEK293-Zellen, die allerdings eine zentrale Bedeutung im methodischen Ansatz einnehmen und für die Schlussfolgerungen von besonderer Bedeutung sind. Die Planung der Experimente erfolgte in enger Abstimmung mit meinem Doktorvater; ich führte die Ableitungen eigenständig durch, wertete sie aus und hinterlegte die Dokumentation. Mein Anteil beinhaltete weiterhin beim erstellen der Publikation die methodische Beschreibung der Patch-Clamp-Technik und Unterstützung bei der Diskussion der einschlägigen Versuchsergebnisse.

Der Inhalt dieser Erklärung wurde mir in das Englische übersetzt und ich bestätige deren Richtigkeit.

Shanghai, 15. Juni 2012



Prof. Dr. med. Haihong Wang

Gesehen und Bestätigt durch die Ko-Autoren der Publikationen (E-Mail-Nachweise liegen bei):

Bibliographische Beschreibung

Prof. Dr. med. Haihong Wang

Amino acid residues constituting the agonist binding site of the human P2X3 receptor and subunit stoichiometry of heteromeric P2X2/3 and P2X2/6 receptors

Universität Leipzig, kumulative Dissertation

51 S., 71 Lit., 0 Tab., 2 Abb.

Referat

Homotrimeric P2X3 and heteromeric P2X2/3 receptors are present in sensory ganglia and participate in pain perception. In order to develop pharmacological antagonists for these receptors, it is important to clarify which amino acid (AA) residues constitute the agonist binding pouch as well as to learn the stoichiometry of the receptor subunits forming a heteromeric receptor. We expressed the homomeric human (h)P2X3 receptor or its mutants in HEK293 cells and measured the ATP-induced responses by the whole-cell patch-clamp method. For the binding-site mutants, all conserved and some non-conserved AAs in the four nucleotide binding segments (NBSs) of the P2X3 subunit were sequentially replaced by alanine. Especially the positively charged AAs Lys and Arg appeared to be of critical importance for the agonist effects. We concluded that groups of AAs organized in NBSs rather than individual amino acids appear to be responsible for agonist binding at the P2X3 receptor. These NBSs are located at the interface of the three subunits forming a functional receptor. We were also interested to find out, whether two heteromeric receptors (P2X2/3 and P2X2/6), where P2X2 combines with two different partners, have an obligatory subunit stoichiometry of 1:2 or whether the subunit stoichiometry may be variable. For this purpose we used non-functional P2X2, P2X3 and P2X6 subunit-mutants to investigate the composition of heteromeric P2X2/3 and P2X2/6 receptors. The subunit stoichiometry of P2X2/3 and P2X2/6 was found to be 1:2 and 2:1, respectively. Thus, recognitions sites between P2X2 and its partners rather than random association may govern the subunit compositions of the receptor trimers.

I. Introduction

Pain as a sensory quality

The Taxonomy Committee of the International Association for the Study of Pain (IASP) describes pain as being „An unpleasant sensory and emotional experience associated with actual or potential tissue damage, or described in terms of such damage” (Mac-Farlane et al., 1997). Painful sensations may be classified according to their duration as acute or chronic. Acute pain has an important signalling function in order to avoid tissue damage (e.g. by triggering a spinal reflex to remove a finger from the hot stove plate or by forcing an individual to immobilize his injured extremity). However, chronic pain may become a self-containing illness, inducing unnecessary hardship for a patient (e.g. cancer pain). A second possibility to classify pain is according to its source (superficial or deep). Injury to the skin causes superficial pain, whereas ischemia of the heart or overt distension of hollow visceral organs produces deep pain. A special type of chronic pain, termed neuropathic, will be the primary subject of this Thesis.

Neuropathic pain can be defined as a condition resulting from non-inflammatory dysfunction of the peripheral (PNS) or central nervous system (CNS), without nociceptor stimulation or trauma. The development of chronic pain following peripheral nerve injury has been attributed to the occurrence of three different processes in the spinal cord: increased excitability, decreased inhibition and structural reorganization of the cells (Woolf and Doubell, 1994). The classic symptoms are (1) stimulus-independent pain, (2) hyperalgesia (increased pain response to a suprathreshold noxious stimulus), and (3) allodynia (pain elicited by a normally non-noxious, e.g. tactile stimulus) (Woolf and Mannion, 1999). Neuropathic pain can result from peripheral nerve trauma (deafferentation, amputation), infection (post-herpetic neuralgia), human immunodeficiency syndrome-associated neuralgia, or metabolic disturbance (diabetic pain). An excruciating, usually unilateral type of neuropathic pain occurs in the distribution of the trigeminal nerves (trigeminal neuralgia); it is triggered by e.g. a light touch at the cheek. A common characteristic of neuropathic pain states is their relative insensitivity to treatment by opioids. In general, neuropathic pain is rather resistant to pharmacological therapy with the exception of trigeminal neuralgia which is treated by anticonvulsants (carbamazepine, sodium valproate, phenytoin) blocking voltage-sensitive sodium

channels. In conclusion, there is a great need for drugs to treat neuropathic pain efficiently and without tolerable side-effects.

Neuronal circuitry for pain processing and sensation in the PNS and CNS

The cell bodies of primary sensory neurons are located in the trigeminal ganglia (TG) as well as dorsal root ganglia (DRG), and innervate the head and the body, respectively (Hunt and Mantyh, 2001; Mantyh et al., 2002; Todd, 2010).

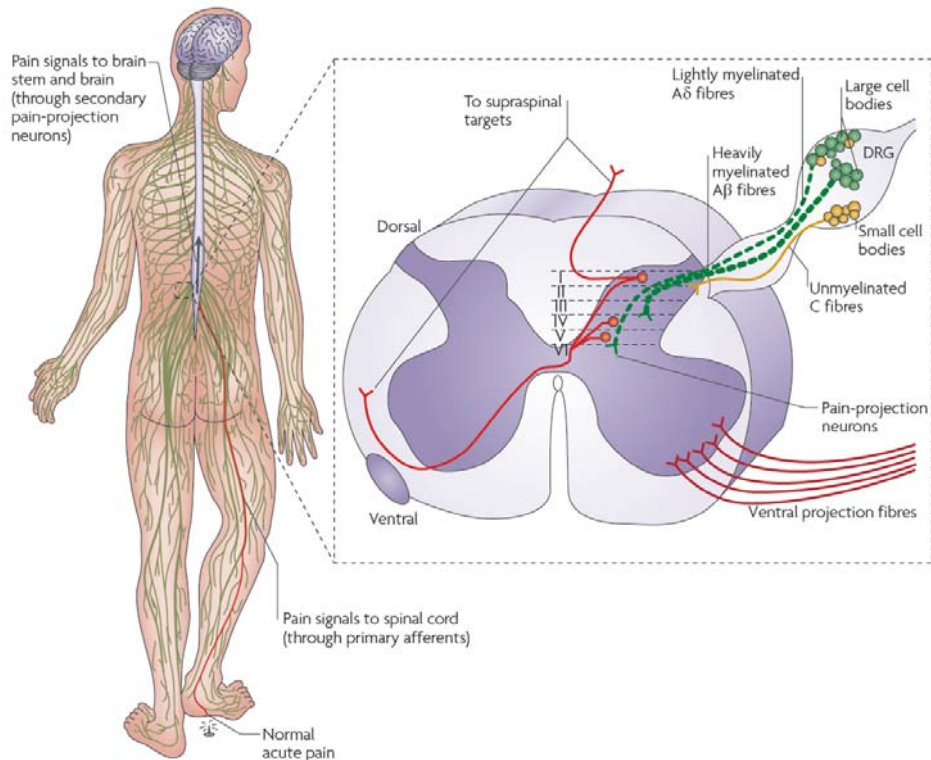


Abb. 1. **Nociception.** Normal pain signalling in the body is transmitted to the spinal cord dorsal horn through nociceptors. Primary afferent terminals project onto pain projection neurons in laminae I, IV and V in the spinal cord dorsal horn. The cell bodies of primary afferent neurons are situated in the dorsal root ganglia (DRG) and are classified into large and small types. C and A δ fibres have small cell bodies, whereas faster-conducting A β fibres have larger cell bodies. Pain signalling to supraspinal targets is *via* ipsilateral or contralateral ascending fibre bundles, the latter ones forming e.g. the spinothalamic tract (Milligan and Watkins, 2009; for more detailed explanation see text).

Nociceptive small-sized TG and DRG neurons are the origin of thin, unmyelinated C fibres, whereas medium-sized sensory neurons with a similar pain-sensing function send myelinated A δ fibres to the periphery. Of the whole spectrum of primary afferent nerves, larger-diameter, myelinated fibre-types known as A β fibres are low threshold mechanoreceptors, and a group of C- and A δ -fibres are thermoreceptive. Nociceptors

have the main function to detect and convert environmental stimuli that are perceived as harmful into electrochemical signals transmitted to the CNS (Mantyh et al., 2002).

Thus, TG and DRG neurons are pseudounipolar, by innervating with their longer peripheral processes the skin and visceral organs, while their central, shorter processes project to the dorsal horn of the spinal cord. In general, myelinated low-threshold mechanoreceptive afferents arborize in an area extending from lamina II to V); nociceptive and thermoreceptive A δ and C afferents innervate lamina I and most of lamina II (Todd, 2010). Lamina II consists almost exclusively of interneurons, which establish contact with the lamina I output neurons whose projections ascend at the contralateral side of the spinal cord to higher areas of the brain. Main supraspinal targets for lamina I projection neurons include the caudal ventrolateral medulla, the nucleus of the solitary tract, the periaqueductal grey matter and certain nuclei of the thalamus (Gauriau and Bernard, 2004). The nucleus ventralis posterior thalami sends further fibre tracts to the parietal and frontal lobes of the cerebral cortex, where the localization of painful stimuli within the organism takes place and these stimuli become associated with the subjective attribute of 'unpleasant' sensory information. Eventually, serotonergic and noradrenergic axons descend from the raphe nuclei and nucleus locus coeruleus, respectively, to the spinal cord and terminate diffusely throughout the dorsal horn (Zoli et al., 1999). Another descending pathway consists of GABAergic axons from the rostral ventromedial medulla that synapse with lamina II interneurons (Kato et al., 2006). Thus, these interneurons synapse with pain-sensing sensory neurons from the periphery, pain-modulating pathways from higher brain areas, and with neighbouring interneurons, thereby integrating multiple information before transmitting it to the lamina I output neurons.

It has been already mentioned that chronic pain is a deleterious condition causing unnecessary suffering to the individual. Hyperalgesia/allodynia as symptoms of chronic pain stages can result from a number of different modifications leading to an increased responsiveness and stronger output from lamina I nociceptive projection neurons (Larsson and Broman, 2011). A well-established mechanism of central sensitization is modification of synaptic strength in the superficial dorsal horn. Intense electrical or natural noxious stimulation induce potentiation of C-fibre synapses in the dorsal horn (Drdla and Sandkühler, 2008), similar to the NMDA receptor-dependent long-term potentiation (LTP) evident in glutamatergic synapses also in other parts of the CNS (Kessel and Malinow, 2009).

Transformation of thermal, mechanical and chemical stimuli into electrical activity by nociceptors; nociceptor-targeted therapeutic approaches

Most C fibre terminals are polymodal nociceptors and respond to all forms of noxious stimulation (thermal, mechanical and chemical), albeit with various degrees of sensitivity. They are endowed with a whole range of receptors, of which transient receptor potential channels (TRPs) and acid-sensing ion channels (ASICs) have an eminent significance.

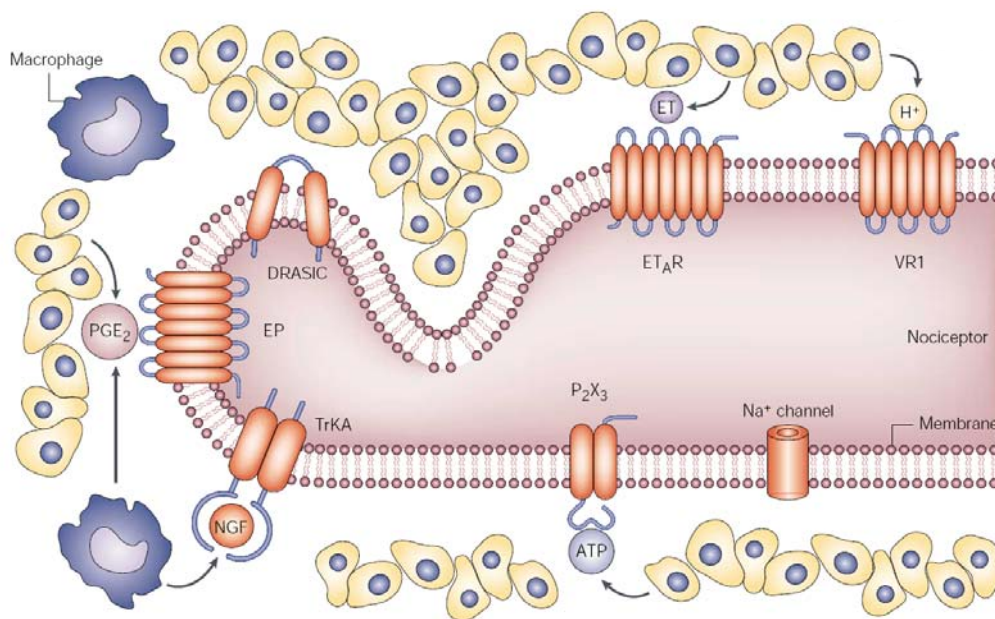


Abb. 2. **Detection by sensory neurons of noxious stimuli produced by damaged or inflamed cells.** Nociceptors use several types of receptors to detect and transmit signals about noxious stimuli that are produced after acute or chronic cell injury. VR1, TRPV1 receptor; ET, endothelin; ET_AR, endothelin-A receptor; DRASIC, dorsal root acid sensing ion channel, EP, prostaglandin receptor; NGF, nerve growth factor; TrkA, tyrosine kinase receptor. (Mantyh et al., 2002; for further details see text).

TRP ion channels are important for vision, olfaction, taste, mechanosensation, osmoregulation and thermosensation (Clapham, 2003; Patapoutian et al., 2009). The role of TRP channels in pain and thermosensation was first suggested by the finding that mammalian transient receptor potential vanilloid 1 (TRPV1) is activated by noxious heat, extracellular protons, and capsaicin the irritating ingredient of chilli peppers (Caterina et al., 1997). Six of the 28 TRP channels from the three distinct subclasses are activated by temperature (TRPV1-4, TRPM8, TRPA1) and are expressed in sensory neurons or in skin keratinocyte cells, which are peripheral targets of these nerves (Dhaka et al., 2006). The heat-sensitive TRPV1 and TRPA1

are co-localized in a subgroup of DRG and TG neurons; TRPM8 is expressed in another subgroup of sensory neurons that respond to innocuous cold temperatures (Papatopoutian et al., 2009). The protein sequences of the TRPs contain six putative transmembrane helices S1-S6 and a putative pore region between S5 and S6; they represent subunits of a tetrameric channel. The opening of TRPs allows the non-selective passage of cations and thereby causes depolarization and the generation of conducted action potentials in C fibres.

ASICs are cationic channels that are directly gated by extracellular protons. They belong to the epithelial sodium channel superfamily (Deval et al., 2010). Each ASIC subunit (ASIC1-4) has two hydrophobic transmembrane domains, flanking a large extracellular loop. Resolution of the crystal structure of the chicken ASIC1 channel has shown that three subunits are necessary to form a functional channel (Jasti et al., 2007). ASIC currents activate transiently upon extracellular acidification, the activation threshold, pH sensitivity and current kinetics depending on the subunit composition of the channel. Among ASICs, ASIC1 and ASIC3 are the most sensitive to protons, being activated by very small acidification. Conversely, ASIC2 currents are activated by more pronounced acidification (Deval et al., 2010).

Experimental evidence for the existence of acid-activated ion channels on sensory neurons isolated from DRG and TG has been provided as early as 1980 (Krishtal and Pidoplichko, 1980). In the meantime it has been documented that ASICs are involved in cutaneous and deep somatic pain, visceral pain, and heart and lung nociception (Wemmie et al., 2006). In addition the distribution of ASICs and TRPV1 appeared to exhibit very little overlap in rat DRG, indicating complementary distribution and function (Molliver et al., 2005).

In addition to these two groups of important pain-sensing receptors, autacoids such as prostaglandins (Sawynok, 2003), and opioids (Fields, 2004; Cahill et al., 2006) as well as non-opioid peptides (e.g. bradykinin; Campos et al., 2006) may also modulate nociceptor function at the C-fibre terminals themselves. Receptors for these compounds are supposed to be associated with chronic pain states, and become up-regulated during inflammation. It is quite clear, however, that the primary site of action of opioids is in the CNS and that of prostaglandins in the periphery. Nevertheless, opioid effects in the periphery and prostaglandin effects at spinal sites have also been documented (Zhang et al., 2004; Zeilhofer and Brune, 2006).

All these channels and receptors are possible targets of pain therapy, although opioids and non-steroidal inflammatory drugs (NSAIDs) still remain the prototypic analgesics. NSAIDs are classic blockers of prostaglandin synthesis, with no selectivity for any of the cyclooxygenase subtypes (COX-1 or COX-2). In contrast, specific COX-2 inhibitors were originally supposed to be devoid of the side effects of NSAIDs exhibiting inherent gastrointestinal and renal toxicity. However, later it was observed that COX-2 inhibitors are cardiovascular risk factors, a finding which seriously limited their therapeutic applicability. More recently, new analgesic targets are emerging such as various types of voltage-sensitive sodium channels (Dib-Hajj et al., 2007; Liu and Wood, 2011). Individual isoforms of voltage-gated sodium channels have been linked to particular types of pain. Nav1.7 is a useful target for ameliorating acute mechanical pain and inflammatory pain. Strong evidence suggests that selective blockers for Nav1.9 could be used to treat inflammatory pain and blockers for Nav1.8 could have clinical benefit for visceral pain.

Release mechanisms for nucleotides and their fate in the extracellular space

It has been suggested in the early seventies of the last century that the purine nucleotide ATP is a transmitter of the enteric nervous system (Burnstock et al., 1970). Later on, excitatory junction potentials in the vas deferens were found to be due to ATP released as a co-transmitter together with noradrenaline (Burnstock and Verkhatsky, 2010). According to the present stage of our knowledge extracellular ATP is an almost general signalling molecule in the CNS and PNS involved in neuronal degeneration, central control of autonomic functions, neural-glial interactions, control of vessel tone, sensory transduction and the physiology of special senses (Burnstock, 2006).

In addition to the exocytotic secretion of ATP from nerve terminals and probably also astrocytes (Hamilton and Attwell, 2010), stimulation of astrocytes by pharmacological means as well as by mechanical or osmotic stimulation may release ATP by four alternative mechanisms (Illes and Alexandre, 2004). Firstly, by ATP-binding cassette (ABC) proteins, such as the multidrug resistance-associated protein (Ballerini et al., 2002); secondly by connexin hemichannels providing the substrate for gap junction formation (Cotrina et al., 2000); and thirdly, by osmolytic transporters linked to cation channels (Darby et al., 2003). Eventually, ATP and more generally

speaking nucleotides may leave injured cells by passing their cell membranes towards the extracellular space.

ATP and other nucleotides act after their release at membrane localized receptors (see below). Their effect is terminated by rapid enzymatic degradation by ecto-nucleotidases, which are important, because ATP metabolites (ADP, adenosine) act as physiological ligands for various purinergic receptors. Thus, the ecto-nucleotidases not only control the life-time of nucleotides but by degrading or interconverting the originally released ligands, they also produce agonists for additional P2 and P1 receptors (Zimmermann and Braun, 1999). The ecto-nucleotidase families consist of nucleoside triphosphate diphosphohydrolase (NTPDase), nucleotide pyrophosphatase (NPP), alkaline phosphatase, and 5'-nucleotidase (Abbracchio et al., 2009).

Nucleotide receptor-types

Burnstock suggested, based on purely pharmacological conclusions (rank order of agonist potencies and preferential antagonists), that P2 receptors may be classified into the P1 (sensitive to adenosine) and P2 (sensitive to ATP) types. Later he came up with the proposal that the P2 receptors belong to two major classes: a P2X family of ligand-gated ion channels and a P2Y family of G protein-coupled receptors (Abbracchio and Burnstock, 1994). This original suggestion became widely accepted after the cloning of all known P2 receptor types (North, 2002; Khakh et al., 2001; Abbracchio et al., 2006).

P2X receptor-channels form a family of seven subunits, referred to as P2X1 through P2X7 (Khakh and North, 2006). The subunits consist of two transmembrane domains, a large extracellular loop containing the ATP binding site, as well as intracellular N- and C-terminal tails. Biochemical evidence indicates that both homomeric and heteromeric receptors occur as stable trimers (Nicke et al., 1998). In fact, heteromultimeric assemblies of two subunits of the composition P2X1/2, P2X1/4, P2X1/5, P2X2/3, P2X2/6 and P2X4/6 were also described (Coddou et al., 2011). These receptors combined the biophysical and pharmacological properties of the original subunits. Co-immunoprecipitation experiments with epitope-tagged subunits demonstrated that only P2X6 was unable to form homooligomers and P2X7 was the only exception of constituting heterooligomeric complexes (Torres et al., 1999).

Neuronal P2X receptors in the CNS appear to belong mostly to the P2X2, P2X4 or P2X4/6 types (Illes and Alexandre, 2004). The neuronal localization of P2X7 receptor-channels is still a matter of debate, although it is quite clear that they are situated at astrocytes, oligodendrocytes and microglial cells in great abundance (Sperlagh et al., 2006; Illes et al., 2012). These receptors change their ion selectivity during longer-lasting exposure to ATP. Recently neuronal P2X2, P2X2/3 and P2X4 receptor-channels were also found to progressively dilate during prolonged or repetitive ATP applications (Khakh et al., 1999). It was reported that in addition to larger cations also bulky fluorescent dyes (e.g. Yo-Pro-1) may enter the cell interior (Pelegri and Surprenant, 2006). However, the suggestion that not the dilation of the receptor-channel itself but rather the coupling of P2X7 receptors to pannexin-1 channels accounts for the cellular uptake of these molecules, has recently been questioned.

P2Y receptor proteins show the typical features of G protein-coupled receptors (GPCRs) (Abbracchio et al., 2006; Köles et al., 2009). They have an extracellular N terminus containing several potential glycosylation sites, seven transmembrane (TM) domains and an intracellular C terminus that contains several consensus binding/phosphorylation sites for protein kinases. Some positively charged residues in TM domains 3, 6 and 7 seem to be crucial for receptors activation by agonists.

So far the P2Y family comprises of eight cloned and functionally defined mammalian subtypes (P2Y_{1,2,4,6,11,12,13,14}); their pharmacological profiles and preferences for coupling to heterotrimeric G protein-subtypes are different. The original idea was that a GPCR is a monomeric transmembrane protein, which upon ligand binding interacts with a heterotrimeric G protein and, in consequence, initiates events characteristic for receptor activation (Köles et al., 2008). However, this view was revised, as a growing body of evidence indicated that GPCRs exist as oligomeric complexes. Combinations of A₁ adenosine receptors with P2Y₁ or P2Y₂ nucleotide receptors were described, and similarly P2Y₁/P2Y₁₁ and P2Y₄/P2Y₆ receptors were also shown to exist in close physical association.

ATP-sensitive P2 receptors and pain sensation

In sensory ganglia, all seven cloned mammalian P2X receptors are present (Chizh and Illes, 2000; Wirkner et al., 2007). Six of them (P2X1-6) were detected with distinct distribution patterns in primary afferent neurons of the rat by means of

immunohistochemistry and in situ hybridization. In DRG neurons, P2X2 and P2X3 receptor mRNA and protein were expressed at comparably high magnitude, while the other subtypes were expressed at much lower quantities.

Nociceptive C-fibre neurons are comprised of both peptidergic (endowed with receptor tyrosine kinase [TrkA] for nerve growth factor [NGF]) and non-peptidergic neurons (lacking TrkA). A subpopulation of non-peptidergic C-fibre neurons express the receptor complex for glial cell-derived neurotrophic factor (GDNF) also labelled by isolectin B4 from *Griffonia simplicifolia* (Molliver et al., 1997). The majority of P2X3-positive neurons belongs to the GDNF-sensitive population and expresses TRPV1 receptor-channels (Wirkner et al., 2007).

ATP and most of its structural agonists evoke rapidly desensitizing inward currents in acutely dissociated rat DRG neurons possessing homomeric P2X3 receptors (Chen et al., 1995). α,β -methylene ATP (α,β -meATP) activates these receptors with a considerable selectivity over all other P2X-types except P2X1 and the heteromeric P2X2/3. Indeed, in rat nodose neurons, P2X2/3 receptors predominate, where α,β -meATP causes slowly desensitizing currents (Lewis et al., 1995). It is assumed that both receptor types are situated at the peripheral terminals of sensory neurons and respond to ATP released by chronic noxious tissue damage. In fact, exogenously applied ATP induces acute pain in humans and animals, which is inhibited by P2 receptor antagonists, but endogenous ATP does not appear to be involved in acute thermal and mechanical pain, as these responses were unchanged in P2X3-knockout mice (Cockayne et al., 2000; Kennedy, 2005). More recent studies are, however, consistent with a role of P2X3 receptors in the pain associated with chronic inflammation and neuronal injury (Donnelly-Roberts et al., 2008). Gene knockout methods, antisense oligonucleotides and small interfering RNA (siRNA) technologies, as well as a selective P2X3 antagonist uniformly support this assumption. Thus, in contrast to acute pain, ATP-gated cationic channels of the P2X3- and P2X2/3-types may contribute to pain sensation in inflammatory/neuropathic pain as well as migraine, and visceral/cancer pain (Wirkner et al., 2007).

In addition to the peripheral terminals and cell bodies of sensory neurons, P2X3 receptors are also situated at their central terminals in the spinal cord dorsal horn. ATP was found to increase the electrophysiologically measured release of glutamate from DRG nerve terminals in lamina II of the spinal cord (Nakatsuka et al., 2003). The increase was transient and inhibited by P2 receptor antagonists indicating the

involvement of P2X3 receptors. In partial agreement with these results, in the projection field of A δ fibres in lamina V, ATP and α,β -meATP caused long-lasting increase in glutamate release, probably mediated by other subtypes of P2X receptors (Nakatsuka and Gu, 2001).

Whereas P2X3 receptors are mostly expressed at small DRG neurons, P2Y receptors appear to be equally expressed in small, large and medium-sized sensory neurons (Gerevich and Illes, 2004). When the receptor protein was identified with immunohistochemistry, P2Y₁ receptors were identified on TRPV1- and P2X3-bearing small diameter neurons of the rat DRG (Gerevich et al., 2004). The activation of P2Y₁ receptors by ADP or its structural analogue ADP- β -S inhibited N-type Ca²⁺ channels, with no effect on any other type of Ca²⁺ channel. The effects of ADP- β -S were abolished by P2Y₁-selective antagonists. Finally, intrathecally applied ADP- β -S prolonged the nociceptive threshold in the tail-flick test, indicating spinally induced analgesia. It was suggested that while spinal P2X3 receptors increase the release of glutamate onto lamina II neurons, P2Y₁ receptors have an opposite effect and are thereby analgesic.

We began to understand the role of ATP in neuropathic pain, when it was discovered that P2X4 receptors are intimately involved in tactile allodynia and hyperalgesia accompanying this pain state (Burnstock et al., 2011). P2X4 receptors facilitate the release of brain-derived neurotrophic factor (BDNF) from microglia in the spinal cord and cause a depolarizing shift in the anion reversal potential of spinal lamina I neurons that invert the polarity of current activated by the previously inhibitory transmitter GABA (Coull et al., 2005). Thus, the activity of the lamina I output neurons critically involved in the transmission of painful information to higher brain centres is facilitated. P2X7 receptors utilize another transduction pathway to cause pain (Burnstock et al., 2011). They increase the release of proinflammatory interleukin-1 β and PGE₂ from macrophages and microglia, sensitizing nociceptors in peripheral tissues or pain-transmitting neurons in the CNS (Clark et al., 2010). Astrocytes are also key players in chronic pain mechanisms secreting the classic immune signals: cytokines and chemokines (Milligan and Watkins, 2009).

References

- Abbracchio MP, Burnstock G (1994) Purinoceptors: are there families of P2X and P2Y purinoceptors? *Pharmacol Ther* 64:445-475.
- Abbracchio MP, Burnstock G, Boeynaems JM, Barnard EA, Boyer JL, Kennedy C, Knight GE, Fumagalli M, Gachet C, Jacobson KA, Weisman GA (2006) International Union of Pharmacology LVIII: update on the P2Y G protein-coupled nucleotide receptors: from molecular mechanisms and pathophysiology to therapy. *Pharmacol Rev* 58:281-341.
- Abbracchio MP, Burnstock G, Verkhratsky A, Zimmermann H (2009) Purinergic signalling in the nervous system: an overview. *Trends Neurosci* 32:19-29.
- Ballerini P, Di IP, Ciccarelli R, Nargi E, D'Alimonte I, Traversa U, Rathbone MP, Caciagli F (2002) Glial cells express multiple ATP binding cassette proteins which are involved in ATP release. *Neuroreport* 13:1789-1792.
- Burnstock G, Campbell G, Satchell D, Smythe A (1970) Evidence that adenosine triphosphate or a related nucleotide is the transmitter substance released by non-adrenergic inhibitory nerves in the gut. *Br J Pharmacol* 40:668-688.
- Burnstock G (2006) Historical review: ATP as a neurotransmitter. *Trends Pharmacol Sci* 27:166-176.
- Burnstock G, Verkhratsky A (2010) Vas deferens--a model used to establish sympathetic cotransmission. *Trends Pharmacol Sci* 31:131-139.
- Burnstock G, Krugel U, Abbracchio MP, Illes P (2011) Purinergic signalling: from normal behaviour to pathological brain function. *Prog Neurobiol* 95:229-274.
- Cahill CM, Holdridge SV, Morinville A (2007) Trafficking of delta-opioid receptors and other G-protein-coupled receptors: implications for pain and analgesia. *Trends Pharmacol Sci* 28:23-31.
- Campos MM, Leal PC, Yunes RA, Calixto JB (2006) Non-peptide antagonists for kinin B1 receptors: new insights into their therapeutic potential for the management of inflammation and pain. *Trends Pharmacol Sci* 27:646-651.
- Caterina MJ, Schumacher MA, Tominaga M, Rosen TA, Levine JD, Julius D (1997) The capsaicin receptor: a heat-activated ion channel in the pain pathway. *Nature* 389:816-824.
- Chen CC, Akopian AN, Sivilotti L, Colquhoun D, Burnstock G, Wood JN (1995) A P2X purinoceptor expressed by a subset of sensory neurons. *Nature* 377:428-431.

- Chizh BA, Illes P (2001) P2X receptors and nociception. *Pharmacol Rev* 53:553-568.
- Clapham DE (2003) TRP channels as cellular sensors. *Nature* 426:517-524.
- Clark AK, Staniland AA, Marchand F, Kaan TK, McMahon SB, Malcangio M (2010) P2X7-dependent release of interleukin-1beta and nociception in the spinal cord following lipopolysaccharide. *J Neurosci* 30:573-582.
- Cockayne DA, Hamilton SG, Zhu QM, Dunn PM, Zhong Y, Novakovic S, Malmberg AB, Cain G, Berson A, Kassotakis L, Hedley L, Lachnit WG, Burnstock G, McMahon SB, Ford AP (2000) Urinary bladder hyporeflexia and reduced pain-related behaviour in P2X3-deficient mice. *Nature* 407:1011-1015.
- Coddou C, Yan Z, Obsil T, Huidobro-Toro JP, Stojilkovic SS (2011) Activation and regulation of purinergic P2X receptor channels. *Pharmacol Rev* 63:641-683.
- Cotrina ML, Lin JH, Lopez-Garcia JC, Naus CC, Nedergaard M (2000) ATP-mediated glia signaling. *J Neurosci* 20:2835-2844.
- Coull JA, Beggs S, Boudreau D, Boivin D, Tsuda M, Inoue K, Gravel C, Salter MW, De KY (2005) BDNF from microglia causes the shift in neuronal anion gradient underlying neuropathic pain. *Nature* 438:1017-1021.
- Darby M, Kuzmiski JB, Panenka W, Feighan D, MacVicar BA (2003) ATP released from astrocytes during swelling activates chloride channels. *J Neurophysiol* 89:1870-1877.
- Deval E, Gasull X, Noel J, Salinas M, Baron A, Diochot S, Lingueglia E (2010) Acid-sensing ion channels (ASICs): pharmacology and implication in pain. *Pharmacol Ther* 128:549-558.
- Dhaka A, Viswanath V, Patapoutian A (2006) TRP ion channels and temperature sensation. *Annu Rev Neurosci* 29:135-161.
- Dib-Hajj SD, Cummins TR, Black JA, Waxman SG (2007) From genes to pain: Na v 1.7 and human pain disorders. *Trends Neurosci* 30:555-563.
- Donnelly-Roberts D, McGaraughty S, Shieh CC, Honore P, Jarvis MF (2008) Painful purinergic receptors. *J Pharmacol Exp Ther* 324:409-415.
- Drdla R, Sandkuhler J (2008) Long-term potentiation at C-fibre synapses by low-level presynaptic activity in vivo. *Mol Pain* 4:18.
- Fields H (2004) State-dependent opioid control of pain. *Nat Rev Neurosci* 5:565-575.
- Gauriau C, Bernard JF (2004) A comparative reappraisal of projections from the superficial laminae of the dorsal horn in the rat: the forebrain. *J Comp Neurol* 468:24-56.

- Gerevich Z, Illes P (2004) P2Y receptors and pain transmission. *Purinergic Signal* 1:3-10.
- Gerevich Z, Borvendeg SJ, Schroder W, Franke H, Wirkner K, Norenberg W, Furst S, Gillen C, Illes P (2004) Inhibition of N-type voltage-activated calcium channels in rat dorsal root ganglion neurons by P2Y receptors is a possible mechanism of ADP-induced analgesia. *J Neurosci* 24:797-807.
- Hamilton NB, Attwell D (2010) Do astrocytes really exocytose neurotransmitters? *Nat Rev Neurosci* 11:227-238.
- Hunt SP, Mantyh PW (2001) The molecular dynamics of pain control. *Nat Rev Neurosci* 2:83-91.
- Illes P, Alexandre RJ (2004) Molecular physiology of P2 receptors in the central nervous system. *Eur J Pharmacol* 483:5-17.
- Illes P, Verkhatsky A, Burnstock G, Franke H (2011) P2X Receptors and Their Roles in Astroglia in the Central and Peripheral Nervous System. *Neuroscientist*.
- Jasti J, Furukawa H, Gonzales EB, Gouaux E (2007) Structure of acid-sensing ion channel 1 at 1.9 Å resolution and low pH. *Nature* 449:316-323.
- Kato G, Yasaka T, Katafuchi T, Furue H, Mizuno M, Iwamoto Y, Yoshimura M (2006) Direct GABAergic and glycinergic inhibition of the substantia gelatinosa from the rostral ventromedial medulla revealed by in vivo patch-clamp analysis in rats. *J Neurosci* 26:1787-1794.
- Kennedy C (2005) P2X receptors: targets for novel analgesics? *Neuroscientist* 11:345-356.
- Kessels HW, Malinow R (2009) Synaptic AMPA receptor plasticity and behavior. *Neuron* 61:340-350.
- Khakh BS, Bao XR, Labarca C, Lester HA (1999) Neuronal P2X transmitter-gated cation channels change their ion selectivity in seconds. *Nat Neurosci* 2:322-330.
- Khakh BS, Burnstock G, Kennedy C, King BF, North RA, Seguela P, Voigt M, Humphrey PP (2001) International Union of Pharmacology. XXIV. Current status of the nomenclature and properties of P2X receptors and their subunits. *Pharmacol Rev* 53:107-118.
- Khakh BS, North RA (2006) P2X receptors as cell-surface ATP sensors in health and disease. *Nature* 442:527-532.

- Koles L, Gerevich Z, Oliveira JF, Zadori ZS, Wirkner K, Illes P (2008) Interaction of P2 purinergic receptors with cellular macromolecules. *Naunyn Schmiedebergs Arch Pharmacol* 377:1-33.
- Krishtal OA, Pidoplichko VI (1980) A receptor for protons in the nerve cell membrane. *Neuroscience* 5:2325-2327.
- Larsson M, Broman J (2011) Synaptic plasticity and pain: role of ionotropic glutamate receptors. *Neuroscientist* 17:256-273.
- Lewis C, Neidhart S, Holy C, North RA, Buell G, Surprenant A (1995) Coexpression of P2X2 and P2X3 receptor subunits can account for ATP-gated currents in sensory neurons. *Nature* 377:432-435.
- Liu M, Wood JN (2011) The roles of sodium channels in nociception: implications for mechanisms of neuropathic pain. *Pain Med* 12 Suppl 3:S93-S99.
- MacFarlane BV, Wright A, O'Callaghan J, Benson HA (1997) Chronic neuropathic pain and its control by drugs. *Pharmacol Ther* 75:1-19.
- Mantyh PW, Clohisy DR, Koltzenburg M, Hunt SP (2002) Molecular mechanisms of cancer pain. *Nat Rev Cancer* 2:201-209.
- Milligan ED, Watkins LR (2009) Pathological and protective roles of glia in chronic pain. *Nat Rev Neurosci* 10:23-36.
- Molliver DC, Wright DE, Leitner ML, Parsadanian AS, Doster K, Wen D, Yan Q, Snider WD (1997) IB4-binding DRG neurons switch from NGF to GDNF dependence in early postnatal life. *Neuron* 19:849-861.
- Molliver DC, Immke DC, Fierro L, Pare M, Rice FL, McCleskey EW (2005) ASIC3, an acid-sensing ion channel, is expressed in metaboreceptive sensory neurons. *Mol Pain* 1:35.
- Nakatsuka T, Gu JG (2001) ATP P2X receptor-mediated enhancement of glutamate release and evoked EPSCs in dorsal horn neurons of the rat spinal cord. *J Neurosci* 21:6522-6531.
- Nakatsuka T, Tsuzuki K, Ling JX, Sonobe H, Gu JG (2003) Distinct roles of P2X receptors in modulating glutamate release at different primary sensory synapses in rat spinal cord. *J Neurophysiol* 89:3243-3252.
- Nicke A, Baumert HG, Rettinger J, Eichele A, Lambrecht G, Mutschler E, Schmalzing G (1998) P2X1 and P2X3 receptors form stable trimers: a novel structural motif of ligand-gated ion channels. *EMBO J* 17:3016-3028.
- North RA (2002) Molecular physiology of P2X receptors. *Physiol Rev* 82:1013-1067.

- Patapoutian A, Tate S, Woolf CJ (2009) Transient receptor potential channels: targeting pain at the source. *Nat Rev Drug Discov* 8:55-68.
- Pelegrin P, Surprenant A (2006) Pannexin-1 mediates large pore formation and interleukin-1 β release by the ATP-gated P2X7 receptor. *EMBO J* 25:5071-5082.
- Sawynok J (2003) Topical and peripherally acting analgesics. *Pharmacol Rev* 55:1-20.
- Sperlagh B, Vizi ES, Wirkner K, Illes P (2006) P2X7 receptors in the nervous system. *Prog Neurobiol* 78:327-346.
- Todd AJ (2010) Neuronal circuitry for pain processing in the dorsal horn. *Nat Rev Neurosci* 11:823-836.
- Torres GE, Egan TM, Voigt MM (1999) Hetero-oligomeric assembly of P2X receptor subunits. Specificities exist with regard to possible partners. *J Biol Chem* 274:6653-6659.
- Wemmie JA, Price MP, Welsh MJ (2006) Acid-sensing ion channels: advances, questions and therapeutic opportunities. *Trends Neurosci* 29:578-586.
- Wirkner K, Sperlagh B, Illes P (2007) P2X3 receptor involvement in pain states. *Mol Neurobiol* 36:165-183.
- Woolf CJ, Doubell TP (1994) The pathophysiology of chronic pain--increased sensitivity to low threshold A β -fibre inputs. *Curr Opin Neurobiol* 4:525-534.
- Woolf CJ, Mannion RJ (1999) Neuropathic pain: aetiology, symptoms, mechanisms, and management. *Lancet* 353:1959-1964.
- Yagi J, Wenk HN, Naves LA, McCleskey EW (2006) Sustained currents through ASIC3 ion channels at the modest pH changes that occur during myocardial ischemia. *Circ Res* 99:501-509.
- Zeilhofer HU, Brune K (2006) Analgesic strategies beyond the inhibition of cyclooxygenases. *Trends Pharmacol Sci* 27:467-474.
- Zhang N, Rogers TJ, Caterina M, Oppenheim JJ (2004) Proinflammatory chemokines, such as C-C chemokine ligand 3, desensitize mu-opioid receptors on dorsal root ganglia neurons. *J Immunol* 173:594-599.
- Zimmermann H (1996) Biochemistry, localization and functional roles of ectonucleotidases in the nervous system. *Prog Neurobiol* 49:589-618.
- Zimmermann H, Braun N, Kegel B, Heine P (1998) New insights into molecular structure and function of ectonucleotidases in the nervous system. *Neurochem Int* 32:421-425.

Zimmermann H, Braun N (1999) Ecto-nucleotidases--molecular structures, catalytic properties, and functional roles in the nervous system. *Prog Brain Res* 120:371-385.

Zoli M, Jansson A, Sykova E, Agnati LF, Fuxe K (1999) Volume transmission in the CNS and its relevance for neuropsychopharmacology. *Trends Pharmacol Sci* 20:142-150.

II. Scientific background and aims of my thesis

ATP binding-sites of P2X3 receptors; subunit composition of P2X2/3 and P2X2/6 heteromeric receptors

My thesis is based on two publications which I authored and co-authored, respectively during a one year stay in Leipzig. Because the specific questions investigated in them have been described in a detailed manner, and will be presented in the enclosed publications, I will give only an overall summary both of the scientific background and the discussion of the data obtained. All references to the relevant literature can be found in these publications.

Our first paper deals with the ATP binding site of homomeric P2X3 receptors. The following evidence from the scientific literature supplied convincing evidence for the three subunit composition of all P2X receptors: (1) Single channel analysis of P2X receptor currents indicated 2-3 sequential binding steps; (2) The kinetic behaviour of P2X receptor currents was simulated with an allosteric model describing channel opening in the di- or tri-liganded state; (3) Atomic force microscopy provided evidence for three receptor subunits; (4) Fluorescence energy transfer and electron microscopy supplied a rough structure of three interacting subunits; (5) The crystal structure of a zebrafish P2X4 receptor mutant confirmed the existence of a trimeric subunit composition.

For many years, knowledge on the amino acid (AA) residues possibly involved in agonist and antagonist binding, allosteric modulation, desensitization and channel-gating of P2X receptors was derived from mutagenesis studies (replacement of the potentially relevant amino acids [AAs] usually by Ala or Cys). These studies uniformly suggested that at the agonist-binding site negatively charged phosphate groups of ATP occupy some positively charged AAs, specifically Lys or Arg in the extracellular loop of the receptor. Whereas originally it was assumed that each P2X subunit contains one individual binding site for ATP, it became soon clear that binding

probably occurs at the interface between two neighbouring subunits. The Leipzig group concluded on the basis of theoretical considerations and a survey of the relevant literature that conserved AAs organized in four clusters (termed nucleotide binding segments (NBS) are important for ATP binding.

Our second paper dealt with the subunit composition of two heteromeric P2X receptors (P2X2/3, P2X2/6) containing as one of the constituents P2X2. As mentioned previously, P2X2/3 receptors occur in sensory neurons and respond to ATP (or α,β -meATP) with slowly desensitizing currents. P2X6 receptors are an interesting member of the P2X family in that homomeric P2X6 do not express at the plasma membrane. However, the combination with P2X2 enables P2X6 to traffick and insert into the plasma membrane, although the potency of ATP at homomeric P2X2 is higher than at heteromeric P2X2/6. In addition, P2X6 acts as a modulatory unit by changing the functional properties of P2X2.

The subunit stoichiometry of P2X2/3 was found to be 1:2, but there are no comparable data available for P2X2/6. In a detailed investigation, two homologous AAs participating in agonist binding were replaced individually with Ala to yield inactive mutants of P2X2 and P2X3 subunits; combination of the mutant P2X3 with wild-type (wt) P2X2 resulted in non-functional receptors, whereas the opposite combination was fully active. Unfortunately, there were no accompanying biochemical data presented to confirm that the functionally silent AA mutants of P2X2 and P2X3 and their compositions with their wt counterparts still exhibited undisturbed trafficking behaviour and were expressed at the cell surface.

The aims of the present work

Our aims were twofold:

1. Do certain individual (conserved or non-conserved) AAs at the supposed ATP binding sites of the human (h)P2X3 receptor determine its affinity to agonists or are the complete NBSs a pre-requisite for an undisturbed receptor function?
2. Does the subunit stoichiometry of hP2X2/6 conform with that of hP2X2/3, or in other words does 1 P2X2 subunit associate with two P2X6 subunits or is the opposite combination valid?

Amino Acid Residues Constituting the Agonist Binding Site of the Human P2X3 Receptor*[§]

Received for publication, July 26, 2010, and in revised form, November 16, 2010. Published, JBC Papers in Press, November 22, 2010, DOI 10.1074/jbc.M110.167437

Mandy Bodnar^{†1}, Haihong Wang^{†1,2}, Thomas Riedel[†], Stefan Hintze[‡], Erzsebet Kato[‡], Ghada Fallah[§], Helke Gröger-Arndt[‡], Rashid Giniatullin[¶], Marcus Grohmann[‡], Ralf Hausmann[§], Günther Schmalzing[§], Peter Illes^{‡3}, and Patrizia Rubini[‡]

From the [†]Rudolf-Boehm Institute of Pharmacology and Toxicology, University of Leipzig, 04107 Leipzig, Germany, the [§]Department of Molecular Pharmacology, University Hospital of Rheinisch Westfaelische Technische Hochschule Aachen University, 52074 Aachen, Germany, and the [¶]Department of Neurobiology, A.I. Virtanen Institute, 70211 Kuopio, Finland

Homomeric P2X3 receptors are present in sensory ganglia and participate in pain perception. Amino acid (AA) residues were replaced in the four supposed nucleotide binding segments (NBSs) of the human (h) P2X3 receptor by alanine, and these mutants were expressed in HEK293 cells and *Xenopus laevis* oocytes. Patch clamp and two-electrode voltage clamp measurements as well as the Ca²⁺ imaging technique were used to compare the concentration-response curves of the selective P2X_{1,3} agonist α,β -methylene ATP obtained at the wild-type P2X3 receptor and its NBS mutants. Within these NBSs, certain Gly (Gly-66), Lys (Lys-63, Lys-176, Lys-284, Lys-299), Asn (Asn-177, Asn-279), Arg (Arg-281, Arg-295), and Thr (Thr-172) residues were of great importance for a full agonist response. However, the replacement of further AAs in the NBSs by Ala also appeared to modify the amplitude of the current and/or [Ca²⁺]_i responses, although sometimes to a minor degree. The agonist potency decrease was additive after the simultaneous replacement of two adjacent AAs by Ala (K65A/G66A, F171A/T172A, N279A/F280A, F280A/R281A) but was not altered after Ala substitution of two non-adjacent AAs within the same NBS (F171A/N177A). SDS-PAGE in the Cy5 cell surface-labeled form demonstrated that the mutants appeared at the cell surface in oocytes. Thus, groups of AAs organized in NBSs rather than individual amino acids appear to be responsible for agonist binding at the hP2X3 receptor. These NBSs are located at the interface of the three subunits forming a functional receptor.

ATP-gated, cation-permeable P2X receptor channels form a family of seven subunits, referred to as P2X1 through P2X7 (1). The subunits consist of two transmembrane domains, a large extracellular loop containing the ATP binding site, as

well as intracellular N- and C-terminal tails. Biochemical evidence indicates that both homomeric and heteromeric receptors occur as stable trimers (2–4).

Mutagenesis studies at homomeric P2X receptors uniformly suggested that the negatively charged phosphate groups of ATP occupy some positively charged amino acids (AAs),⁴ specifically Lys or Arg, in the extracellular loop of the receptor (5–7). Moreover, aromatic Phe residues were assumed to be associated with binding the adenine ring of ATP (8). Molecular models were generated on the basis of these studies, under the assumption that each subunit of the P2X receptor family contains one individual binding site (9, 10). The three-subunit composition of P2X receptors was supported in addition to the already mentioned biochemical evidence (2) by a wealth of further data. (a) Single channel analysis of P2X receptor currents indicated 2–3 sequential binding steps (11, 12). (b) The kinetic behavior of P2X receptor currents was simulated with an allosteric model describing channel opening in the di- or triliganded state (13, 14). (c) Atomic force microscopy provided evidence for three receptor subunits, which moved away from the central pore as the channel opened (15, 16). (d) Fluorescence resonance energy transfer and electron microscopy supplied a rough structure of three interacting subunits (17). (e) The crystal structure of a zebrafish (zf) P2X4 receptor mutant supported the existence of corresponding intersubunit pockets as the binding site for ATP (17, 18).

Because in P2X receptors, instead of a few amino acid residues, four clusters of AAs, termed nucleotide binding domains (NBD1–4 (19); here nucleotide binding segments; NBS1–4), were identified as possible docking places for ATP (see Fig. 1A), we investigated by Ala scanning mutagenesis the functional significance of these NBSs. For this purpose, the human (h) recombinant P2X3 receptor, located at sensory neurons and participating in pain sensation (20, 21), was expressed in HEK293 cells or *Xenopus laevis* oocytes, and the P2X_{1,3} receptor-selective α,β -methylene ATP (α,β -meATP) was used as an agonist (22). In contrast to α,β -meATP, ATP itself would have the drawback of also activating P2Y recep-

* This work was supported by grants from the Deutsche Forschungsgemeinschaft (Grants IL 20/11-3; WI 1674/4-1; and IL20/18-2) and the Volkswagen Foundation (Grant I/82 940).

[§] The on-line version of this article (available at <http://www.jbc.org>) contains supplemental Figs. 1 and 2.

[†] Both authors contributed equally to this work.

² Present address: Dept. of Physiology, Medical School, Tongji University, Shanghai 200092, China.

³ To whom correspondence should be addressed: Rudolf-Boehm-Institute of Pharmacology and Toxicology, University of Leipzig, Haertelstrasse 16-18, D-04107 Leipzig, Germany. Tel.: 49-341-9724614; Fax: 49-341-9724609; E-mail: Peter.Illes@medizin.uni-leipzig.de.

⁴ The abbreviations used are: AA, amino acids; NBS, nucleotide binding segment; h, human; r, rat; zf, zebrafish; ORI, oocyte Ringer's solution; α,β -meATP, α,β -methylene ATP; FR, fluorescence ratio; TNP-ATP, 2'-(3')-O-(2,4,6-trinitrophenyl)adenosine 5'-triphosphate; BzATP, dibenzoyl-ATP.

P2X3 Receptor Agonist Binding Site

tors negatively interacting with the stimulatory effect at P2X3 (23).

P2X1 and P2X3 receptors show, in contrast to all other P2X receptor subtypes, a rapidly desensitizing behavior; this may be due to differences in either the AA composition/length of the N or C terminus (24–27) or the AA composition/length of the second transmembrane domain (27). Moreover, the phosphorylation of consensus protein kinase C sites at the extracellular loop of the P2X3 receptor might also modify the agonist-induced desensitization (28, 29). Eventually, rapid desensitization may also depend on agonist binding to a non-conserved AA at the extracellular loop, which is absent in the slowly desensitizing receptor types. Thus, patch clamp and two-electrode voltage clamp measurements, as well as the Ca^{2+} imaging technique, were used to investigate the role of all conserved and some non-conserved AA residues arranged in NBSs and located at the interface of two subunits for determining the amplitude and time course of the agonist-induced responses.

EXPERIMENTAL PROCEDURES

Culturing of HEK293-hP2X3 Cells—HEK293 cells were kept in Dulbecco's modified Eagle's medium also containing 4.5 mg/ml D-glucose (Invitrogen), 2 mM L-glutamine (Sigma-Aldrich), 10% fetal bovine serum (Invitrogen) at 37 °C and 10% CO_2 in humidified air.

Site-directed Mutagenesis and Transfection Procedures—The human P2X3 receptor (hP2X3) cDNA (GenBank™ accession number NM-002559.2) was subcloned per PstI and EcoRI restriction sites into pIRES2-EGFP vector from Clontech Laboratories for independent expression of P2X3 and EGFP, creating the pIR-P2 plasmid. All P2X3 receptor mutants were generated by introducing replacement mutations into the pIR-P2 construct using the QuikChange site-directed mutagenesis protocol from Stratagene according to the instruction manual. HEK293 cells were plated in plastic dishes (electrophysiology) or onto coverslips (Ca^{2+} imaging) 1 day before transient transfection. 0.5 μg of plasmid DNA per dish was combined with 10 μl of PolyFect reagent from Qiagen and 100 μl of Opti-MEM (Invitrogen). After 10 min of incubation, the lipid-DNA complexes were introduced to the cells. Approximately 18 h after transfection, the medium was replaced with Opti-MEM to remove residual plasmid DNA.

Whole-cell Patch Clamp Recordings—Whole-cell patch clamp recordings were performed 2–3 days after the transient transfection of HEK293 cells, at room temperature (20–22 °C), using an Axopatch 200 B patch clamp amplifier (Molecular Devices). The pipette solution contained (in mM): 140 CsCl, 1 CaCl_2 , 2 MgCl_2 , 10 HEPES, and 11 EGTA, pH adjusted to 7.4 using CsOH. The external physiological solution contained (in mM): 135 NaCl, 4.5 KCl, 2 CaCl_2 , 2 MgCl_2 , 10 HEPES, and 10 glucose, pH adjusted to 7.4 using NaOH. The pipette resistances were 3–6 megaohms. The liquid junction potential (V_{LJ}) between the bath and pipette solution at 21 °C was calculated and was found to be 4.5 mV. Holding potential values given in this study were corrected for V_{LJ} . All recordings were made at a holding potential of –65 mV. Data were filtered at 2 kHz with the inbuilt filter of the amplifier, digi-

tized at 5 kHz, and stored on a laboratory computer using a Digidata 1440 interface and pClamp 10.2 software (Molecular Devices).

Drugs were dissolved in the external solution and locally superfused to single cells (detected by their EGFP fluorescence), using a rapid solution change system (SF-77B Perfusion Fast-Step, Warner Instruments; 10–90% rise time of the junction potential at an open pipette tip was 1–4 ms; but see below). Concentration-response curves were established by applying increasing concentrations of α,β -methylene ATP (α,β -meATP; Sigma-Aldrich) for 2 s. The intervals between applications were 5 min for 0.03–1 μM and 7 min for 3–300 μM . Under these conditions, agonist responses were reproducible at the given concentrations (30).

In experiments investigating the kinetics of P2X3 currents, α,β -meATP (100 μM) was applied for 10 s with 7-min intervals three times in total. The current induced by the second application was used for calculations. The decay phases of the curves were fitted by the following biexponential equation

$$y = A_1 \times e^{-t/\tau_{des1}} + A_2 \times e^{-t/\tau_{des2}} + P \quad (\text{Eq. 1})$$

using the in-built function of the pClamp 10.2 software (Molecular Devices), where A_1 and A_2 are the relative amplitudes of the first and second exponential, τ_{des1} and τ_{des2} are the desensitization time constants, and P is the plateau. The onset time constants ($\tau_{on(10-90\%)}$) were calculated from the individual recordings under the assumption that despite the relatively slow local application, they give a rough approximation of the kinetics of channel opening.

Macroscopic Conductance Kinetics—Macroscopic conductance kinetics were analyzed by a hidden Markov model (see supplemental Fig. 2A, panel a; derived from Ref. 14) that includes binding, gating, and desensitization. Kinetic modeling and fitting were performed by the QuB software (31). To estimate solution exchange times of the rapid superfusion system used, 150 mM KCl was applied to the cell. The time constant of this test pulse (~140 ms) was determined by a single exponential fit and used for modeling the wash in and wash out of α,β -meATP.

High α,β -meATP concentrations induce large and rapidly activating currents, leading to a reduced membrane potential. Hence, for kinetic fits, the whole-cell conductance σ was calculated from the measured current I , the access resistance R_a , the membrane resistance R_m , and the holding potential U_h , using the following equation.

$$\sigma = \frac{(R_a + R_m)^2}{R_a^2 R_m + R_a R_m^2 + \frac{R_m^2 U_h}{I}} \quad (\text{Eq. 2})$$

Ca^{2+} Microfluorometry—HEK293 cells were loaded 2–3 days after transient transfection with the Ca^{2+} -sensitive fluorescent dye Fura-2 acetoxymethyl ester (2.5 μM ; Sigma-Aldrich) at 37 °C for 30 min in culture medium. To remove extracellular traces of the dye, the cells were then washed in physiological solution of the same composition as that used for patch clamp measurements. Cells plated onto coverslips were mounted into a perfusion chamber and placed on the

stage of an inverted microscope (IX-70; Olympus) with epifluorescence optics and a cooled CCD camera (IMAGO; Till Photonics). Throughout the experiments, cells were continuously superfused at 0.8 ml/min by means of a roller pump with external solution. Intracellular Fura-2 was alternately excited at 340 and 380 nm, and the emitted light was measured at a wavelength of 510 nm. The TILL vision software (3.3 Till Photonics) was used for data acquisition, system control, and later, off-line analysis. The fluorescence ratio (FR; 340/380 nm) provides a relative measure of the cytosolic free Ca^{2+} concentration ($[\text{Ca}^{2+}]_i$).

For the determination of concentration-response relationships, α,β -meATP was pressure-injected locally, by means of a computer-controlled DAD12 superfusion system (ALA Scientific Instruments, Inc.). The application time was 5 s, and the intervals between two subsequent agonist applications were kept, independent of the concentration used, at 15 min.

Expression of P2X3 Receptors and Their Mutants in *X. laevis* Oocytes—An oocyte expression plasmid harboring the cDNA for an N-terminally hexahistidine-tagged (His-tagged) hP2X3 subunit was available from a previous study. Replacement mutations were introduced by QuikChange site directed-mutagenesis (Stratagene). All constructs were verified by restriction analysis and nucleotide sequencing. Capped cRNAs were synthesized and injected into collagenase-defolliculated *X. laevis* oocytes using a Nanoliter 2000 injector (World Precision Instruments) as described previously (2, 32). Oocytes were cultured at 19 °C in sterile oocyte Ringer's solution (ORi: 90 mM NaCl, 1 mM KCl, 1 mM CaCl_2 , 1 mM MgCl_2 , and 10 mM Hepes, pH 7.4) supplemented with 50 $\mu\text{g}/\text{ml}$ gentamycin.

Two-electrode Voltage Clamp Electrophysiology—2–3 days after cRNA injection, current responses were evoked by α,β -meATP as indicated, at ambient temperature (21–24 °C), and recorded by conventional two-electrode voltage clamp with a Turbo TEC-05 amplifier (npi Electronics) at a holding potential of -60 mV as described previously (33). Oocytes were continuously perfused by gravity (5–10 ml/min) in a small flow-through chamber with a nominally calcium-free ORi solution (designated Mg-ORi), in which CaCl_2 was replaced by equimolar MgCl_2 to avoid a possible contribution of endogenous Ca^{2+} -dependent Cl^- channels to the α,β -meATP response.

Dilutions of agonists and antagonists in Mg-ORi were prepared daily and applied by bath perfusion. Switching between bath solutions was controlled by a set of magnetic valves, enabling computer-controlled applications of compounds (Cell-Work Lite 5.1 software; npi Electronics). For concentration-response analysis, rapidly desensitizing hP2X3 receptors were first repetitively activated in 1-min intervals by 10-s applications of 100 μM α,β -meATP (which is maximally effective at the wild-type (WT) hP2X3 receptor) until constant current responses were obtained (for further experimental details, see Ref. 33).

Protein Labeling, Purification, and PAGE—cRNA-injected oocytes were metabolically labeled by overnight incubation with L- ^{35}S methionine and, just before protein extraction, additionally surface-labeled with Cy5 NHS ester, an amine-reactive, membrane-impermeant fluorescent dye (34). His-

tagged proteins were purified by nickel-nitrilotriacetic acid agarose (Qiagen) chromatography from digitonin (1%, w/v) extracts of oocytes and analyzed by blue native PAGE as described previously (2, 3). Where indicated, samples were treated before blue native PAGE for 1 h at 37 °C with 0.1% (w/v) SDS or a combination of 0.1% (w/v) SDS and 100 mM DTT, to induce partial dissociation of hP2X3 complexes.

For SDS-urea-PAGE, proteins were denatured by incubation with reducing SDS sample buffer for 15 min at 56 °C and electrophoresed in parallel with ^{14}C -labeled molecular mass markers (Rainbow, Amersham Biosciences) on SDS-urea-PAGE gels (10% acrylamide). SDS-urea-PAGE gels were scanned wet with a fluorescence scanner (Typhoon, GE Healthcare) for visualization of fluorescently labeled plasma membrane-bound proteins and then dried and exposed to a phosphor screen for subsequent PhosphorImager (Storm 820, GE Healthcare) detection of ^{35}S incorporation. The figures were prepared by using ImageQuant TL v2005 (Amersham Biosciences) for contrast adjustments and Adobe Photoshop CS 8.0 for level adjustment and cropping.

Homology Modeling—We modeled, based on the published crystal structure of the zfp2X4 channel in its closed state (18), the extracellular loop and transmembrane areas of the hP2X3 receptor. The software used was Modeler 9, version 7 (35). The alignment was determined by the align2D function, which also takes the secondary structure of the template into consideration. Homology modeling was made with the loop-model function with high optimization settings. Visualization of the results was by VMD (36).

Data Analysis—Concentration-response curves for α,β -meATP were fitted by using a three-parametric Hill plot (SigmaPlot; SPSS). The figures show mean \pm S.E. values of n experiments. One-way analysis of variance followed by Holm-Sidak post hoc test was used for statistical analysis. We compared the various current and $[\text{Ca}^{2+}]_i$ parameters (amplitude and/or time course) of the mutants within NBS1–4 with the WT data. A probability level of 0.05 or less was considered to reflect a statistically significant difference.

RESULTS

Agonist Sensitivity of hP2X3 Receptor Mutants

Patch Clamp Investigations—The underlined, conserved AA residues in NBS1–4 of hP2X3 were sequentially replaced by Ala, one or two at a time (Fig. 1A). In addition, the conserved Ala-283 was substituted by Asp or Arg. We have also chosen non-conserved AA residues in each NBS and replaced them by Ala (Fig. 1A). The functional significance of AAs was checked by using the P2X1,3-selective α,β -meATP as an agonist.

The hP2X3 receptor or its mutants were transiently expressed either in HEK293 cells or in *X. laevis* oocytes. Fig. 1B documents the agonist application protocols in WT HEK293-hP2X3 cells. When recorded by the whole-cell variant of the patch clamp technique, at a holding potential of -65 mV, α,β -meATP had already caused a prominent desensitization of the inward current during its 2-s superfusion period (Fig. 1B, panel a). We kept a 5–7-min interval between the applica-

P2X3 Receptor Agonist Binding Site

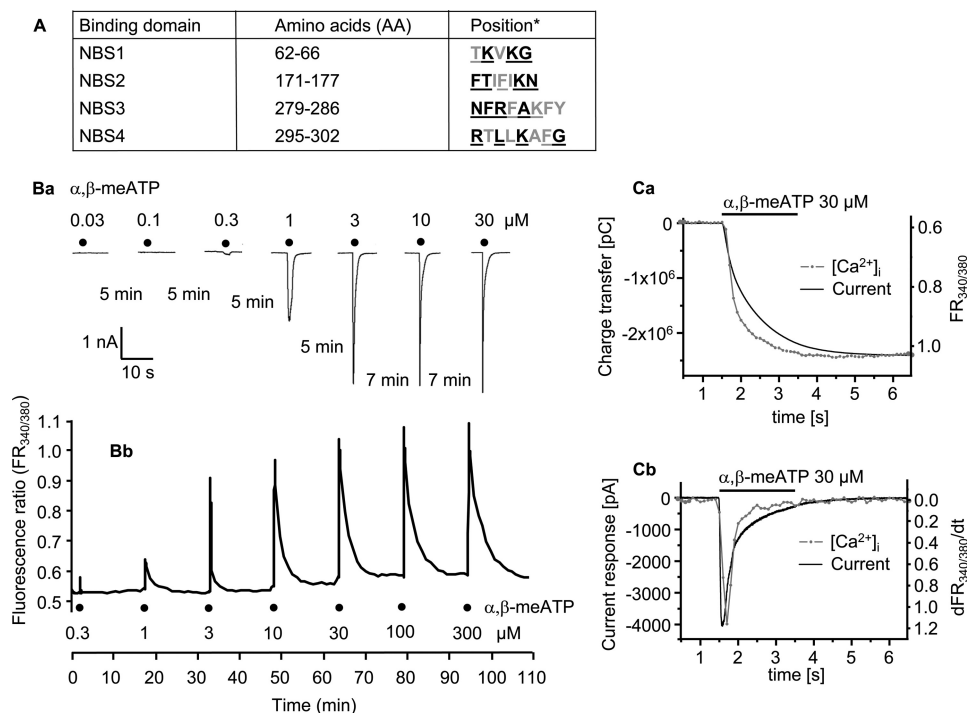


FIGURE 1. Current responses to α,β -meATP of the WT hP2X3 receptor and its NBS mutants in HEK293 cells. *A*, AA residues of the supposed nucleotide binding segments (NBS1–4). **Bold characters**, conserved AAs; **underlined characters**, substitution by Ala. *B*, *panel a*, whole-cell current responses, induced by α,β -meATP (0.03–30 μM), were recorded with the patch clamp technique at a holding potential of -65 mV. Increasing concentrations of the agonist were locally superfused for 2 s with 5- or 7-min intervals as indicated. *Panel b*, increases in the intracellular calcium concentration ($[\text{Ca}^{2+}]_i$) were induced by α,β -meATP (0.3–300 μM). Increasing concentrations of the agonist were locally superfused for 5 s with 15-min intervals. The cells were labeled with the calcium-sensitive fluorescent dye Fura-2, and fluorescence ratio ($\text{FR}_{340/380}$) measurements were made with a dual wavelength spectrometer (alternating excitation at 340 and 380 nm). The changes in FR were used as a measure of $[\text{Ca}^{2+}]_i$. Representative tracings are shown in both *panels a* and *b*. *C*, *panel a*, α,β -meATP (30 μM)-induced charge transfer measured by the patch clamp technique and fluorescence ratio determined by Ca^{2+} imaging as a function of time. The time courses of these responses were similar. Two representative experiments are shown out of a total of three (current response) and four ($[\text{Ca}^{2+}]_i$ transients) similar ones (2-s application time). *pC*, picocolombs. *Panel b*, the current response to α,β -meATP (30 μM) and the differentiated $\text{FR}_{340/380}/\text{dt}$ also have similar time courses. The recordings from *panel a* were replotted in *panel b*.

tion of successively increasing α,β -meATP concentrations to allow recovery of agonist sensitivity. α,β -meATP caused a concentration-dependent increase of the intracellular $[\text{Ca}^{2+}]_i$ transients in HEK293-hP2X3 cells as well, with a slow decline to the pre-drug level. In these experiments, we superfused α,β -meATP for 5 s and correspondingly prolonged the application intervals from 5–7 to 15 min (Fig. 1*B*, *panel b*). It is noteworthy that extracellular Ca^{2+} appeared to enter the cells via the P2X3 receptor channels only because a Ca^{2+} -free bath medium almost abolished the effect of α,β -meATP (37). Finally, the α,β -meATP-induced inward currents and $[\text{Ca}^{2+}]_i$ transients were strongly depressed by the P2X1–3 antagonist TNP-ATP or the P2X3-selective antagonist A317491 (37).

In the following experiments, we singly or doubly replaced all conserved AA residues within NBS1–4 of the hP2X3 subunit by Ala (Fig. 2); the only exception was the neutral Ala-283 itself, which was substituted by the negatively charged Asp or the positively charged Arg. Then, we transfected both the WT receptor and its NBS mutants into HEK293 cells and compared the current responses measured by the patch clamp technique. The concentration-response curve for α,β -meATP at the WT receptor yielded an EC_{50} of 2.66 ± 0.67 μM , an I_{max} of $4,110 \pm 310$ pA, and a Hill coefficient of 1.47 ± 0.47 ($n = 8$ –12). It is noteworthy that the EC_{50} values correlated well with those reported previously, both by ourselves (30) and by other authors (38).

When concentration-response curves were determined for α,β -meATP at the mutant receptors, it became evident that several AA substitutions interfered with the agonist effect. First of all, replacement of Ala-283 by Asn or Arg caused a decrease in the activity of α,β -meATP. It was not possible to determine EC_{50} or I_{max} values at the A283D and A283R mutants because no clear maximum of the concentration-response curve was reached up to 300 μM . The current amplitudes at this α,β -meATP concentration were 380.7 ± 95.9 pA (A283D; $n = 6$) and $2,996 \pm 1,553$ pA (A283R; $n = 5$), respectively; a statistically significant inhibition was observed only when the I_{max} value at the WT receptor ($4,110 \pm 310$ pA; see above) was compared with effect of α,β -meATP (300 μM) at the A283D mutant. Thus, AAs carrying a negative or positive charge at position 283 perturbed the ability of the receptor channel to open.

In NBS1, the amino acid residues Lys-63 and Gly-66, in NBS2, the residues Thr-172, Lys-176, and Asn-177, in NBS3, the residues Asn-279, Arg-281, and Lys-284, and eventually in NBS4, the residues Lys-299 and Arg-295 were essential for the agonist response. Although of less importance, modifications at Lys-65 (NBS1), Phe-174 (NBS2), Phe-280 and Phe-282 (NBS3), and Gly-302 (NBS4) also caused moderate changes. Replacements of Thr-62 (NBS1), Phe-171 (NBS2), and Leu-297 or F301A (NBS4) by Ala had no effect. There was no obligatory relationship between an AA being con-

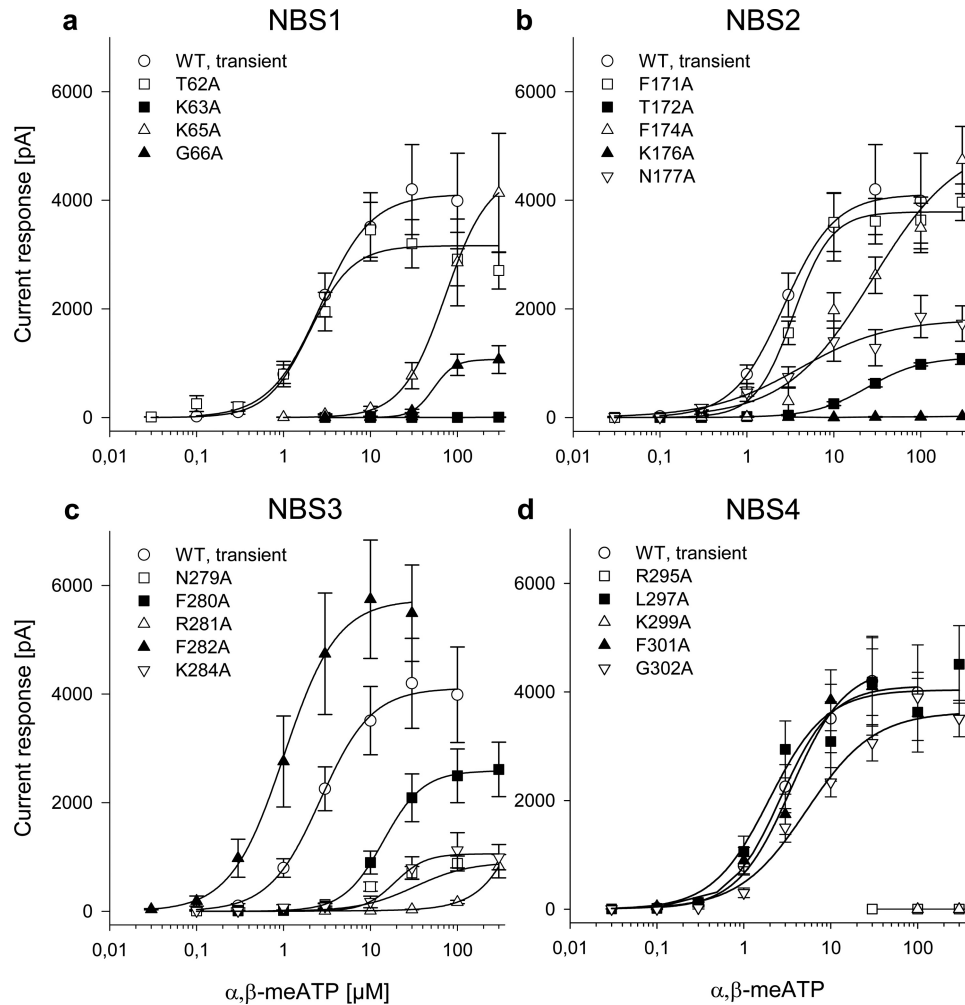


FIGURE 2. **Current responses to α,β -meATP in HEK293 cells transfected with the WT hP2X3 receptor and its mutants.** Whole-cell patch clamp recordings were made as described in the legend for Fig. 1. Concentration-response curves for α,β -meATP were constructed both for the WT hP2X3 receptor and for its point mutants, where the indicated AAs in their nucleotide binding segments were replaced by Ala (in Fig. 1A, see *underlined* one-letter coding of AAs). Ala was sequentially introduced to substitute individual AAs in NBS1 (a), NBS2 (b), NBS3 (c), and NBS4 (d). Each symbol indicates the mean \pm S.E. of 5–13 cells.

served or non-conserved and the magnitude of inhibition. Some conserved (*e.g.* Lys-63) and non-conserved (*e.g.* Lys-284) AAs were both of great importance for the agonist effect, whereas other non-conserved (*e.g.* Thr-62) and conserved (*e.g.* Phe-171) AAs were of minor significance. It turned out to be especially interesting that although some single mutations of adjacent, conserved AAs in NBS1, -2, and -3 failed to abolish the current response, the respective double mutations (K65A/G66A, F171A/T172A, N279A/F280A, F280A/R281A) caused complete inhibition (supplemental Fig. 1). However, the double mutation of two non-adjacent, conserved AAs (F171A/N177A) within NBS2 did not decrease the α,β -meATP response further when compared with F171A alone.

Ca²⁺ Imaging Studies—The evaluation of the α,β -meATP concentration-response curves for [Ca²⁺]_i transients in HEK293 cells transfected with the WT hP2X3 receptor yielded an EC₅₀ value of 1.86 \pm 0.21 μ M, an Δ FR_{max} of 0.45 \pm 0.01, and a Hill coefficient of 3.16 \pm 0.64 (*n* = 14–19) (Fig. 3). The agonist effects were modified by mutations of individual AAs within NBS1–4 to Ala. Moreover, the replacement of Ala-283 by Asp or Arg decreased the α,β -meATP-induced

increase of [Ca²⁺]_i. It was not possible to determine EC₅₀ or I_{max} values at the A283D and A283R mutants because no clear maximum of the concentration-response curve was reached up to 300 μ M. The [Ca²⁺]_i transients at this agonist concentration were 0.15 \pm 0.01 (A283D; *n* = 32) and 0.35 \pm 0.04 (A283R; *n* = 35), respectively; a statistically significant inhibition was observed when the Δ FR_{max} value at the WT receptor (0.45 \pm 0.01; see above) was compared with the effect of α,β -meATP (300 μ M) at both mutants. Thus, AAs carrying a negative or positive charge at position 283 perturbed the ability of the receptor to interact with its agonist.

All these changes were basically similar to the situation when current responses were used as a measure of agonist potency. However, in contrast to patch clamp measurements, where T62A, F172A, L297A, and F301A did not considerably modify the α,β -meATP sensitivity, Ca²⁺ imaging also demonstrated small changes with these mutants. It should be kept in mind that because of the possibility to measure [Ca²⁺]_i simultaneously in many cells, the number of experiments was in this case higher than with patch

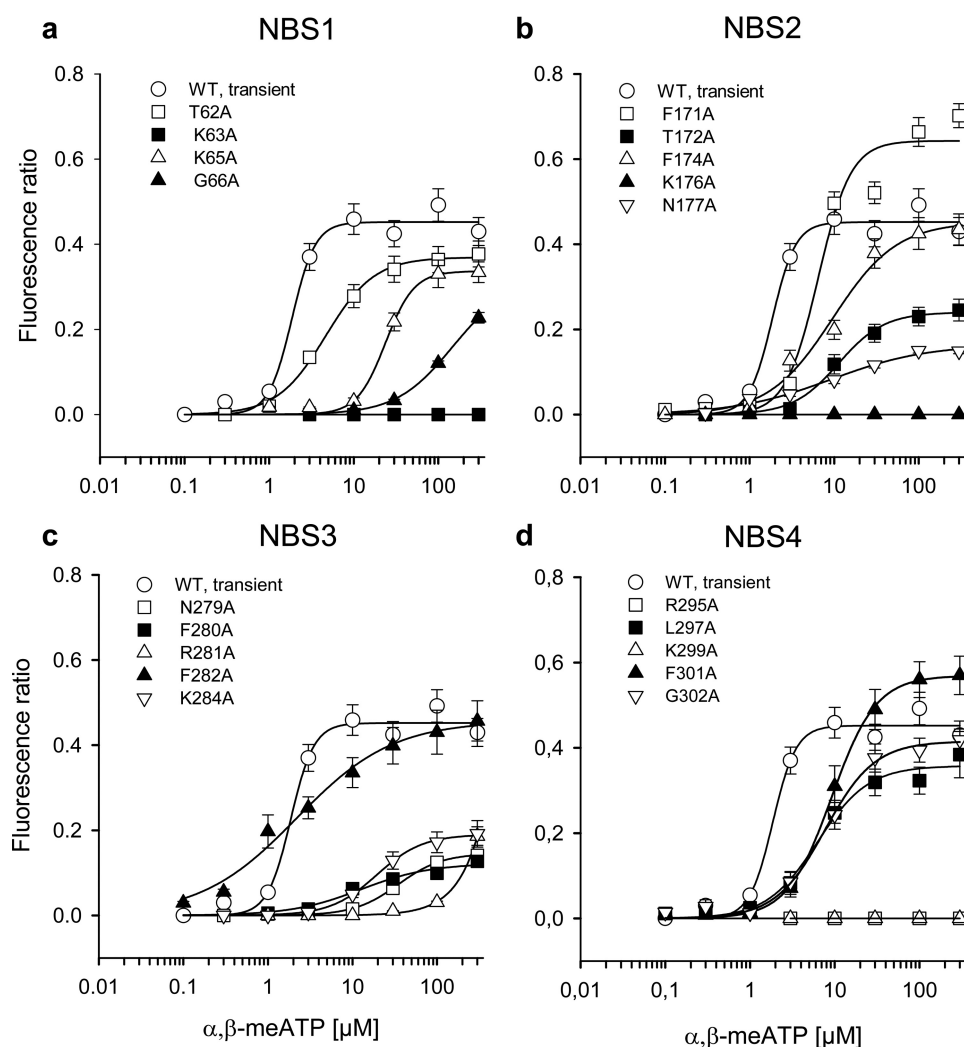


FIGURE 3. **Increases of intracellular calcium by α,β -meATP in HEK293 cells transfected with the WT hP2X3 receptor and its mutants.** FR measurements were made as described in the legend for Fig. 1 and were taken as a measure of $[Ca^{2+}]_i$. Concentration-response curves for α,β -meATP were constructed both for the WT hP2X3 receptor and for its point mutants, where the indicated AAs in their nucleotide binding segments were replaced by Ala (in Fig. 1A, see *underlined* one-letter coding of AAs). Ala was sequentially introduced to substitute individual AAs in NBS1 (a), NBS2 (b), NBS3 (c), and NBS4 (d). Each symbol indicates the mean \pm S.E. of 9–20 cells.

clamp recordings, where each cell had to be patched separately. We assume that the combination of these two methods allows a more reliable observation of subtle changes than the measurement of current responses or $[Ca^{2+}]_i$ transients alone (39, 40).

It is certainly true that electrophysiology directly determines the cationic fluxes through the P2X3 receptor channel, whereas $[Ca^{2+}]_i$ transients are only a consequence of the entry of Ca^{2+} via this receptor channel into the intracellular space. However, the two methods equally well describe the same phenomenon. In representative experiments, we integrated the α,β -meATP (30 μM) currents through the WT P2X3 receptor to obtain the total amount of transferred charge ($n = 3$) and found its time course similar to that of the $[Ca^{2+}]_i$ transients (measured as fluorescence ratio; ΔFR) ($n = 4$; Fig. 1C, panel a). Then, the shape of the current response to α,β -meATP was compared with that of the differentiated $[Ca^{2+}]_i$ response and was found to perfectly correlate (Fig. 1C, panel b) (41); rapid desensitization was a characteristic fea-

ture of the receptor when either method was used for recording.

Comparison of Data Obtained by Patch Clamp Measurements and Ca^{2+} Imaging Studies

Fig. 4 summarizes the data obtained by electrophysiology and Ca^{2+} imaging. The EC_{50} and the maximal effect E_{max} (I_{max} and ΔFR_{max} , respectively) values calculated from the concentration-response curves are shown both for the WT receptor and for its Ala-substituted single or double mutants. As already mentioned above, qualitatively identical results were obtained by the two techniques, although quantitative differences exist. With some of the mutants, no clear maximum of the concentration-response curve (and as a consequence EC_{50} or E_{max} values) could be determined with one or both of these techniques. With these limitations in mind, there was no response to α,β -meATP at the K63A, K176A, R295A, and K299A mutants, in agreement with the suggestion that certain positively charged AAs are associated with

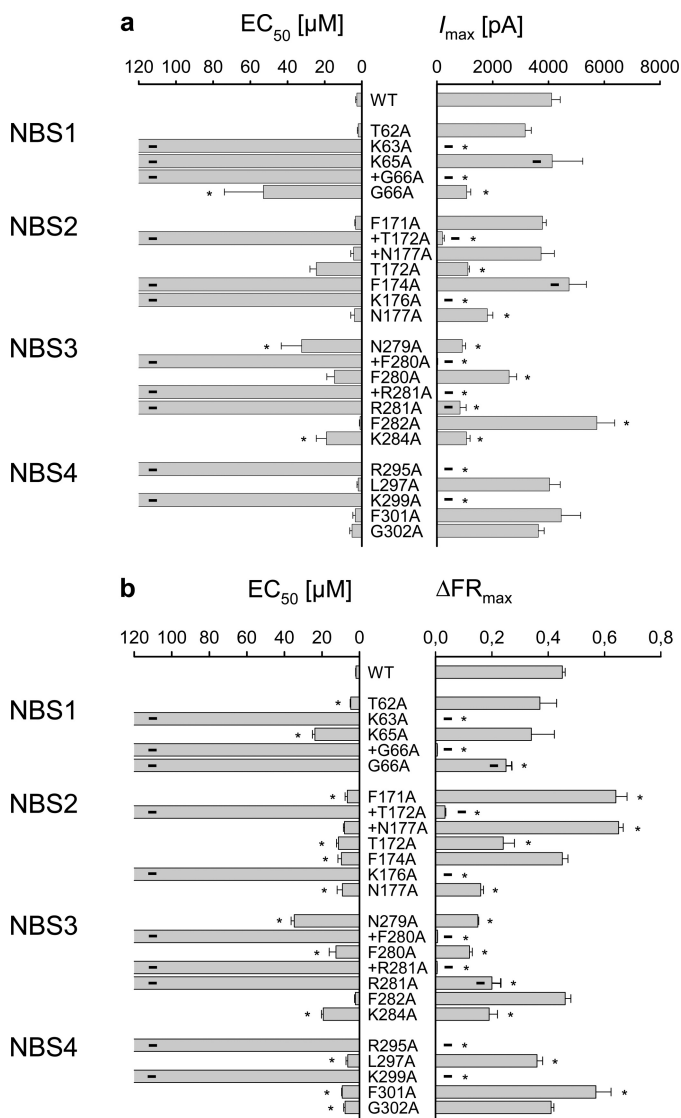


FIGURE 4. Summary of α,β -meATP concentration-response curves for the hP2X3 receptor and its NBS mutants in HEK293 cells. Curves presented in Figs. 2 and 3, and supplemental Fig. 1 were fitted as described under "Experimental Procedures" to obtain the EC_{50} and E_{max} (I_{max} or ΔFR_{max}) values. On the left-side graph, the EC_{50} values of the indicated mutants are expressed in μM . On the right-side graph, the E_{max} values of the same mutants are expressed in pA and ΔFR , respectively. Current (a) and FR (b) measurements are indicated for each single and double mutant. Each symbol indicates mean \pm S.E. of 4–13 (a) and 9–20 (b) cells. With several mutants, no clear maximum of the concentration-response curve was reached, and therefore neither the EC_{50} nor the E_{max} values could be reliably determined. In such cases, the EC_{50} values were not indicated, and the E_{max} values were replaced with the effect of the highest agonist concentration tested (300 μM ; designated by a thick line). *, $p < 0.05$; statistically significant difference from the respective value measured with the WT receptor.

the binding of the negatively charged phosphate groups of ATP (5–7). The changes in EC_{50} and E_{max} with the additional mutants, as well as the experiments with mutating Ala-283 to Asp or Arg, confirmed our assumption that all conserved AAs in the NBSs play some role in agonist binding, the stabilization of the secondary protein structure, or the transduction of receptor binding to channel gating. A comparable function of at least some of the non-conserved AAs was also evident.

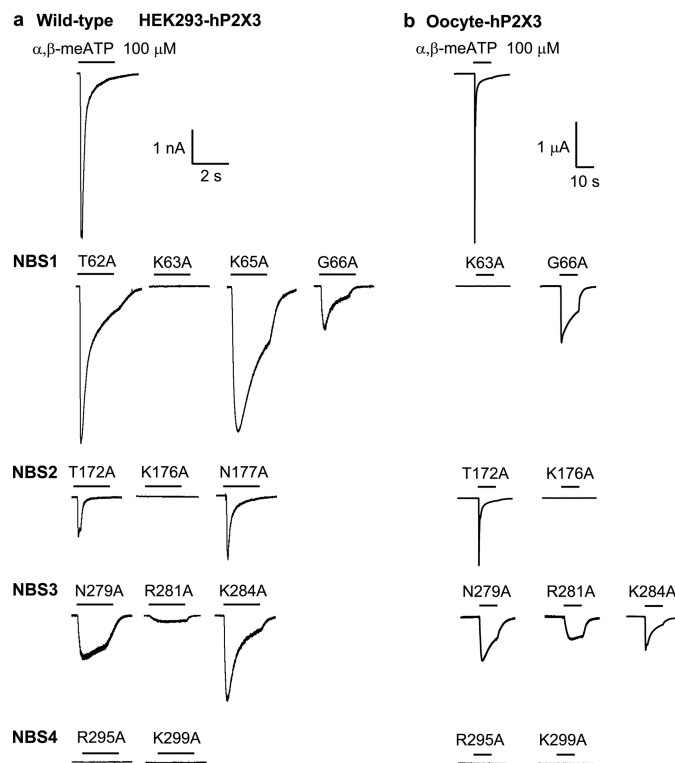


FIGURE 5. Original recordings of α,β -meATP-induced currents at hP2X3 receptors or its NBS mutants. The expression systems of the HEK293 cell (a, left panel; experimental conditions were as described in the legend for Fig. 1) or the *Xenopus laevis* oocyte (b, right panel; holding potential, -60 mV; agonist application was for 10 s every 1 min) were used. a, α,β -meATP (100 μM) effects are shown at those mutants only, where either the amplitude or the time course of the current responses appeared to be modified in comparison with the WT receptor. b, α,β -meATP (100 μM) effects are shown at nine selected mutants only, where the amplitude and/or the time course of current responses appeared to be modified in comparison with the WT receptor. These mutants were tested for assembly and surface expression in the oocyte system in the following experiments (Fig. 6B). Representative recordings for 5–14 experiments are shown.

Activation, Gating, and Desensitization of hP2X3 Receptor Mutants

A further question to be answered was whether some of the mutations altered the shape of the current response by interfering with channel activation or desensitization. Fig. 5a shows original tracings of α,β -meATP (100 μM) responses on mutants, where the current amplitude, its activation time, or the rate of desensitization appeared to change in comparison with the WT receptor. It is noteworthy that a slower rate of desensitization (higher τ_{des1} , τ_{des2} values; see below) may also be caused by a slower gating of the P2X3 receptor channel. In these experiments, α,β -meATP was applied for only 2 s; the rate constants were calculated from similar experiments with 10-s application times (not shown; see "Experimental Procedures"). According to expectations, WT P2X3 exhibited a rapid activation time constant (τ_{on} , 38 ± 4 ms) and an extremely rapid fading of the current amplitude with the two desensitization time constants τ_{des1} (935 ± 128 ms) and τ_{des2} (133 ± 12 ms; $n = 8$ each). The T62A, F171A, and L297A mutants exhibited current amplitudes similar to those of the WT receptor (Figs. 2 and 4); neither their τ_{on} nor their τ_{des1}/τ_{des2} values differed in a statistically significant manner from the WT controls. The mutation of Lys-65 to Ala did not

P2X3 Receptor Agonist Binding Site

change the current amplitude but prolonged the onset time constant τ_{on} (270 ± 50 ms; $p < 0.05$) and increased both desensitization time constants (τ_{des1} , $4,121 \pm 945$ ms; τ_{des2} , 690 ± 95 ms; $n = 7$; $p < 0.05$). The G66A mutant exhibited smaller current responses than the WT receptor, with a reduction of the rise and decay times (τ_{on} , 310 ± 45 ms; τ_{des1} , $5,477 \pm 1,480$ ms; τ_{des2} , 740 ± 105 ms; $n = 10$; $p < 0.05$). The current responses at the T172A and N177A mutants were also smaller than those at the WT receptor, although the rate of desensitization was unaltered. Eventually, smaller amplitudes were accompanied either by decelerated (N279A, τ_{on} , 487 ± 60 ms; τ_{des1} , $21,830 \pm 7,060$ ms; τ_{des2} , $2,168 \pm 501$ ms; $n = 9$; $p < 0.05$) or by practically non-existent desensitization (R281A), at least during the 2–10-s application times of the present experiments. In the case of K284A, the τ_{on} values increased (151 ± 18 ms; $p < 0.05$), whereas the τ_{des1} ($2,376 \pm 133$ ms) and τ_{des2} values (418 ± 30 ms; $n = 10$ and $p > 0.05$ each) did not alter.

For the WT P2X3 receptor and a number of its mutants, we constructed kinetic fits of the α,β -meATP-induced currents by using a hidden Markov model obtained by simplification of the model of Karoly *et al.* (14). The rate constants characterizing transitions between the unbound, closed-state receptor (C_1), and the receptor binding one- (C_2), two (C_3)-, or three (C_4)-agonist molecules, as well as the two open-state receptors (O_5 , O_6) and the two desensitized receptors (C_7 , C_8) are shown for WT P2X₃ on the [supplemental Fig. 2A, panel a](#). By using the on- and off-rate constants, the shape and amplitude of the α,β -meATP (0.3–300 μM)-induced currents could be computer-modeled; the quality of the fits can be judged by the close parallelism of the *black lines* (original tracings) and the current traces (*orange lines*) calculated with the indicated rate constants for binding (C_1 – C_4), gating (C_3 – O_5 ; C_4 – O_6), and desensitization (C_3 – C_7 and O_5 – C_7 ; C_4 – C_8 and O_6 – C_8). Best fits for the α,β -meATP currents were computed by modifying the rate constants as indicated in the individual panels of [supplemental Fig. 2](#). By comparing these constants with those of the WT receptor, it appears that in the case of K65A (*B*) and F280A (*D*), binding was altered, whereas in the case of F174A (*C*), both binding and gating were altered. Thus, selected mutations within NBS1–3 are suggested to modify agonist binding to a variable degree, although in some cases, gating may also be affected. The quality of the best fit for R281A (*E*) was moderate, indicating on the one hand changes in binding, but on the other hand raising the possibility of additional complicating factors such as the interruption of hydrogen bonds formed between Arg-281 and Glu-156 on the same subunit and/or Asp-76 on the neighboring subunit (see “Homology Modeling of the hP2X3 Receptor” below). Similarly, the modification of the rate constants failed to produce a good fit for agonist currents at Lys-284 (not shown). This may be due to the fact that Lys-284 is situated at the entry of the ion pore region and is not directed toward the binding groove. We simplified the model of Karoly *et al.* (14) by omitting the kinetic constants determining high affinity desensitization and the recovery from desensitization but maintained those involved in the early phase of desensitization. Of course, this simplification means a loss of quality, but the obtained fits

should be sufficient to decide whether binding and/or gating are responsible for the modified amplitudes and time courses of the current responses.

Assembly and Plasma Membrane Trafficking of hP2X3 Receptor Mutants

To check for expression system-specific differences and also to assess their assembly capacitance, we expressed selected mutants (K63A, G66A, T172A, K176A, N279A, R281A, K284A, R295A, and K299A), which responded in HEK cells with rather small or even no current amplitudes to α,β -meATP (100 μM) in *X. laevis* oocytes. The α,β -meATP concentration-response curve of oocyte-expressed WT hP2X3 receptors exhibited EC_{50} and E_{max} values of 3.14 ± 0.75 μM and 3.68 ± 0.41 μA , respectively; the Hill coefficient was 1.28 ± 0.49 ($n = 6$ each). In agreement with the patch clamp data in HEK293 cells, the α,β -meATP (100 μM)-induced current responses were markedly depressed or even abolished on the selected mutants in comparison with WT hP2X3 receptor currents (Fig. 6A). In addition, changes in the speed of activation and desensitization were also comparable in recordings from oocytes and HEK293 cells (compare Fig. 5b with 5a). It should be noted, however, that because of the relatively slow application speed and the short inter-application interval of α,β -meATP (100 μM) (see “Experimental Procedures”), no time constants for activation/desensitization were calculated for oocytes.

The mutations may affect the assembly and cell surface expression of the hP2X3 mutants. To address this issue, we used the nine single mutants with impaired function in the oocyte expression system, which has the strong advantage that the cell integrity needed for reliable cell surface labeling can be easily assessed by visual inspection. Assembly (Fig. 6B, *panel a*) and cell surface expression (Fig. 6B, *panel b*) were investigated by blue native PAGE in the [³⁵S]methionine-labeled form and by SDS-PAGE in the Cy5 cell surface-labeled form, respectively. Like the WT hP2X3 receptor subunit, all P2X3 mutants with impaired function were also capable of assembling to homotrimers (Fig. 6B, *panel b*). All mutants appeared at the cell surface, albeit at different levels (note for example the rather weak surface expression of R295A and K299A). Thus, with these two mutants, the failure of α,β -meATP (100 μM) to induce a current response (Fig. 6A) may be due at least partly to the low degree of plasma membrane expression. However, in the case of all other mutants investigated in the oocyte system, the trafficking to the cell membrane was roughly equal with that of the WT receptor.

Homology Modeling of the hP2X3 Receptor

Eventually, based on the published crystal structure of the zfP2X4 (18), we modeled the hP2X3 receptor. The NBSs shown to be involved in agonist binding were situated at opposite sites of the same subunit (Fig. 7B) and were therefore able to form a binding pocket only at the interface of two adjacent subunits (Fig. 7A, *panels a* and *b*). Of the conserved residues investigated, many were oriented toward the groove of the pocket, indicating that they may bind ATP directly (Lys-63, Lys-65, Lys-176, Asn-279, Arg-281, Arg-295, Lys-

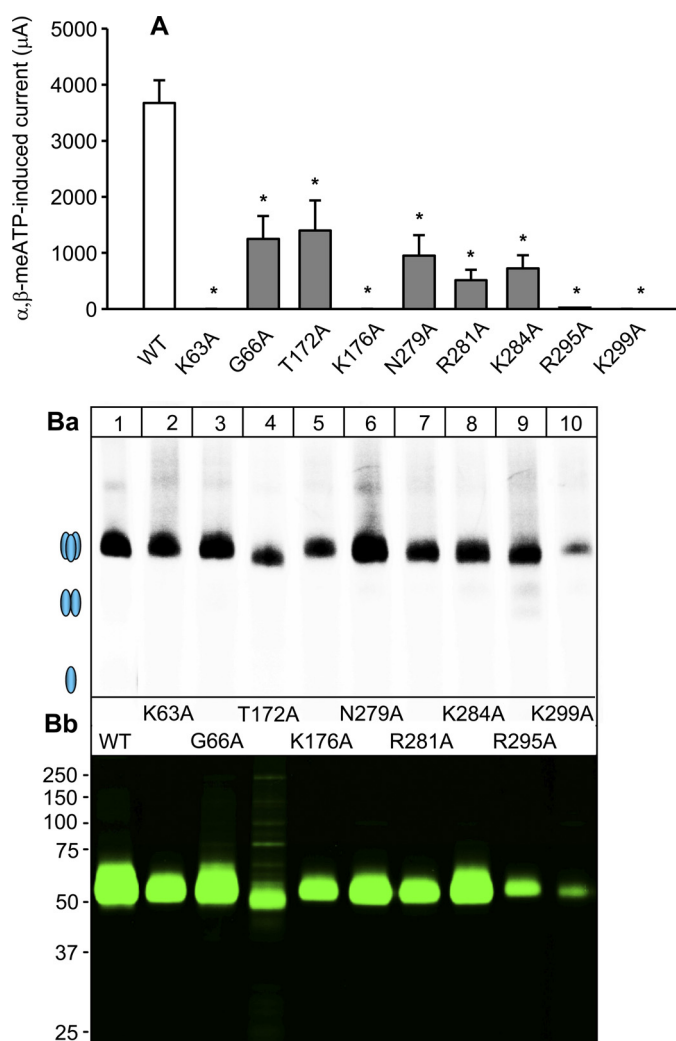


FIGURE 6. Sensitivity to α,β -meATP and assembly and surface expression of hP2X3 mutants in *X. laevis* oocytes. *A*, typical two-electrode voltage clamp current traces recorded from oocytes expressing the hP2X₃ receptor or its selected NBS mutants as indicated. α,β -meATP (100 μ M) caused smaller current amplitudes at all nine mutants tested than at the WT receptor. Mutants K63A, K276A, and K299A were unable to mediate any current response. Each symbol indicates mean \pm S.E. of 5–6 oocytes. *, $p < 0.05$; statistically significant difference from the WT receptor. *B*, [³⁵S]methionine-labeled oocytes were chased for 24 h and surface-labeled with the membrane-impermeant fluorescent Cy5 dye prior to protein purification by non-denaturing nickel-nitrilotriacetic acid chromatography. *B*, *panel a*, oligomeric state of the P2X3 proteins as visualized by blue native PAGE and ³⁵S phosphorimaging. The ovals schematically illustrate the migration positions of the non-denatured trimeric state and dimeric and monomeric states produced by partial or complete denaturation with SDS treatment, respectively. *Panel b*, aliquots of the same samples shown in *panel a* were denatured with reducing SDS-PAGE sample buffer, resolved by SDS-urea-PAGE, and visualized in their Cy5-labeled surface form by Typhoon fluorescence scanning. Each mutant was analyzed at least twice with identical results.

299); our experiments confirm that Ala substitution of these AA residues causes marked changes in the amplitude and/or gating and possibly desensitization kinetics of the current responses. In contrast, some of the conserved AA residues, such as Thr-172, Asn-177, and Phe-280, were oriented away from the groove, although their replacement with Ala caused pronounced changes, suggesting that they may participate in transducing conformational information changes from the binding pocket to the ion channel. Ala-283 is located rela-

tively far from the binding pocket; however, the substitution of Ala by negatively (Asn) or positively (Arg) charged AAs had prominent effects. Ala substitution of the non-conserved AAs Thr-62, Phe-174, Phe-282, and Phe-301 caused only minor changes, irrespective of their orientation toward (Phe-174, Phe-301) or away (Thr-62, Phe-282) from the binding pocket. Replacement of the non-conserved Lys-284 by Ala had a marked effect both on the current amplitude and on its time course. However, structural considerations in conjunction with our poor kinetic fits make the involvement of this AA in agonist binding unlikely (see “Activation, Gating, and Desensitization of hP2X3 Receptor Mutants”).

DISCUSSION

P2X3 receptors are mostly limited to the neuronal pathways involved in the perception and conduction of painful stimuli (20, 21). This highly circumscribed distribution in the peripheral and central nervous system is a prerequisite to develop new drugs for the selective treatment of pain. The peripheral terminals of sensory neurons, situated for example in dorsal root ganglia, possess P2X3 receptors, which react to ATP released by all types of nociceptive stimuli. Antagonists at these receptors have been shown to effectively block both hyperalgesia and allodynia in different models of pathological pain (42).

In view of the great significance of P2X3 receptors for future therapeutic strategies to medicate various pain states, we set out to investigate the AA residues involved in agonist binding, the more so because in contrast to most P2X receptor types, in the case of P2X3, we dispose of some selective agonists and antagonists (22). Our purpose was to characterize the ATP binding site of the P2X3 receptor to alleviate the computer-assisted design of new antagonists for therapeutic purposes. Although mutagenesis studies at P2X1 (6, 8, 43, 44), P2X2 (7, 45), and P2X4 (39, 40) have identified several AA residues of the respective receptors, which are indispensable for agonist binding, similar information for P2X3 receptors is scarce (45) (Table 1). Bioinformatics and receptor modeling suggested the existence of four putative ATP binding sites per each subunit (19, 46). The possibility of there being more than one ATP binding site per monomer cannot be ruled out at the present (17) but is rather unlikely. More importantly, instead of individual amino acids, groups of AAs organized in four nucleotide binding segments were proposed to mediate the nucleotide effects (19).

In the present study, we systematically replaced all conserved AAs in the NBSs of the hP2X3 subunit (plus 1–2 non-conserved AAs in each NBS) and searched for changes in agonist potency by means of electrophysiology and Ca²⁺ imaging in two expression systems (HEK293 cells, *X. laevis* oocytes). In the first place, we confirmed our previous results relating to the critical importance of a few positively charged AAs (K63A, K65A, K176A, R281A, R295A, K299A (37, 45)). Then, the involvement of a range of further AAs in agonist binding, agreeing with a comparable role of these AAs in the hP2X1, rP2X2, and rP2X4, was also documented (Table 1 and references cited therein). However, we report in addition three key findings. 1) Unequivocal, although sometimes minor, changes

P2X3 Receptor Agonist Binding Site

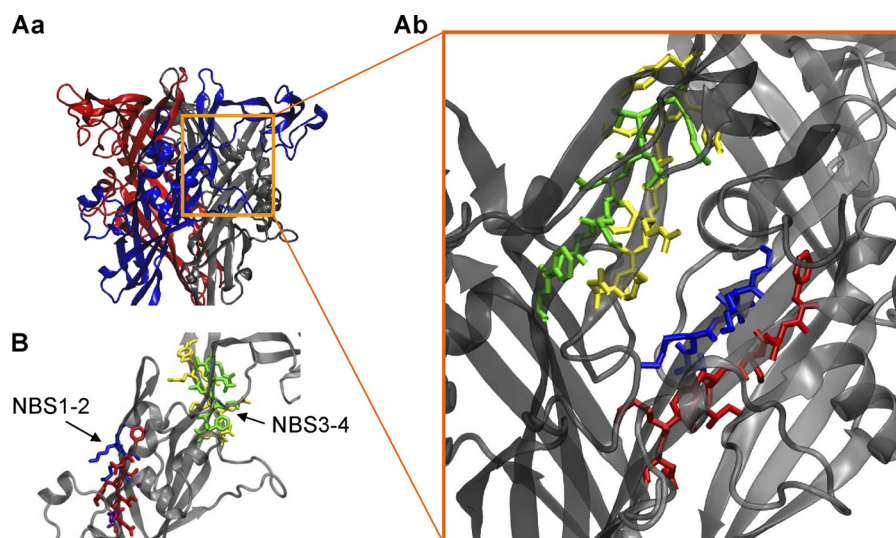


FIGURE 7. **Model of the hP2X3 receptor.** *A, panel a*, extracellular loop of the hP2X3 trimer. The individual subunits are labeled by different colors. *Panel b*, detailed view of the supposed binding site at the interface of two neighboring subunits containing four binding segments (NBSs). Color coding of the amino acid residues is: blue, NBS1; red, NBS2; yellow, NBS3; green, NBS4. *B*, NBS1–2 and NBS3–4 are located at opposite sites of a single subunit.

TABLE 1

Nucleotide binding segments of P2X receptors

Closed circle, major decrease in activity; *open circle*, slight decrease in activity or change only with Ca^{2+} imaging; *h*, human receptor; *r*, rat receptor; *zf*, zebrafish receptor mutant; conserved amino acids are indicated with bold lettering.

P2X receptor-type	NBS1	NBS2	NBS3	NBS4
hP2X1 ¹	67-71 V K L K G	185-191 F T L F I K N	290-297 N F R F A R H F	305-312 R H L F K V F G
rP2X2 ²	68-72 T K V K G	183-189 F T L I K N	288-295 N F R F A K Y Y	304-311 R T L I K A F G
hP2X3 ³	62-66 T K V K G	171-177 F T L F K N	279-286 N F R F A K Y Y	295-302 R T L I K A F G
rP2X4 ⁴	66-70 T K A K G	185-191 F T L L V K N	293-300 N F R F A K Y Y	309-316 R T L T K A Y G
zfP2X4 ⁵	69-73 T K V K G	188-194 F T V L I K N	296-303 N F R F A K Y Y	312-319 R T L I K G Y G

¹ Mutagenesis by alanine or cysteine with ATP or BzATP as agonists (6, 8, 44, 45).

² Mutagenesis by alanine or cysteine with ATP as the agonist (7, 45).

³ Replacement of alanine-283 by aspartate or arginine, or replacement of all residual investigated amino acids by alanine with α,β -meATP as the agonist (present study).

⁴ Mutagenesis by alanine or cysteine with ATP as the agonist (39, 40, 45).

⁵ Prediction based on the crystal structure (18, 45).

occurred in the amplitude of the current and/or $[\text{Ca}^{2+}]_i$ response when further conserved (Phe-171, Leu-297) or non-conserved (Thr-62, Phe-174, Lys-284, Phe-301) AAs were replaced by Ala or Ala itself was substituted by other AAs (A283D, A283R). 2) The agonist potency decrease was additive when two adjacent AAs were replaced simultaneously by Ala (Lys-65/Gly-66, Phe-171/Thr-172, Asn-279/Phe-280, Phe-280/Arg-281) but was not altered after Ala substitution of two non-adjacent AAs of the same NBS (Phe-171/Asn-177). 3) The decrease in current amplitude was accompanied in many cases by a pronounced decrease in the activation and/or desensitization rate of the receptor mutants (K65A, G66A, N279A). With R281A, a depression of the current amplitude was not accompanied by a concomitant change in the speed of activation or desensitization.

Signals that regulate intracellular trafficking of P2X receptors and thereby their membrane expression are usually associated with the N (47) or C terminus of these receptors (48, 49). Disrupting some of the conserved disulfide bridges of the extracellular loop of P2X subunits also markedly depresses their trafficking to the cell surface (50, 51). However, in this case, the normal folding of the protein appears to be altered, and the trafficking defects might be due to a failure to pass the quality check test that takes place in the endoplasmic reticulum rather than due to a trafficking defect *per se*. Thus, it was not astonishing that the present mutations in the NBSs in general did not modify the insertion of the P2X3 receptor mutants into the cell membrane of oocytes. A major change occurred only with R295A and K299A, which were expressed at a lower quantity, partially explaining the abolition of current amplitudes in the voltage clamp recordings. In the case of all other mutants, the decrease of the current response was certainly not the consequence of a disturbed trafficking behavior.

An inventive approach demonstrated by co-expression of wild-type P2X3 and a mutant P2X2, where Lys-69 or -308 was mutated to Ala, that the resulting P2X2/3 receptor functioned normally but not when both Lys residues were mutated to Ala (52). However, co-expression of wild-type P2X2 with a correspondingly mutated P2X3 subunit (K63A or K299A) produced non-functional heteromers. Thus, the failure to rescue function in the P2X2 subunit with both Lys residues mutated, by wild-type P2X3, suggests that residues from two different subunits interact in agonist binding. Similarly, the replacement of two conserved residues, Lys-68 and Phe-291 (Lys-63, Phe-280; P2X3 numbering), by cysteine led to disulfide cross-linking between neighboring P2X1 subunits (53). Because mutation of these residues results in a decreased ATP potency and cysteine cross-linking is prevented in the presence of ATP, an intersubunit ATP binding site was proposed to operate. In agreement with this idea, our P2X3 receptor model, developed on the basis of the crystal structure of the P2X4

receptor (18), suggested in conjunction with the mutagenesis results that NBS1–2 and NBS3–4 as a whole shape the binding pocket for ATP. These findings lend support to our previous hypothesis (19, 46) that instead of a few amino acid residues as generally believed, at least four NBSs are needed for the docking of ATP to the P2X3 receptor. The kinetic modeling of the agonist-induced currents on some of the receptor mutants suggested the involvement of AA residues (Lys-65, Phe-174, Phe-280, Arg-281) in ligand binding, although a gating function could also be attributed to Phe-174. In accordance with these results, the use of the full agonist ATP and the partial agonist BzATP for P2X1 suggested that certain AAs of the extracellular loop have a gating function (8). The homology modeling of the receptor structure documented that a few conserved AA residues, such as Thr-172, Asn-177, and Phe-280, were in the closed state oriented away from the groove, although their replacement with Ala caused marked changes, suggesting that they may participate in transducing conformational information changes from the binding pocket to the ion channel. In addition, the replacement of Gly-66 by Ala markedly depressed both the current and the $[Ca^{2+}]_i$ responses. It is quite possible that the flexible nature of this AA would allow conformational changes to occur, as suggested for Gly-250 in P2X1 receptors (43).

In conclusion, polypeptide clusters, rather than individual AAs, might be responsible for agonist binding, gating, and desensitization of P2X3 receptors.

Acknowledgments—We are grateful to Sara Wiese, Nanette Messermer, and Martin Fuchs for methodological help. We thank Dr. Kerstin Wirkner for useful discussions.

REFERENCES

- Khakh, B. S., and North, R. A. (2006) *Nature* **442**, 527–532
- Nicke, A., Bäumer, H. G., Rettinger, J., Eichele, A., Lambrecht, G., Mutschler, E., and Schmalzing, G. (1998) *EMBO J.* **17**, 3016–3028
- Aschrafi, A., Sadtler, S., Niculescu, C., Rettinger, J., and Schmalzing, G. (2004) *J. Mol. Biol.* **342**, 333–343
- Illes, P., and Alexandre Ribeiro, J. (2004) *Eur. J. Pharmacol.* **483**, 5–17
- Freist, W., Verhey, J. F., Stühmer, W., and Gauss, D. H. (1998) *FEBS Lett.* **434**, 61–65
- Ennion, S., Hagan, S., and Evans, R. J. (2000) *J. Biol. Chem.* **275**, 29361–29367
- Jiang, L. H., Rassendren, F., Surprenant, A., and North, R. A. (2000) *J. Biol. Chem.* **275**, 34190–34196
- Roberts, J. A., and Evans, R. J. (2004) *J. Biol. Chem.* **279**, 9043–9055
- Vial, C., Roberts, J. A., and Evans, R. J. (2004) *Trends Pharmacol. Sci.* **25**, 487–493
- Evans, R. J. (2009) *Eur. Biophys. J.* **38**, 319–327
- Ding, S., and Sachs, F. (1999) *J. Gen. Physiol.* **113**, 695–720
- Riedel, T., Lozinsky, I., Schmalzing, G., and Markwardt, F. (2007) *Biophys. J.* **92**, 2377–2391
- Sokolova, E., Skorinkin, A., Fabbretti, E., Masten, L., Nistri, A., and Giniatullin, R. (2004) *Br. J. Pharmacol.* **141**, 1048–1058
- Karoly, R., Mike, A., Illes, P., and Gerevich, Z. (2008) *Mol. Pharmacol.* **73**, 224–234
- Nakazawa, K., Yamakoshi, Y., Tsuchiya, T., and Ohno, Y. (2005) *Eur. J. Pharmacol.* **518**, 107–110
- Shinozaki, Y., Sumitomo, K., Tsuda, M., Koizumi, S., Inoue, K., and Torimitsu, K. (2009) *PLoS Biol.* **7**, e103
- Young, M. T. (2010) *Trends Biochem. Sci.* **35**, 83–90
- Kawate, T., Michel, J. C., Birdsong, W. T., and Gouaux, E. (2009) *Nature* **460**, 592–598
- Mager, P. P., Weber, A., and Illes, P. (2004) *Curr. Top. Med. Chem.* **4**, 1657–1705
- Chizh, B. A., and Illes, P. (2001) *Pharmacol. Rev.* **53**, 553–568
- Wirkner, K., Sperlagh, B., and Illes, P. (2007) *Mol. Neurobiol.* **36**, 165–183
- Jarvis, M. F., and Khakh, B. S. (2009) *Neuropharmacology* **56**, 208–215
- Gerevich, Z., Zadori, Z., Müller, C., Wirkner, K., Schröder, W., Rubini, P., and Illes, P. (2007) *Br. J. Pharmacol.* **151**, 226–236
- Koshimizu, T., Koshimizu, M., and Stojilkovic, S. S. (1999) *J. Biol. Chem.* **274**, 37651–37767
- He, M. L., Koshimizu, T. A., Tomić, M., and Stojilkovic, S. S. (2002) *Mol. Pharmacol.* **62**, 1187–1197
- Fountain, S. J., and North, R. A. (2006) *J. Biol. Chem.* **281**, 15044–15049
- Zhou, Z., Monsma, L. R., and Hume, R. I. (1998) *Biochem. Biophys. Res. Commun.* **252**, 541–545
- Wirkner, K., Stanchev, D., Köles, L., Klebingat, M., Dihazi, H., Flehmig, G., Vial, C., Evans, R. J., Fürst, S., Mager, P. P., Eschrich, K., and Illes, P. (2005) *J. Neurosci.* **25**, 7734–7742
- Stanchev, D., Flehmig, G., Gerevich, Z., Nörenberg, W., Dihazi, H., Fürst, S., Eschrich, K., Illes, P., and Wirkner, K. (2006) *Neurosci. Lett* **393**, 78–83
- Gerevich, Z., Zadori, Z. S., Köles, L., Kopp, L., Milius, D., Wirkner, K., Gyires, K., and Illes, P. (2007) *J. Biol. Chem.* **282**, 33949–33957
- Milescu, L. S., Akk, G., and Sachs, F. (2005) *Biophys. J.* **88**, 2494–2515
- Schmalzing, G., Gloor, S., Omay, H., Kröner, S., Appelhans, H., and Schwarz, W. (1991) *Biochem. J.* **279**, 329–336
- Hausmann, R., Rettinger, J., Gerevich, Z., Meis, S., Kassack, M. U., Illes, P., Lambrecht, G., and Schmalzing, G. (2006) *Mol. Pharmacol.* **69**, 2058–2067
- Becker, D., Woltersdorf, R., Boldt, W., Schmitz, S., Braam, U., Schmalzing, G., and Markwardt, F. (2008) *J. Biol. Chem.* **283**, 25725–25734
- Fiser, A., and Sali, A. (2003) *Methods Enzymol.* **374**, 461–491
- Humphrey, W., Dalke, A., and Schulten, K. (1996) *J. Mol. Graph.* **14**, 33–38
- Fischer, W., Zadori, Z., Kullnick, Y., Gröger-Arndt, H., Franke, H., Wirkner, K., Illes, P., and Mager, P. P. (2007) *Eur. J. Pharmacol.* **576**, 7–17
- North, R. A., and Surprenant, A. (2000) *Annu. Rev. Pharmacol. Toxicol.* **40**, 563–580
- Yan, Z., Liang, Z., Tomic, M., Obsil, T., and Stojilkovic, S. S. (2005) *Mol. Pharmacol.* **67**, 1078–1088
- Zemkova, H., Yan, Z., Liang, Z., Zelinkova, I., Tomic, M., and Stojilkovic, S. S. (2007) *J. Neurochem.* **102**, 1139–1150
- Egan, T. M., and Khakh, B. S. (2004) *J. Neurosci.* **24**, 3413–3420
- Donnelly-Roberts, D., McGaraughty, S., Shieh, C. C., Honore, P., and Jarvis, M. F. (2008) *J. Pharmacol. Exp. Ther.* **324**, 409–415
- Digby, H. R., Roberts, J. A., Sutcliffe, M. J., and Evans, R. J. (2005) *J. Neurochem.* **95**, 1746–1754
- Roberts, J. A., Digby, H. R., Kara, M., El Ajouz, S., Sutcliffe, M. J., and Evans, R. J. (2008) *J. Biol. Chem.* **283**, 20126–20136
- Browne, L. E., Jiang, L. H., and North, R. A. (2010) *Trends Pharmacol. Sci.* **31**, 229–237
- Mager, P. P., and Illes, P. (2006) *Expert Opin. Drug Discov.* **1**, 202–309
- Ormond, S. J., Barrera, N. P., Qureshi, O. S., Henderson, R. M., Edwardson, J. M., and Murrell-Lagnado, R. D. (2006) *Mol. Pharmacol.* **69**, 1692–1700
- Chaumont, S., Jiang, L. H., Penna, A., North, R. A., and Rassendren, F. (2004) *J. Biol. Chem.* **279**, 29628–29638
- Murrell-Lagnado, R. D., and Qureshi, O. S. (2008) *Mol. Membr. Biol.* **25**, 321–331
- Newbolt, A., Stoop, R., Virginio, C., Surprenant, A., North, R. A., Buell, G., and Rassendren, F. (1998) *J. Biol. Chem.* **273**, 15177–15182
- Ennion, S. J., and Evans, R. J. (2002) *Mol. Pharmacol.* **61**, 303–311
- Wilkinson, W. J., Jiang, L. H., Surprenant, A., and North, R. A. (2006) *Mol. Pharmacol.* **70**, 1159–1163
- Marquez-Klaka, B., Rettinger, J., Bhargava, Y., Eisele, T., and Nicke, A. (2007) *J. Neurosci.* **27**, 1456–1466

ATP Binding Site Mutagenesis Reveals Different Subunit Stoichiometry of Functional P2X2/3 and P2X2/6 Receptors*[§]

Received for publication, January 21, 2012, and in revised form, February 27, 2012. Published, JBC Papers in Press, February 29, 2012, DOI 10.1074/jbc.M112.345207

Ralf Hausmann^{‡1}, Mandy Bodnar^{§1}, Ronja Woltersdorf[‡], Haihong Wang[§], Martin Fuchs[§], Nanette Messemer[§], Ying Qin[§], Janka Günther[‡], Thomas Riedel[§], Marcus Grohmann^{‡§}, Karen Nieber[¶], Günther Schmalzing[‡], Patrizia Rubini^{§2}, and Peter Illes^{§2,3}

From the [‡]Department of Molecular Pharmacology, University Hospital of Rheinisch Westfaelische Technische Hochschule, Aachen University, 52074 Aachen, Germany, the [§]Rudolf Boehm Institute of Pharmacology and Toxicology, University of Leipzig, Haertelstrasse 16-18, 04107 Leipzig, Germany, and the [¶]Department of Pharmacology for Natural Sciences, Institute of Pharmacy, University of Leipzig, 04103 Leipzig, Germany

Background: Heteromeric P2X receptors increase the diversity of rapid ATP signaling.

Results: Non-functional P2X2, P2X3, and P2X6 subunit mutants were used to investigate the composition of heteromeric P2X2/3 and P2X2/6 receptors.

Conclusion: The subunit stoichiometry of P2X2/3 and P2X2/6 is 1:2 and 2:1, respectively.

Significance: Recognition sites between P2X2 and its partners rather than random association may govern the subunit composition of the receptor trimers.

The aim of the present experiments was to clarify the subunit stoichiometry of P2X2/3 and P2X2/6 receptors, where the same subunit (P2X2) forms a receptor with two different partners (P2X3 or P2X6). For this purpose, four non-functional Ala mutants of the P2X2, P2X3, and P2X6 subunits were generated by replacing single, homologous amino acids particularly important for agonist binding. Co-expression of these mutants in HEK293 cells to yield the P2X2 WT/P2X3 mutant or P2X2 mutant/P2X3 WT receptors resulted in a selective blockade of agonist responses in the former combination only. In contrast, of the P2X2 WT/P2X6 mutant and P2X2 mutant/P2X6 WT receptors, only the latter combination failed to respond to agonists. The effects of α,β -methylene-ATP and 2-methylthio-ATP were determined by measuring transmembrane currents by the patch clamp technique and intracellular Ca^{2+} transients by the Ca^{2+} -imaging method. Protein labeling, purification, and PAGE confirmed the assembly and surface trafficking of the investigated WT and WT/mutant combinations in *Xenopus laevis* oocytes. In conclusion, both electrophysiological and biochemical investigations uniformly indicate that one subunit of P2X2 and two subunits of P2X3 form P2X2/3 heteromeric receptors, whereas two subunits of P2X2 and one subunit of P2X6 constitute P2X2/6 receptors. Further, it was shown that already two binding sites of the three possible ones are sufficient to allow these receptors to react with their agonists.

Cys-loop, pentameric (1–3), and tetrameric (4, 5) ligand-gated ion channels usually consist of the heteromeric composition

of structurally divergent subunits. Homomeric assemblies of identical subunits are, however, to a minor extent also possible (e.g. for the 5HT₃ receptor and certain neuronal nicotinic and GABA_A receptor subtypes). More recently, an additional ATP-gated ionotropic receptor family has been discovered by cloning seven distinct P2X receptor subunits from mammalian species (P2X1 to -7) (6–9). Again, P2X subunits appeared to form not only homomeric receptor channels but also heteromeric ones. Original work based on co-immunoprecipitation with epitope-tagged subunits demonstrated that only P2X6 was not able to form homooligomers, and P2X7 was the only exception of constituting heterooligomeric complexes (10). Subsequently, it was found that P2X1/2 (11, 12), P2X1/4 (13), P2X1/5 (14), P2X2/3 (15), P2X2/6 (16), and P2X4/6 (17) receptors combine the original pharmacological and biophysical properties of their parent subunits. The huge diversity of native P2X receptors and their characteristics, often differing from those of the recombinant receptors, have been explained by the existence of heteromeric subunit compositions (18).

Despite these findings relating to recombinant receptors and the evidence that three subunits form both homomeric and heteromeric P2X receptors (6, 19, 20), two further points still need extensive clarification. First, only P2X2/3 (sensory ganglia) (21, 22), P2X1/5 (astrocytes) (23, 24), and probably P2X2/6 (neural stem cells) (25, 26) receptors were shown to occur under native conditions, whereas native P2X1/2, P2X1/4, and P2X4/6 receptors were hitherto not identified. Second, the subunit stoichiometry of functional P2X2/3 receptors appears to be 1:2 (27, 28), but for the residual heteromeric receptors, there are no comparable data available.

In the case of the P2X2/3 receptor, two homologous amino acid (AA)⁴ residues participating in agonist binding were

* This work was supported by Deutsche Forschungsgemeinschaft Grant FOR 748 and the Volkswagen Foundation.

[§] This article contains supplemental Figs. 1 and 2.

¹ Both authors contributed equally to this work.

² Both authors contributed equally to this work.

³ To whom correspondence should be addressed. Tel.: 49-341-9724614; Fax: 49-341-9724609; E-mail: Peter.Illes@medizin.uni-leipzig.de.

⁴ The abbreviations used are: AA, amino acid; NBS, nucleotide binding segment; hP2X2, hP2X3, and hP2X6, human P2X2, P2X3, and P2X6, respectively; 2-MeSATP, 2-methylthio-ATP; α,β -meATP, α,β -methylene-ATP; BN, blue native.

replaced individually with alanine to yield inactive mutants of P2X2 and P2X3 subunits; combination of the mutant P2X3 with wild-type (WT) P2X2 resulted in a non-functional receptor, whereas the opposite combination was fully active (28). Unfortunately, there were no accompanying biochemical data presented to confirm that the functionally silent AA mutants of P2X2 and P2X3 and their compositions with their WT counterparts still exhibited undisturbed trafficking behavior and were expressed at the cell surface.

In P2X receptors, instead of a few AA residues, four clusters of AAs, termed nucleotide binding domains (NBD1 to -4) (29) (here nucleotide binding segments, NBS1 to -4), were identified as possible docking places for ATP. NBS1 and -2 appear to be located at one subunit, whereas NBS3 and -4 are situated at the neighboring subunit (30) in accordance with the recently described crystal structure of the zebrafish P2X4 receptor (31).

The aim of the present experiments was to find out whether two heteromeric receptors (P2X2/3 and P2X2/6), where P2X2 combines with two different partners, have an obligatory subunit stoichiometry of 1:2 or whether the subunit stoichiometry may be variable. For this purpose, we used the ATP structural analogues 2-methylthio-ATP (2-MeSATP) and α,β -methylene-ATP (α,β -meATP) as well as non-functional mutants of P2X2 and P2X3 with a single Ala mutation in NBS1 to -4 each. Moreover, we also used homologous mutants of P2X6 to clarify the subunit stoichiometry of the P2X2/6 receptor. Electrophysiological measurements and Ca^{2+} imaging as well as protein labeling, purification, and PAGE suggested that P2X2/6 receptors consist of two P2X2 subunits and one P2X6 subunit and thereby differ from P2X2/3 receptors.

EXPERIMENTAL PROCEDURES

Culturing of HEK293 Cells—HEK293 cells were kept in Dulbecco's modified Eagle's medium also containing 4.5 mg/ml D-glucose (Invitrogen), 2 mM K-glutamine (Sigma-Aldrich), 10% fetal bovine serum (Invitrogen) at 37 °C and 10% CO_2 in humidified air.

Site-directed Mutagenesis and Transfection Procedures—The human P2X2 (hP2X2_A), hP2X3 (gift of J. N. Wood, University College, London, UK), and hP2X6 (gift of A. Surprenant, University of Manchester, Manchester, UK) cDNAs were subcloned at PstI and EcoRI restriction sites into pIRES2-EGFP (P2X3 and P2X6) or pIRES2-Ds-Red (P2X2) vectors from Clontech for independent expression of the respective P2X subunit and EGFP or Ds-Red, creating the pIR-P2X plasmid. All P2X subunit mutants were generated by introducing replacement mutations into the pIR-P2X construct using the QuikChange site-directed mutagenesis protocol from Stratagene according to the instruction manual. HEK293 cells were plated in plastic dishes (electrophysiology) or onto coverslips (Ca^{2+} imaging) 1 day before transient transfection. 0.5 μg of plasmid DNA (homomeric P2X2, P2X3, and P2X6 receptors; heteromeric P2X2/3 and P2X2/6 receptors, 1:2 ratio) or 0.75 μg of plasmid DNA (P2X2/6 receptors, 1:4 ratio) was combined with 10 μl of Polyfect reagent from Qiagen and 100 μl of Opti-MEM (Invitrogen).

Whole-cell Patch Clamp Recordings—Whole-cell patch clamp recordings were made after transient transfection of

HEK293 cells, at room temperature (20–22 °C), using an Axopatch 200B patch clamp amplifier (Molecular Devices) as described previously (30). Transfected HEK293 cells were searched for by means of a reverse differential interference contrast microscope with epifluorescent optics (Axiovert 100, Zeiss). The pipette solution contained 140 mM CsCl, 1 mM CaCl_2 , 2 mM MgCl_2 , 10 mM HEPES, and 11 mM EGTA, pH adjusted to 7.3 using CsOH. When 2-MeSATP was used as an agonist, GDP- β -S (300 μM) was also included, in order to eliminate the negative interaction between P2Y and P2X receptors in HEK293 cells (31). The external physiological solution contained 135 mM NaCl, 4.5 mM KCl, 2 mM CaCl_2 , 2 mM MgCl_2 , 10 mM HEPES, and 10 mM glucose, pH adjusted to 7.4 using NaOH. The pipette resistances were 3–6 megaohms. Holding potential values were corrected for the calculated liquid junction potential between the bath and pipette solution. All recordings were made at a holding potential of –65 mV. Data were filtered at 2 kHz with the built-in filter of the amplifier, digitized at 5 kHz, and stored on a laboratory computer using a Digidata 1440 interface and pClamp 10.2 software (Molecular Devices).

Drugs were dissolved in the external solution and locally superfused over single cells (detected by their EGFP and/or DS-Red fluorescence), using a rapid solution change system (SF-77B Perfusion Fast Step, Warner Instruments). Concentration-response curves were established by applying increasing concentrations of α,β -meATP or 2-MeSATP (both from Sigma-Aldrich) for 2 s. The intervals between applications were kept at 5 min throughout. Under these conditions, agonist responses were reproducible, with the exception of those to 2-MeSATP at HEK293-P2X3 cells; the marked desensitization at higher concentrations of 2-MeSATP (>3 μM) was in accordance with the reported long period of time required to regain 50% of control peak amplitude when determined with a paired-pulse protocol (32) (see also supplemental Fig. 1Ac, right).

The desensitization time constants (τ_{des1} and τ_{des2}) and the recovery of P2X3 receptors from desensitization were determined as described previously (supplemental Fig. 1Ac, left) (33). For the measurement of the recovery from desensitization, HEK293 cells were stimulated repetitively with α,β -meATP (30 μM ; 2-s pulses) with a progressive increase in the interpulse intervals. We measured the t_{50} value, which is the time needed to regain 50% of maximally recovered currents. Only the τ_{des1} values are indicated, because the rapid phase of desensitization appears to be the more relevant one.

Ca^{2+} Microfluorometry—HEK293 cells were loaded 2–3 days after transient transfection, with the Ca^{2+} -sensitive fluorescent dye Fura-2 acetoxymethyl ester (2.5 μM ; Sigma-Aldrich) at 37 °C for 1 h in culture medium. Cells plated onto coverslips were mounted into the superfusion chamber and placed on the stage of an inverted microscope (IX-70; Olympus) with epifluorescent optics and a cooled CCD camera (IMAGO; Till Photonics). Throughout the experiments, cells were continuously superfused at 0.8 ml/min by means of a roller pump with external solution. Intracellular Fura-2 was alternately excited at 340 and 380 nm, and the emitted light was measured at a wavelength of 510 nm. The Till Vision software (version 3.3, Till Photonics) was used for data acquisition, system control,

Subunit Stoichiometry of P2X Receptors

and, later, off-line analysis. The fluorescence ratio (340/380 nm) provides a relative measure of the cytosolic free Ca^{2+} concentration ($[\text{Ca}^{2+}]_i$).

For the determination of concentration-response relationships, α, β -meATP or 2-MeSATP was pressure-injected locally, by means of a computer-controlled DAD12 superfusion system (ALA Scientific Instruments, Inc.). The application time was 5 s, and the intervals between two subsequent agonist applications were kept, independent of the concentration used, at 15 min. α, β -meATP is a selective P2X1, P2X3, P2X1/2, P2X1/5, and P2X2/3 receptor agonist (34), which does not activate endogenous P2Y receptors of HEK 293 cells (35). In contrast, 2-MeSATP is a non-selective P2X/Y receptor agonist (34, 36), which may cause an increase of $[\text{Ca}^{2+}]_i$ through the activation of G_q protein-coupled P2Y₁ receptors (35). In order to account for this problem, concentration-response curves for 2-MeSATP were constructed at HEK293 cells transfected with P2X2 subunits, P2X6 subunits, or their mutants as well as on mock-transfected cells. $[\text{Ca}^{2+}]_i$ responses caused by 2-MeSATP after mock transfection were subtracted from those obtained after transfection with the respective subunit plasmids (Fig. 3C*b*) and yielded the $[\text{Ca}^{2+}]_i$ transients due to receptor stimulation only.

Expression of P2X2, P2X3, and P2X6 Receptors and Their Mutants in *Xenopus laevis* Oocytes—Oocyte expression plasmids harboring the cDNAs for N-terminally hexahistidine-tagged (His-tagged) hP2X2_A, hP2X3, or hP2X6 subunit have been described previously (12, 30). Replacement mutations or a StrepII affinity tag-encoding sequence 5' of the stop codon were introduced by QuikChange site-directed mutagenesis (Stratagene). Capped cRNAs were synthesized and injected in aliquots of 46 nl into collagenase-defolliculated *X. laevis* oocytes using a Nanoliter 2000 injector (World Precision Instruments) as described previously (37). For expression of the heteromeric P2X2/3 receptor, cRNAs for the P2X2 and P2X3 subunit were co-injected at a 1:2 ratio (w/w). For expression of the heteromeric P2X2/6 receptor, the cRNAs for the P2X2 and P2X6 subunit were co-injected at a 1:4 ratio (w/w). Oocytes were cultured at 19 °C in sterile oocyte Ringer's solution (90 mM NaCl, 1 mM KCl, 1 mM CaCl_2 , 1 mM MgCl_2 , and 10 mM HEPES, pH 7.4) supplemented with 50 $\mu\text{g}/\text{ml}$ gentamycin.

Two-electrode Voltage Clamp Electrophysiology—1–2 days after cRNA injection, current responses were evoked by 2-MeSATP (P2X2 and P2X2/6 receptors) or α, β -meATP (P2X2/3 receptors) as indicated at ambient temperature (21–24 °C), and recorded by conventional two-electrode voltage clamp with a Turbo TEC-05 amplifier (npi Electronics) at a holding potential of –60 mV as described previously (37). For concentration-response analysis, P2X receptor-mediated currents were induced in 60-s intervals by 10-s applications of increasing concentrations of the indicated agonist.

Protein Labeling, Purification, and PAGE—cRNA-injected oocytes were metabolically labeled by overnight incubation with L-[³⁵S]methionine (PerkinElmer Life Sciences) and, just before protein extraction, surface-labeled with the membrane-impermeable fluorescent dye Cy5 NHS ester (GE Healthcare) as described previously (38). Affinity-tagged proteins were purified by non-denaturing Ni^{2+} -NTA chromatography (Qiagen) or Strep-Tactin chromatography (IBA Germany) from

digitonin (1%, w/v) extracts of oocytes as indicated. The P2X receptors were released in the non-denatured state from the Ni^{2+} -NTA-Sepharose or the Strep-Tactin-Sepharose with elution buffer consisting of 1% (w/v) digitonin in 250 mM imidazole/HCl (pH 7.6) or 1% (w/v) digitonin in 0.1 M sodium phosphate buffer, pH 8.0, supplemented with 10 mM biotin, respectively. Native proteins were analyzed by blue native PAGE (BN-PAGE) as described previously (12, 39). Where indicated, samples were treated before BN-PAGE for 1 h at 37 °C with 0.1% (w/v) SDS to induce partial dissociation of P2X receptor complexes. To avoid quenching of the fluorescence by the Coomassie G250 dye, BN-polyacrylamide gels were destained prior to fluorescence imaging by repeated cycles of incubation in 50% (v/v) acetonitrile (Biosolve) supplemented with 25 mM ammonium carbonate as described previously (40). The destained polyacrylamide gel was repeatedly washed in 0.1 M sodium phosphate buffer, pH 8.0, and scanned wet by a Typhoon 9410 scanner (GE Healthcare) for fluorescence detection. For the subsequent visualization of the ³⁵S-labeled proteins, the BN-polyacrylamide gels were dried, exposed to a phosphor screen, and scanned by a PhosphorImager (Storm 820, GE Healthcare).

For reducing SDS-PAGE, proteins were denatured by incubation with SDS sample buffer containing 20 mM DTT for 15 min at 56 °C and electrophoresed in parallel with ¹⁴C-labeled molecular mass markers (Rainbow, Amersham Biosciences) on SDS-polyacrylamide gels (10% acrylamide). SDS-polyacrylamide gels were scanned wet with a fluorescence scanner (Typhoon 9410, GE Healthcare) for visualization of Cy5-labeled plasma membrane-bound proteins, and then we dried the gels for the subsequent detection of ³⁵S incorporation as described above.

The intensity of the fluorescent protein bands was quantified using the ImageQuant TL software version 7.0 (GE Healthcare). Images of polyacrylamide gels were prepared with ImageQuant TL for contrast adjustments. For better visibility of weak and strong protein bands, individual lanes from the same, but differently enhanced, ImageQuant image were cropped and positioned using Adobe Photoshop CS4. Microsoft PowerPoint 2003 was used for labeling. Each experiment was performed at least twice with equivalent results.

Homology Modeling—We modeled, based on the published crystal structure of the zebrafish P2X4 channel in its closed state (31), the extracellular loop and transmembrane areas of the hP2X2, hP2X3, and hP2X6 receptors. The software used was Modeler 9, version 7 (41). The alignment was determined by the align2D function, which also takes the secondary structure of the template into consideration. Homology modeling was made with the loop model function with high optimization settings. Visualization of the results was by VMD (42).

Data Analysis—Concentration-response curves for agonists were fitted by using a three-parametric Hill plot (SigmaPlot; SPSS). The figures show mean \pm S.E. values of *n* experiments. One-way analysis of variance followed by the Holm-Sidak post hoc test was used for multiple comparisons with a control group or multiple pairwise comparisons. The differences between two groups were evaluated by the normality test followed by the Student's *t* test or the rank sum test, as appropriate.

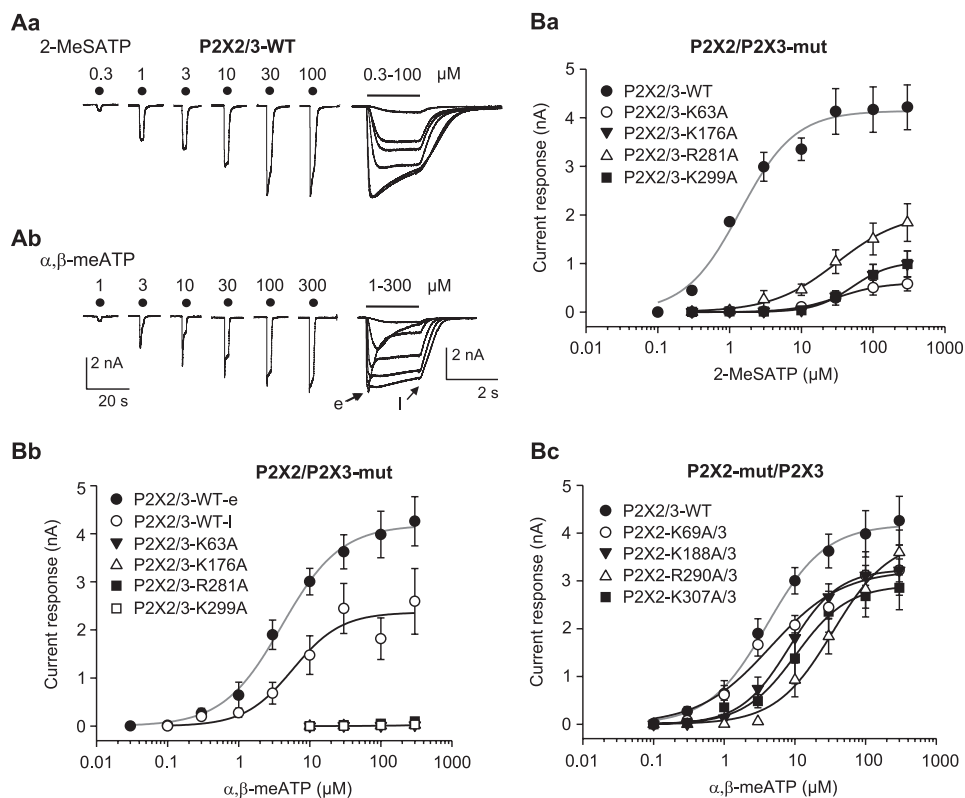


FIGURE 1. Current responses at wild-type (WT) hP2X2/3 receptors and at the combinations of mutant (mut) hP2X2 or hP2X3 subunits with their WT partners expressed in HEK293 cells. *A*, whole-cell currents induced by 2-MeSATP (*Aa*) or α,β -meATP (*Ab*; 0.3–100 μM) were recorded with the patch clamp technique at a holding potential of -65 mV. Increasing concentrations of the two agonists were locally superfused for 2 s with 5-min intervals (as indicated by filled circles or a horizontal bar), and the resulting currents were reproduced at two different time scales (note the divergent calibration bars on the right and left). α,β -meATP caused a rapidly desensitizing early current (*e*), followed by a more constant late current (*l*). *B*, concentration-response relationships constructed for 2-MeSATP (*Ba*) and α,β -meATP (*Bb* and *Bc*) at WT P2X2/3 receptors and their non-functional mutants, whose selected Lys and Arg residues were replaced by Ala. The concentration-response relationships at the WT homomeric or heteromeric receptor are shown in gray. Means \pm S.E. (error bars) of 5–8 experiments are shown. The Hill coefficients for the respective concentration-response curves at WT P2X2/3 receptors were as follows: 1.1 ± 0.2 (2-MeSATP); 1.1 ± 0.1 (α,β -meATP, early), 1.3 ± 0.5 (α,β -meATP, late). The E_{max} and EC_{50} values for the late α,β -meATP concentration-response curves at WT P2X2/3 receptors were $2,365 \pm 241$ pA and 5.7 ± 2.2 μM . For all further E_{max} and EC_{50} values as well as the exact number of experiments, see Table 1.

ate. A probability level of 0.05 or less was considered to reflect a statistically significant difference.

RESULTS

Patch Clamp Investigations in HEK293 Cells—Alanine-scanning mutagenesis in the four NBSs in hP2X3 showed that the conserved K63A, K176A, R281A, and K299A mutants did not react with α,β -meATP (300 μM) at all or responded with very small current amplitudes only (30). The inactivity of the homologous Ala or Cys mutants in P2X1, P2X2, and P2X4 with ATP as an agonist was demonstrated previously (see Refs. 19, 43, and 44).

Both α,β -meATP and 2-MeSATP (0.3–100 μM each) caused fast inward currents at the holding potential of -65 mV (supplemental Fig. 1, *Aa* and *Ab*). The current responses desensitized already during the 2-s application period with a rapid onset, which was similar both for α,β -meATP and 2-MeSATP (30 μM each) (supplemental Fig. 1*Ac*, left). However, the recovery from desensitization, which probably reflects the dissociation of the agonist from the receptor, was much slower for 2-MeSATP than for α,β -meATP (30 μM each) (supplemental Fig. 1*Ac*, right; $p < 0.05$). In accordance with this observation, the E_{max} value of the concentration-response curve for 2-MeSATP was smaller than that of α,β -meATP (supplemental Fig. 1*B*; $p <$

0.05). At the same time, the EC_{50} values of the two agonists also differed. In addition, we investigated the effect of 2-MeSATP (10–300 μM) at the mutant K176A and found that neither this agonist nor α,β -meATP (10–300 μM) caused any current response. Thus, K176A-hP2X3 was an inactive mutant irrespective of the type of agonist used.

In the following experiments, HEK293 cells transfected with WT or mutant P2X2 plus P2X3 cDNA plasmids, in a ratio of 1:2, were superfused with 2-MeSATP (0.1–300 μM) or α,β -meATP (0.03–300 μM) for 2 s every 5 min (Fig. 1, *A* and *B*). Although the E_{max} values and Hill coefficients of the concentration-response curves were comparable, the EC_{50} values of the two agonists differed from each other (Fig. 1, *A* and *B*, and Table 1; the peaks of the agonist-induced currents were evaluated at this stage). By keeping a 5-min interval between the applications of increasing 2-MeSATP concentrations, there was little desensitization within the 2-s application time (Fig. 1*Aa*). By contrast, with the same application protocol, α,β -meATP caused a rapid peak followed by a quasi-steady-state response (at the end of the 2-s superfusion period; Fig. 1*Ab*). Accordingly, a plot of the early peak response against the logarithmic α,β -meATP concentration resulted in a maximum of the curve (Table 1), which was higher than that obtained by plotting the late, quasi-steady-state current against the loga-

Subunit Stoichiometry of P2X Receptors

TABLE 1

Agonist sensitivities of P2X2, P2X3, P2X6, P2X2/3, and P2X2/6 receptors as well as of the combinations of the respective WT and mutant subunits expressed in HEK293 cells

Concentration-response curves for α,β -meATP or 2-MeSATP were determined by the whole-cell patch clamp method.

Receptor	Agonist	E_{\max}	EC_{50}	n
		μA	μM	
P2X2 WT	α,β -meATP		>300	6
P2X3 WT		4,891 \pm 85	2.1 \pm 0.1	7
P2X3-K176A			>300	6
P2X2/3 WT		4,182 \pm 93 ^a	4.1 \pm 0.4	8
P2X2/3-K63A			>300	6
P2X2/3-K176A			>300	6
P2X2/3-R281A			>300	6
P2X2/3-K299A			>300	6
P2X2-K69A/3		3,231 \pm 240 ^b	4.5 \pm 1.4	6
P2X2-K188A/3		3,245 \pm 45 ^b	8.4 \pm 0.4	7
P2X2-R290A/3		3,870 \pm 266	34.3 \pm 6.8 ^b	7
P2X2-K307A/3		2,911 \pm 101 ^b	10.3 \pm 1.2	7
P2X3 WT		2-MeSATP	1,811 \pm 131 ^a	0.9 \pm 0.3
P2X3-K176A			>300	6
P2X2 WT	6,448 \pm 29 ^a		14.4 \pm 0.2 ^a	10
P2X2-K69A			>300	6
P2X2-K188A			>300	6
P2X2-R290A			>300	6
P2X2-K307A			>300	7
P2X2/3 WT	4,140 \pm 139 ^a		1.4 \pm 0.2 ^c	6
P2X2/3-K63A	607 \pm 10 ^b		31.7 \pm 1.4 ^b	7
P2X2/3-K176A	1,042 \pm 32 ^b		51.5 \pm 3.5 ^b	8
P2X2/3-R281A	2,044 \pm 123 ^b		31.6 \pm 5.9 ^b	6
P2X2/3-K299A	1,042 \pm 32 ^b		51.5 \pm 3.5 ^b	6
P2X6 WT			>300	7
P2X2/6 WT	3,202 \pm 145 ^a		30.5 \pm 3.8	10
P2X2/6-K68A	3,385 \pm 144		26.5 \pm 3.2	6
P2X2/6-K191A	3,092 \pm 93		24.3 \pm 2.0	8
P2X2/6-R287A	4,488 \pm 98 ^b		18.2 \pm 1.1 ^b	6
P2X2/6-K305A	4,946 \pm 131 ^b		14.6 \pm 1.2 ^b	7
P2X2-K69A/6		>300	6	
P2X2-K188A/6		>300	6	
P2X2-R290A/6		>300	6	
P2X2-K307A/6		>300	6	

^a $p < 0.05$; statistically significant difference from the respective values at the WT P2X3 receptor (P2X3 WT).

^b $p < 0.05$; statistically significant difference from the respective values at the WT receptor.

^c $p < 0.05$; statistically significant difference from the respective EC_{50} value at the P2X3 WT receptor with α,β -meATP as the agonist.

rhythmic α,β -meATP concentration (Fig. 1Bb). However, the EC_{50} values of the “early” (Table 1) and “late” curves (Fig. 1Bb; $p > 0.05$) were similar. Thus, under our experimental conditions, a mixed P2X3-P2X2/3 initial response with a rapidly desensitizing P2X3 component was followed by a slowly desensitizing P2X2/3 component. It is noteworthy that the P2X2/3 currents could be investigated in isolation, when the receptor mutants were expressed in *X. laevis* oocytes (no early peak current because of strong residual desensitization at a drug-free interval of 1 min; supplemental Fig. 2Aa).

Then we demonstrated that although 2-MeSATP and α,β -meATP equally well activated the WT P2X2/3 receptor, 2-MeSATP still slightly stimulated the P2X2/3 heteromeric receptors containing WT P2X2 and mutant P2X3 (K63A, K176A, R281A, and K299A), whereas α,β -meATP had no effect at all at these complexes (Fig. 1, compare Ba and Bb, and Table 1). By contrast, when WT P2X3 was co-transfected together with the non-functional P2X2 mutants (K69A, K188A, R290A, and K307A) (Fig. 1Bc, and Table 1), at positions homologous to those targeted in the P2X3 mutants, the E_{\max} values of α,β -meATP at all heteromeric receptors only slightly decreased, and all EC_{50} values with the exception of P2X2-R290A/P2X3 did not change (Fig. 1Bc and Table 1). Thus, heteromeric

P2X2/3 receptors lost their original sensitivity toward agonists (α,β -meATP) or became much less sensitive (2-MeSATP) when the P2X3 subunits carried inactivating mutations but were only slightly affected when the P2X2 subunits carried the homologous mutations. These results can be explained by the assumption that one P2X2 subunit associates with two P2X3 subunits to form a P2X2/3 heteromer.

The following experiments were designed to clarify the subunit stoichiometry of P2X2/6 receptors. First of all, we transfected HEK293 cells with P2X6 subunits only and did not obtain any current response to 2-MeSATP (0.3–300 μM ; Fig. 2Aa). Subsequently, transfections were made by P2X2 and P2X6 in combinations of 1:2 and 1:4. The WT P2X2/6 receptors at the 1:2 and 1:4 transfection ratios exhibited decreasing sensitivities to 2-MeSATP; the respective E_{\max} values gradually decreased from the WT P2X2 to P2X2/6 (Fig. 2Aa; $p < 0.05$ each).

The slope of the current responses measured during the last 1 s of agonist application (out of the total 2-s duration) also differed between P2X2 and P2X2/6 ($p < 0.05$) (e.g. at 30 μM 2-MeSATP (inset to Fig. 2Ab; compare also the right panels of Fig. 2, Ca and Cb). At 2-MeSATP concentrations higher than 3 μM , there was an increasingly positive slope for the P2X2 curve up to a concentration of 100 μM , whereas the slope for the P2X2/6 (1:4 transfection ratio) curve was negative in this range of concentrations. The P2X2/6 (1:2 transfection ratio) curve was found to lie between the two other ones.

Gradual acidification of the bath solution from pH 7.4 to 5.4 only slightly increased the amplitudes of the 2-MeSATP (30 μM)-induced P2X2 but not P2X2/6 (1:2 transfection ratio; $p > 0.05$) currents, whereas there was a marked potentiation of the P2X2/6 (1:4 transfection ratio; $p < 0.05$) current amplitudes (Fig. 2, Ba–Bc). The sudden increase in amplitude with acidification observed with the transfection ratio 1:4, in contrast to the transfection ratio 1:2, may indicate that an excess of P2X6 over P2X2 is needed to generate a sufficient amount of P2X2/6 in the plasma membrane. Thus, all three experimental approaches prove that co-transfection with P2X2 and P2X6 subunits resulted in a presumably heteromeric receptor with functional properties differing from P2X2 only if the plasmid cDNA ratios amounted to 1:4. Therefore, this transfection procedure was used for all subsequent investigations.

Fig. 2, Ca and Cb, shows individual concentration response relationships for 2-MeSATP (1–300 μM) at homomeric P2X2 and heteromeric P2X2/6 receptors. As previously mentioned, the Ala replacement of four conserved AA residues in P2X2 at positions homologous to those targeted in P2X3 produced non-functional P2X2 receptors (Fig. 2D and Table 1). When WT P2X2 was used together with P2X6 mutants (K68A, K191A, R287A, and K305A) for co-transfecting HEK293 cells, the E_{\max} and EC_{50} values indicated higher activity for the P2X2/P2X6-R287A and -K305A mutants, when compared with the WT P2X2/6 receptor, but not for the P2X2/P2X6-K68A and -K191A mutants (Fig. 2Ea and Table 1). In contrast, the non-functional P2X2 mutant components abolished the 2-MeATP effects at the respective P2X2/6 receptors. The results can be explained by the assumption that two P2X2 subunits associate with one P2X6 subunit to form a P2X2/6 heteromer (see also

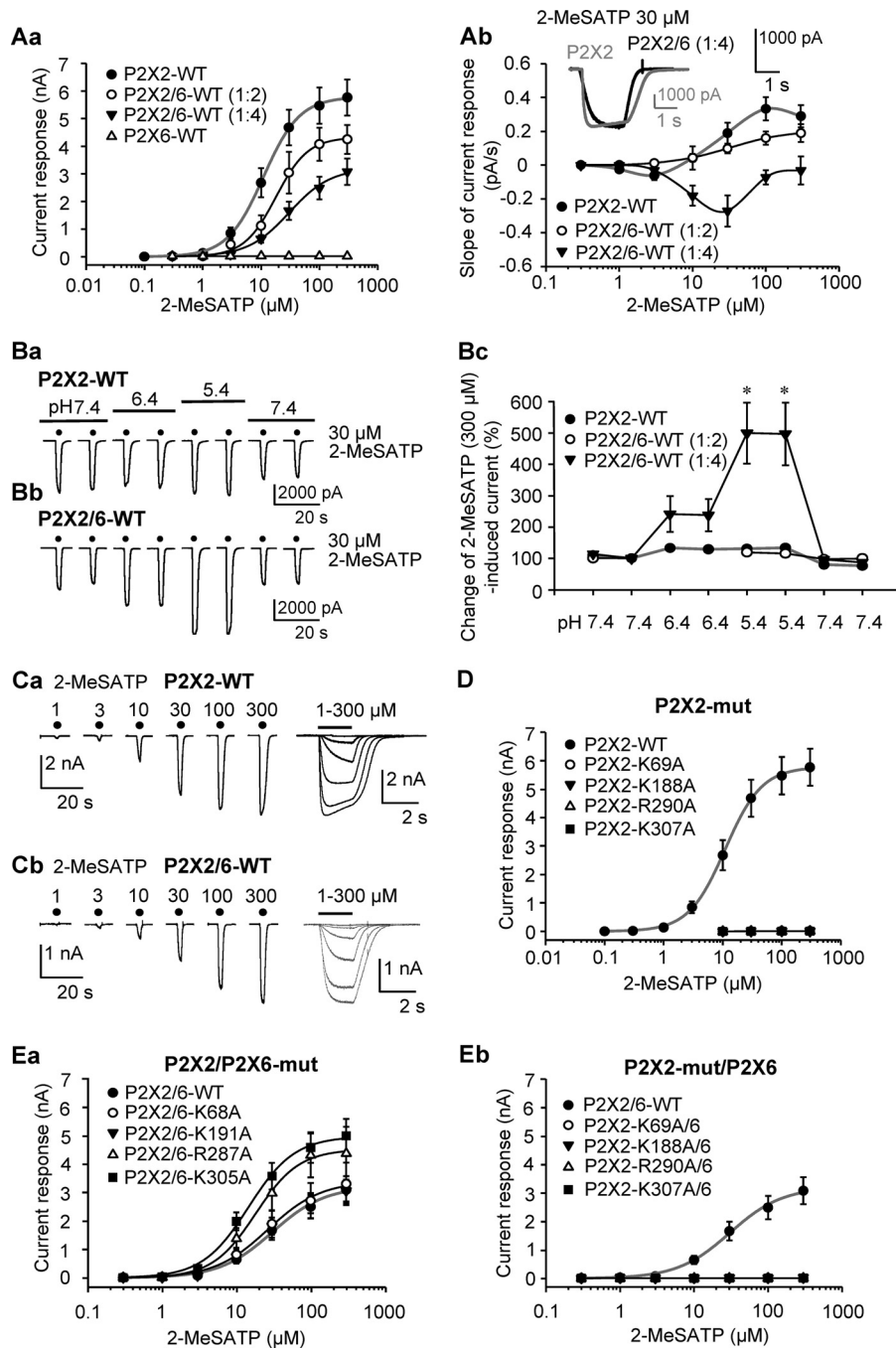


FIGURE 2. Current responses at WT hP2X2, hP2X6, and hP2X2/6 receptors and at the combinations of the respective WT and mutant subunits expressed in HEK293 cells. *A*, whole-cell currents at P2X2 or P2X2/6 (transfection ratios 1:2 or 1:4) receptors induced by 2-MeSATP (0.1–300 μM) were recorded with the patch clamp technique at a holding potential of -65 mV. Increasing concentrations of the two agonists were locally superfused for 2 s with 5-min intervals (for representative recordings and application protocol, see *C*). Shown are concentration-response relationships for the amplitude of the 2-MeSATP-induced current at WT P2X2 and WT P2X2/6 receptors (see transfection ratios in parentheses). Means \pm S.E. (error bars) of 6–10 experiments both in this panel and in all further experiments are shown. The Hill coefficients for the respective WT receptors with 2-MeSATP as an agonist were as follows: P2X2, 1.8 ± 0.1 ; P2X2/6 (1:4 transfection), 1.2 ± 0.1 . For the E_{max} and EC_{50} values as well as the exact number of experiments, see Table 1. The E_{max} and EC_{50} values as well as the Hill coefficients at the P2X2/6 receptor (1:2 transfection) were as follows: $4,327 \pm 116$ nA, 18.6 ± 1.4 μM , and 1.6 ± 0.2 (*Aa*). Shown are concentration-dependent changes of the slopes of the current responses from the beginning of the second s of application until its end (2-s applications in total; *Ab*). The inset shows the amplitude and shape of two representative scaled currents in response to 2-MeSATP (30 μM); the slopes of the current responses measured during the last 1 s of agonist application were 0.19 ± 0.06 pA/s for P2X2 and -0.27 ± 0.09 pA/s for P2X2/6. *B*, dependence of 2-MeSATP (30 μM)-induced current amplitudes on a gradual decrease of the external pH value from 7.4 to 5.4 for P2X2 and P2X2/6 receptors. Shown are representative recordings (*Ba* and *Bb*) and mean percentage changes with respect to the second current response (5-min intervals between agonist applications) at a normal pH of 7.4 (*Bc*). *, $p < 0.05$; statistically significant difference from the effect of 2-MeSATP at the P2X2 receptor. When the statistical comparison was with the predrug value of 100%, the percentage potentiation was by $33.6 \pm 7\%$ (P2X2; $p < 0.05$), $16.1 \pm 11.4\%$ (P2X2/6; transfection ratio 1:2; $p > 0.05$), and $397.2 \pm 99.6\%$ (P2X2/6; transfection ratio 1:4; $p < 0.05$). *C*, original recordings of current responses induced by increasing concentrations of 2-MeSATP at WT P2X2 (*Ca*) and WT P2X2/6 (*Cb*) receptors (indicated by filled circles or a horizontal bar). *D* and *E*, concentration-response relationships constructed for 2-MeSATP at WT and mutant (*mut*) P2X2 (*D*) or WT and mutant P2X2/6 (*E*) receptors; P2X2/6 contained either WT P2X2 and presumably non-functional mutants of P2X6 (*Ea*) or WT P2X6 and non-functional mutants of P2X2 (*Eb*). In the non-functional mutants, selected Lys and Arg residues were replaced by Ala at homologous sites also manipulated in the P2X3 subunits (Fig. 1*D*). The concentration-response relationships at the WT homomeric or heteromeric receptor are gray.

Subunit Stoichiometry of P2X Receptors

the respective oocyte voltage clamp measurements in supplemental Fig. 2, *Da* and *Db*).

Ca²⁺ Imaging in HEK293 Cells—In order to lend more support to our findings, we measured, in addition to the transmembrane current responses, also the [Ca²⁺]_i transients in HEK293 cells bearing P2X2, P2X3, P2X2/3, and P2X2/6 receptors. Whereas α,β -meATP (10–300 μM) caused a rapidly rising and, after its washout, also rapidly declining [Ca²⁺]_i response at homomeric P2X3 receptors (e.g. see Fig. 3*Ab*, *right*), similar concentrations of this agonist induced biphasic responses, slowly recovering to base line at heteromeric P2X2/3 receptors (Fig. 3*Aa*). 2-MeSATP (300 μM) at the P2X2/P2X3-K63A mutant and 2-MeSATP (10 μM) at the WT P2X2/3 receptor evoked [Ca²⁺]_i transients of practically undistinguishable shape (Fig. 3, *Aa* and *Ab*, *left*). It is noteworthy that although α,β -meATP is a selective P2X1, P2X3, P2X1/2, P2X1/5, and P2X2/3 receptor agonist without any activity at the endogenous P2Y receptors of HEK293 cells (see “Experimental Procedures”), its EC₅₀ value for [Ca²⁺]_i transients in HEK293 transfected with WT P2X2/3 receptors was higher than that for transmembrane currents ($p < 0.05$; compare Figs. 1 and 3). The Hill coefficients of the two concentration-response relationships also differed from each other ($p < 0.05$). At the moment, we have no unequivocal explanation for these discrepancies. However, we tentatively suggest that Ca²⁺ influx from the extracellular space may be slightly modified by Ca²⁺-induced Ca²⁺ release from the endoplasmic reticulum and simultaneous sequestration of [Ca²⁺]_i by its intracellular storage sites. In perfect agreement with the patch clamp investigations, Ala substitutions of the relevant AAs in the P2X3 component of the P2X2/3 receptor markedly depressed the α,β -meATP (10–300 μM)-induced current amplitudes (Fig. 3*Ba*). By contrast, replacement of the same AAs by Ala in the P2X2 component of this receptor complex had no major effect (Fig. 3*Bb*).

Because 2-MeSATP is a general P2X/P2Y receptor agonist, the amplitudes of the 2-MeSATP (0.3–300 μM)-induced [Ca²⁺]_i transients in mock-transfected HEK293 cells (mediated by endogenous P2Y receptors) were subtracted from those induced by this agonist in cells transfected with P2X2 or P2X2 plus P2X6 subunits (Fig. 3*Cb*, *left* and *right panels*; see “Experimental Procedures”). Interestingly, this time the [Ca²⁺]_i measurement yielded a lower EC₅₀ value ($p < 0.05$) but identical Hill coefficient ($p > 0.05$) of the 2-MeSATP concentration-response curve as the corresponding values obtained by patch-clamp recording (compare Figs. 1 and 3), a finding that also awaits explanation.

The biphasic [Ca²⁺]_i responses appear to be typical for WT P2X2 receptors (Fig. 3*Cb*, *left*) and heteromeric receptors containing this subunit (for P2X2/6, see Fig. 3*Ca*). Again in agreement with the patch clamp investigations, Ala substitutions of the relevant AAs in the P2X6 component of the P2X2/6 receptor had no major effect on the 2-MeSATP (10–300 μM)-induced [Ca²⁺]_i transients (Fig. 3*Da*), whereas replacement of the homologous AAs in the P2X2 component of this receptor were strongly inhibitory (Fig. 3*Db*).

Two-electrode Voltage Clamp Measurements in *X. laevis* Oocytes—The subunit composition of the above homomeric and heteromeric receptors and their expression at the cell sur-

face were investigated by biochemical methods in the non-mammalian *X. laevis* oocyte expression system. Therefore, it was important to prove that the functional data generated on HEK293 cells and *X. laevis* oocytes are basically identical.

In fact, in oocytes injected with cRNAs for P2X2, P2X3, and P2X6 receptor subunits, we made observations similar to those described for the mammalian cell line HEK293. Non-desensitizing current amplitudes were evoked both by α,β -meATP and 2-MeSATP (1–300 μM each) at P2X2/3 and P2X2/6 receptors, respectively (supplemental Fig. 2, *Aa* and *Ab*). When the P2X2/3 receptor complexes consisted of the P2X2 WT and P2X3 mutant subunits, the α,β -meATP (1–300 μM) current responses were greatly depressed (supplemental Fig. 2*Ca*). By contrast, the expression of the P2X3 WT subunit together with non-functional P2X2 subunits (see Fig. 2*D* and supplemental Fig. 2*B* for HEK293 cells and oocytes, respectively) only slightly displaced the α,β -meATP concentration-response curve of the WT P2X2/3 receptor to the right, indicating a moderate decrease in potency (supplemental Fig. 2*Cb*).

At P2X2/6 receptors, 2-MeSATP up to 300 μM failed to induce a notable current response at P2X2 mutant/P2X6 WT heteromers (supplemental Fig. 2*Db*), whereas the concentration-response curves of 2-MeSATP at P2X2 WT/P2X6 mutant heteromers were only modestly shifted to the left in comparison with those constructed at the WT P2X2/6 receptor (supplemental Fig. 2*Da*).

A shift of the extracellular pH from 7.4 to 5.4 depressed the E_{max} of the 2-MeSATP concentration-response curve from 34.0 ± 1.1 to $25.8 \pm 0.5 \mu\text{A}$ ($n = 6$ each; $p < 0.05$) and the EC₅₀ value from 4.6 ± 0.5 to $3.3 \pm 0.3 \mu\text{M}$ ($p < 0.05$) but did not change its Hill coefficient significantly. Such a decrease of ATP-activated inward currents at rat P2X2/6 receptors by a decrease of the external pH from 7.5 to 5.5 was described previously (16) and appears to be valid for the oocyte expression system but not for HEK293 cells (see Fig. 2*Bc*).

Assembly and Cell Surface Trafficking of P2X2/3 and P2X2/6 Receptors—To assess the impact of the point mutations on the assembly and cell surface expression, BN-PAGE and SDS-PAGE analysis was performed. Like the homomeric wild type and mutant P2X2 receptor (data not shown) and the P2X3 receptor (30), also all of the functionally impaired heteromeric P2X2/3 mutant receptors were capable of assembling to heterotrimers and appearing at the cell surface (Fig. 4*A*, *top*). The significantly larger mass of the P2X2 protomer of 72 kDa as compared with the 55 kDa of the P2X3 protomer is reflected by a clearly detectable retarded migration of the P2X2 protomer and homotrimer in the BN-PAGE (Fig. 4, *A* and *B*, *top*) and the SDS-PAGE (Fig. 4, *A* and *B*, *bottom*) gels, respectively. As expected, the heterotrimeric assemblies of P2X2 WT and P2X3 WT or P2X3 mutant subunits migrated at a lower molecular mass than the homotrimeric P2X2 and significantly above that of the homotrimeric P2X3 receptor, clearly indicating the formation of intermediate sized heteromeric assemblies consisting of P2X2 WT and P2X3 WT or P2X3 mutant subunits (Fig. 4*A*, *top*).

A physically stable interaction between P2X2 WT and P2X3 WT or P2X3 mutant subunits is also apparent from a co-purification assay, in which we co-expressed the His-P2X2-StrepII

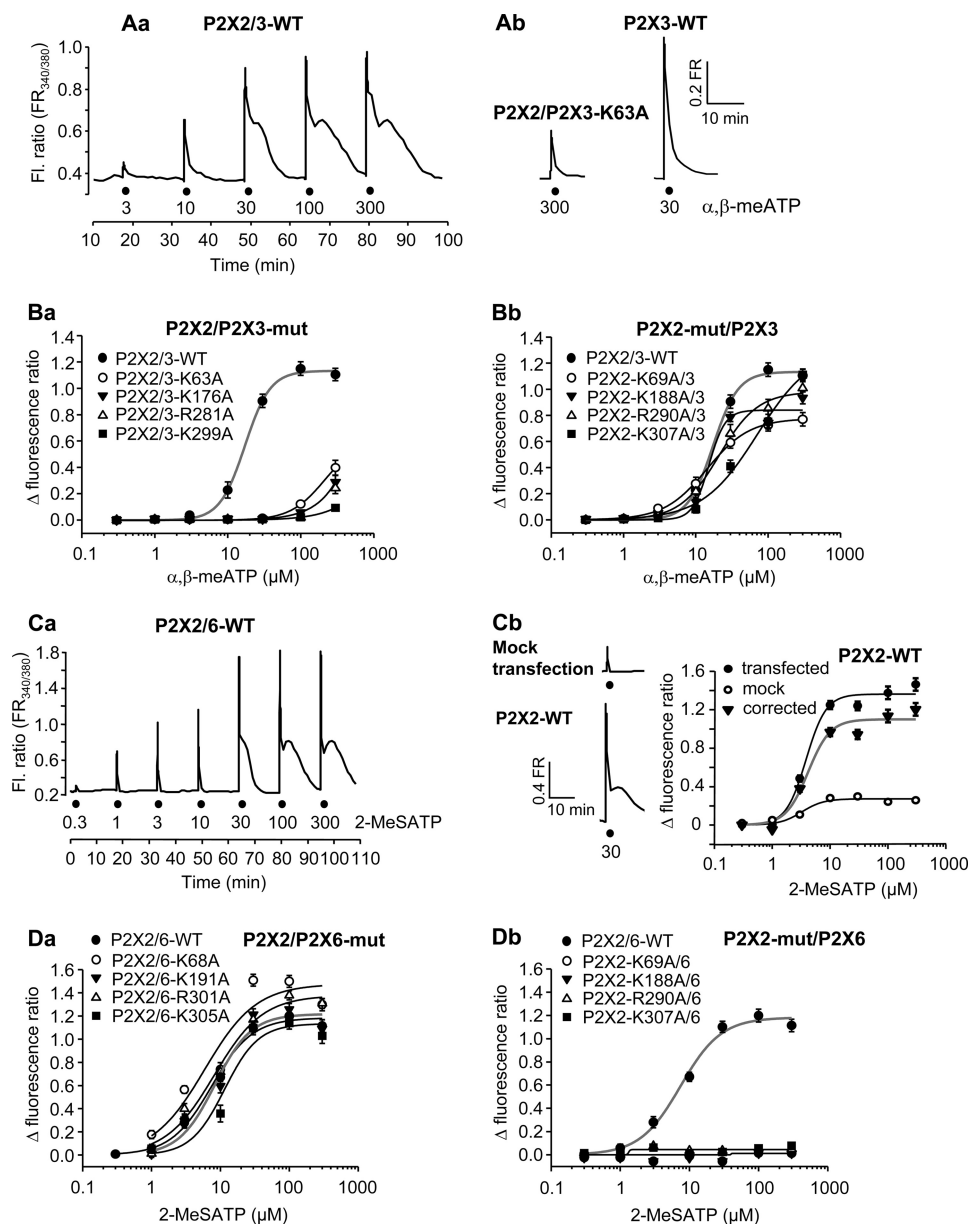


FIGURE 3. Increase of the cytosolic free Ca^{2+} concentration ($[Ca^{2+}]_i$) by Ca^{2+} influx from the extracellular space through wt-hP2X2, hP2X6, and hP2X2/6 receptors and through the combinations of the respective WT and mutant subunits expressed in HEK293 cells. A, Ca^{2+} imaging was carried out on HEK293 cells loaded by the fluorescence dye Fura-2 acetoxymethyl ester. The fluorescent ratio (*Fl. Ratio*; *FR*) provides a relative measure of $[Ca^{2+}]_i$. Increasing concentrations of 2-MeSATP (3–300 μM) were locally superfused for 5 s with 15-min intervals (as indicated by filled circles in the original recording shown). The shape and amplitude of the individual 2-MeSATP-induced $[Ca^{2+}]_i$ transients at WT P2X2/3 receptors (Aa) can be compared with the same parameters at the P2X2/P2X3-K63A mutant (Ab; left) and at the WT P2X3 receptor (Ab; right). B, concentration-response relationships constructed for α,β -meATP at P2X2/3 receptors containing either WT P2X2 and non-functional P2X3 subunits (Ba) or WT P2X3 and non-functional P2X2 subunits (Bb). Concentration-response curves at WT P2X2/3 receptors are also shown. C, original recording for a typical experiment with 2-MeSATP (0.3–300 μM) at WT P2X2/6 receptors. The shape and amplitude of the individual 2-MeSATP-induced $[Ca^{2+}]_i$ transients at WT P2X2/6 receptors (Ca) can be compared with the same parameters at the WT P2X2 receptor (Cb, bottom left) and in mock-transfected cells (Cb, top left). The 2-MeSATP-induced $[Ca^{2+}]_i$ transients measured in mock-transfected HEK293 cells were subtracted from the $[Ca^{2+}]_i$ transients measured in cells transfected with WT P2X2 receptors to yield the concentration-response curve of 2-MeSATP non-contaminated by the release of Ca^{2+} from intracellular pools (Cb, right). D, concentration-response relationships constructed for 2-MeSATP at P2X2/6 receptors, which contained either WT P2X2 and presumably non-functional mutants of P2X6 (Da) or WT P2X6 and non-functional mutants of P2X2 (Db). Concentration-response curves at WT P2X2/6 receptors are also shown. The concentration-response relationships at the WT homomeric or heteromeric receptors are gray. Shown are mean \pm S.E. of 19–42 experiments. The E_{max} and EC_{50} values as well as the Hill coefficients of the corrected WT concentration-response curves were as follows: P2X2/3 and α,β -meATP, 1.134 ± 0.021 , $17.2 \pm 0.9 \mu M$, and 2.5 ± 0.2 ; P2X2 and 2-MeSATP, 1.099 ± 0.072 , $4.1 \pm 0.9 \mu M$, and 2.3 ± 1.0 ; P2X2/6 and 2-MeSATP (1:4 transfection), 1.183 ± 0.043 , $7.4 \pm 0.9 \mu M$, and 1.5 ± 0.2 .

(a protein bearing a C-terminal, nine-AA StrepII tag in addition to the N-terminal hexahistidine tag) as a bait together with WT or mutant His-P2X3 as the prey. Purification using metal affinity chromatography or Strep-Tactin chromatography allowed us to verify the expression of the two proteins (Fig. 4A, bottom)

and to screen for the presence of co-purified His-P2X3 protein (Fig. 4A, bottom), respectively. His-P2X2-StrepII and WT or mutant His-P2X3 proteins could both be isolated by Ni^{2+} -NTA chromatography from the cells in which they were co-expressed. Purification by Strep-Tactin chromatography led to

Subunit Stoichiometry of P2X Receptors

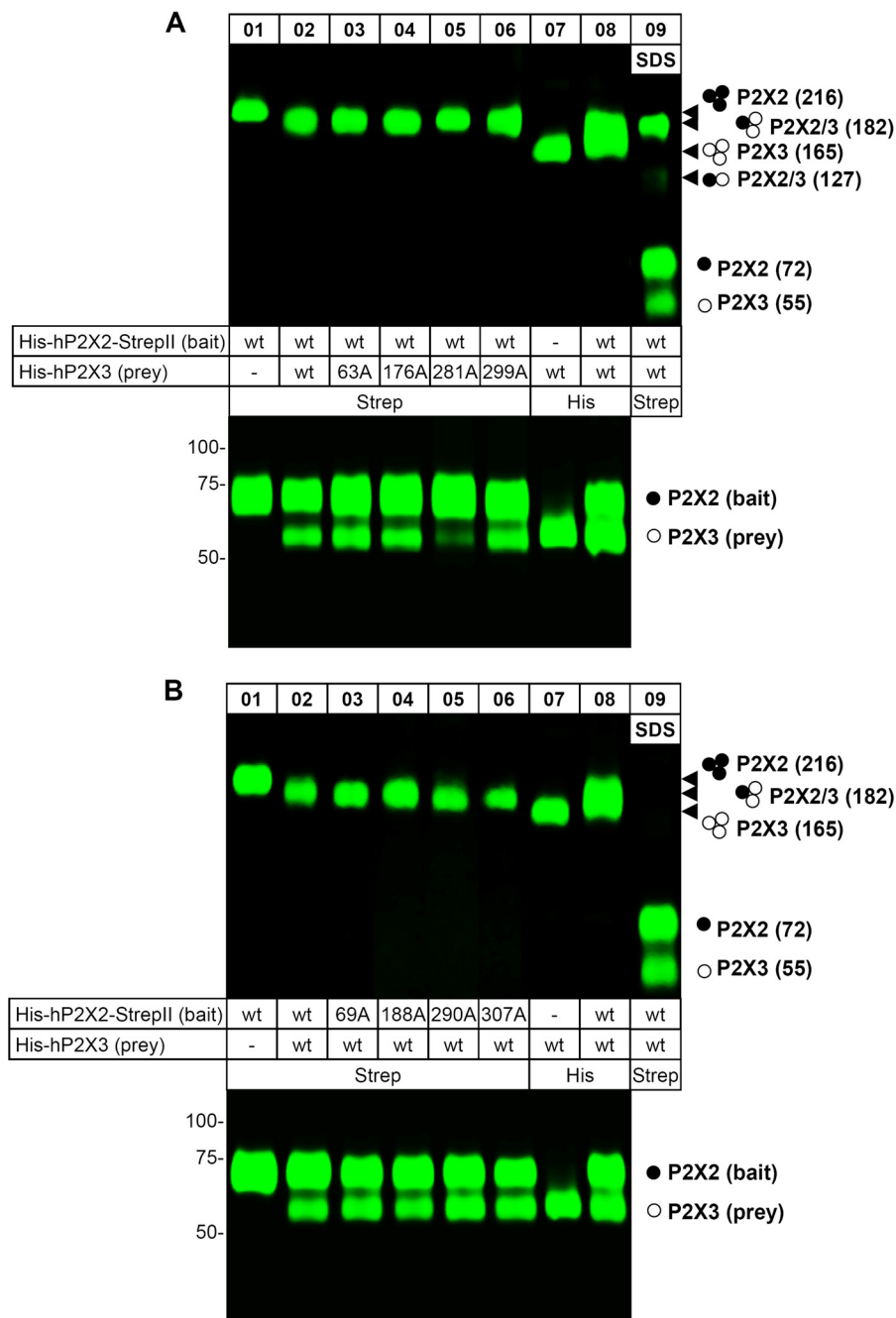


FIGURE 4. The hP2X3 subunit co-assembles and co-purifies with the hP2X2 subunit. The indicated proteins were purified under non-denaturing conditions from *X. laevis* oocytes by Ni^{2+} -NTA chromatography or Strep-Tactin chromatography, as indicated, resolved by BN-PAGE (top) or reducing SDS-PAGE (bottom), and visualized by Typhoon fluorescence scanning. Both the co-assembly of the WT His-hP2X2-StrepII subunit with the His-hP2X3 mutants (A) and the His-hP2X2-StrepII mutants with the WT His-hP2X3 subunit (B) are shown. The rightmost lane designated SDS, shows P2X2/3 protein migration after partial denaturation by a 1-h incubation with 0.1% SDS. The solid and open circles on the right indicate the numbers of hP2X2 and/or hP2X3 subunits, respectively, incorporated in the respective protein band. Migration positions of the corresponding trimeric assemblies are indicated by arrowheads. The numbers given in parenthesis on the right indicate the molecular masses calculated by referring to the SDS-PAGE-derived masses of 72 and 55 kDa for the hP2X2 and the hP2X3 protomer, respectively.

the co-isolation of the non-StrepII-tagged WT or mutant His-P2X3 proteins (Fig. 4A, bottom). When expressed alone, the His-P2X3 was not isolated (data not shown), indicating the absence of nonspecific binding of the His-P2X3 protein to the Strep-Tactin resin and thus confirming the suitability of this method for the analysis of P2X2 and P2X3 protein interaction.

Using the same biochemical techniques, we also found that the co-expression of P2X2 mutant subunits with P2X3 WT

subunits resulted in the formation of heterotrimeric receptors, as judged from the characteristic migration positions in the BN-polyacrylamide gel between those of the P2X2 and P2X3 homomers (Fig. 4B, top). Also, Strep-Tactin affinity purification of co-expressed mutant His-P2X2-StrepII proteins as bait together with WT His-P2X3 as the prey led to the co-isolation of the non-StrepII-tagged WT His-P2X3 proteins (Fig. 4B, bottom).

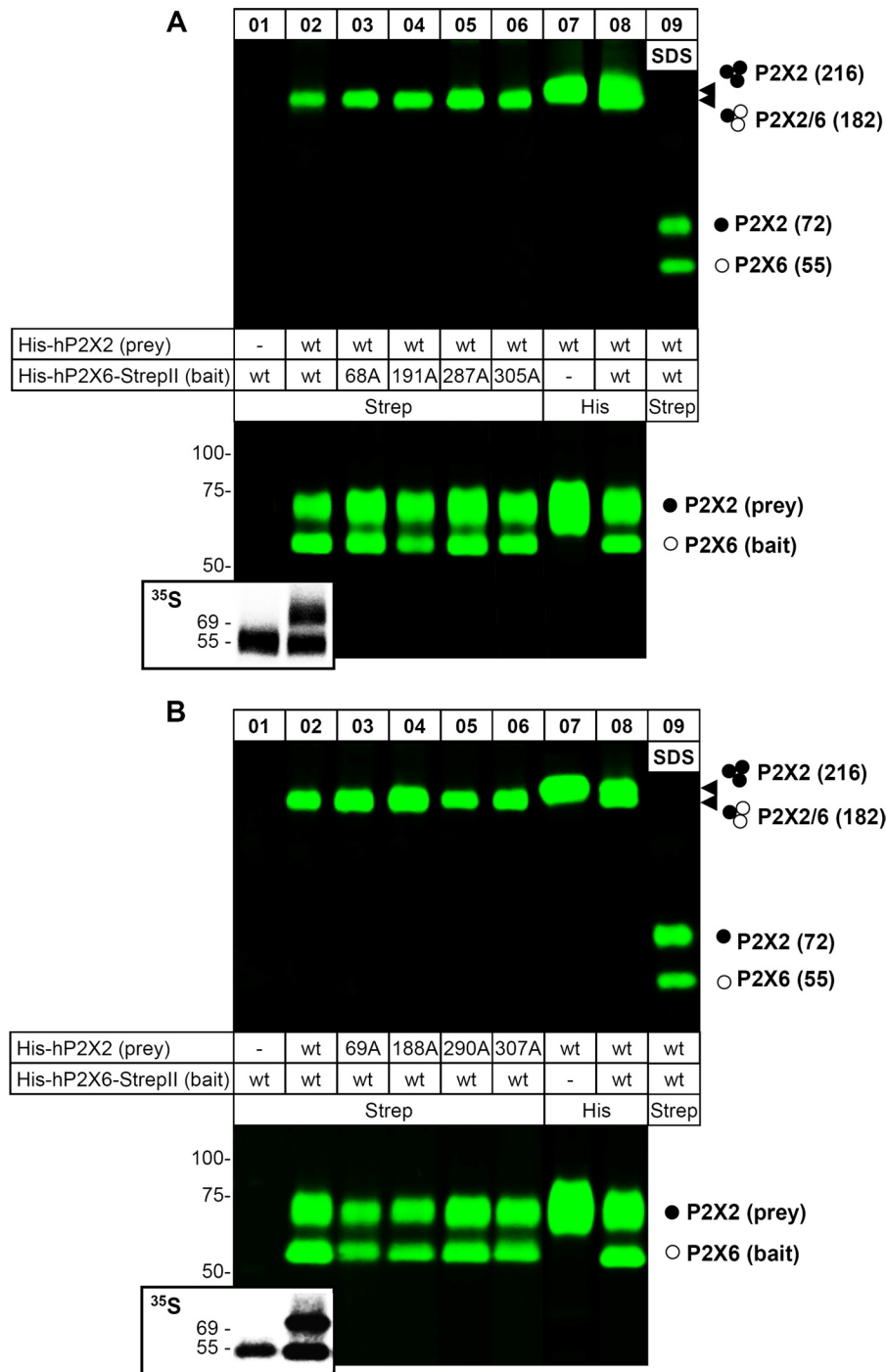


FIGURE 5. The hP2X2 subunit coassembles and co-purifies with the hP2X6 subunit. The indicated proteins were purified under non-denaturing conditions from *X. laevis* oocytes by Ni^{2+} -NTA chromatography or Strep-Tactin chromatography, as indicated, resolved by BN-PAGE (top) or reducing SDS-PAGE (bottom), and visualized by Typhoon fluorescence scanning. The inset of the bottom panel shows the total protein forms from corresponding lanes by [^{35}S]methionine incorporation. Both the co-assembly of the WT His-hP2X2 subunit with the His-hP2X6-StrepII mutants (A) and the His-hP2X2 mutants with the WT His-hP2X6-StrepII subunit (B) are shown. The rightmost lane, designated SDS, shows P2X2/6 protein migration after partial denaturation by a 1-h incubation with 0.1% SDS. The solid and open circles on the right indicate the numbers of hP2X2 and/or hP2X6 subunits, respectively, incorporated in the respective protein band. Migration positions of the corresponding trimeric assemblies are indicated by arrowheads. The numbers given in parenthesis on the right indicate the molecular masses calculated by referring to the SDS-PAGE-derived masses of 72 and 55 kDa for the hP2X2 and the hP2X6 protomer, respectively.

Oocyte-expressed heteromeric P2X2/6 receptors were also analyzed biochemically. Consistent with previous data (12), the singly expressed P2X6 subunit could be detected in the [^{35}S]methionine-labeled total form (Fig. 5, A and B, inset of bottom) but was absent at the plasma membrane (Fig. 5, A and

B, lane 1). However, upon co-expression of the WT or a mutant His-hP2X6-StrepII subunit with the WT His-hP2X2 subunit, a distinct protein band was observed in the BN-polyacrylamide gel that migrated with a lower mass than that of the homomeric P2X2 receptor (Fig. 5A, top). The reduced mass of this protein

Subunit Stoichiometry of P2X Receptors

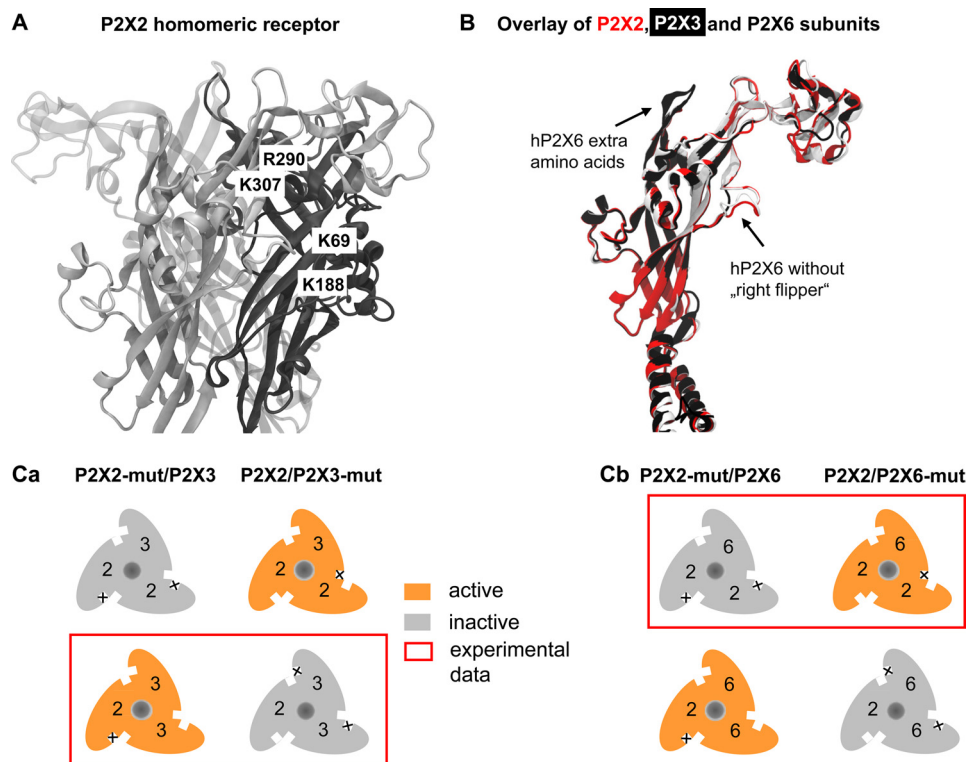


FIGURE 6. Homology model of the P2X2 receptor and of various P2X receptor subunits; schematic representation of the subunit stoichiometry of P2X2/3 and P2X2/6 receptors. A, binding-relevant Lys and Arg residues (Arg²⁹⁰, Lys³⁰⁷, Lys⁶⁹, and Lys¹⁸⁸; P2X2 numbering) of the homomeric hP2X2 receptor. Individual subunits are shown as *black*, *dark gray*, and *light gray* loops. Arg²⁹⁰ and Lys³⁰⁷ are situated at one subunit, and Lys⁶⁹ and Lys¹⁸⁸ are located at the neighboring one. The four AA residues are parts of one of the three agonist binding pouches of the P2X2 receptor. B, overlay of P2X2 (*red*), P2X3 (*light gray*), and P2X6 (*black*) subunits. The *right flipper* of the dolphin-like structure of these subunits is missing in P2X6. C, summary schematic showing the assumed subunit stoichiometry of (P2X2)₁/(P2X3)₂ (Ca) and (P2X2)₂/(P2X6)₁ (Cb). The experimental data obtained by co-expressing WT P2X2, P2X3, and P2X6 subunits and their non-functional mutants with the respective subunit partners supported the above assumption.

band can easily be reconciled with a P2X2/6 heteromer co-assembled of the larger 72-kDa P2X2 subunit and the smaller 55-kDa P2X6 subunit. The presence of the P2X6 subunit in this protein band could be demonstrated by denaturing treatment with 0.1% SDS, which led to the dissociation into two polypeptides, the larger P2X2 and the smaller P2X6 subunit (Fig. 5A, *lane 9, top*). The mass difference of these two polypeptides is also apparent from dissociation of the WT P2X2/6 trimeric protein complex in SDS-PAGE analysis (Fig. 5A, *bottom*).

Strep-Tactin affinity purification of co-expressed WT or mutant His-P2X6-StrepII proteins with WT His-P2X2 as the bait and the prey, respectively, led to the co-isolation of the non-StrepII-tagged WT His-P2X2 protein (Fig. 5A, *bottom*). Co-expression of P2X2 mutant subunits with P2X6 WT subunits resulted also in the formation of heterotrimeric receptors, as evident from the characteristic mobility shift in the BN-polyacrylamide gel toward a lower mass (Fig. 5B, *top*). Also, Strep-Tactin affinity purification of co-expressed WT His-P2X6-StrepII proteins with mutant His-P2X2 as bait and prey, respectively, led to the co-isolation of the non-StrepII-tagged mutant His-P2X2 proteins (Fig. 5B, *bottom*).

Homology Modeling of hP2X2 Receptor and of hP2X2, hP2X3, and hP2X6 Subunits; Schematic Representation of Subunit Stoichiometry of P2X2/3 and P2X2/6 Receptors—Using the published x-ray structure of the zebrafish P2X4 (31) as a template, we homology-modeled the hP2X2 receptor. The individual subunits are shown as *black*, *dark gray*, and *light gray* loops. The

aromatic AA residues replaced by Ala and thereby yielding non-functional mutants are indicated in Fig. 6A; they are located pairwise (Arg²⁹⁰-Lys³⁰⁶ and Lys⁶⁹-Lys¹⁸⁸) at two adjacent subunits and participate in the formation of a binding pocket. The overlay of the P2X2, P2X3, and P2X6 subunits shows that P2X6 does not contain the AAs forming the right flipper of the dolphin shaping all other subunits (Fig. 6B) (19, 31). In addition, P2X6 contains a series of extra AAs between the head and the left flipper.

A summary schematic shows our conclusions. In theory, two subunit stoichiometries are conceivable for the P2X2/P2X3 heterotrimer; 1:2 or 2:1 (Fig. 6C). Because our experiments indicated a loss of function only in the WT P2X2/P2X3 mutant combination (see the *framed assembly* in Fig. 6Ca), the 1:2 stoichiometry is compatible with the present findings. By contrast, for the P2X2/P2X6 heterotrimer, a loss of function was found only in the P2X2 mutant/WT P2X6 combination (see the *framed assembly* in Fig. 6Cb); therefore, in this case the combination 2:1 is compatible with the present findings.

DISCUSSION

The three-subunit composition of homomeric and heteromeric P2X receptors was originally suggested on the basis of biochemical data, including co-immunoprecipitation (6, 7) and BN-PAGE analysis as well as chemical cross-linking of subunits (12, 39). More recently, it was pointed out that co-immunopre-

cipitation may not be able to differentiate between receptor hetero-oligomers and two individual homo-oligomeric receptors closely interacting in the cell membrane (for the supposed P2X4/7 receptor, see Refs. 45 and 46). At the present time, a wealth of data supply compelling evidence for the fact that three subunits form a functional P2X receptor. Our experiments were designed to investigate the subunit composition of two neuronal heteromeric P2X receptors, composed of P2X2 and another partner (P2X3 or P2X6).

α,β -meATP activates recombinant, rapidly desensitizing P2X1 and P2X3 but not slowly desensitizing P2X2 receptors (6, 20, 34). Trinitrophenyl-ATP blocked P2X1, P2X2, and P2X2/3 receptors equally well; by contrast, diinosine pentaphosphate inhibited P2X1 receptors with a much higher affinity than P2X3 receptors (47, 48). Eventually, the selective P2X3 antagonist A-317491 exhibits comparable activities in blocking P2X2 and P2X2/3 receptors (34). Thus, P2X2/3 receptors have a ligand sensitivity resembling that of homomeric P2X3 receptors and non-desensitizing gating characteristics resembling those of homomeric P2X2 receptors (15, 49).

The situation with P2X2/6 receptors appears to be much more complex. Although co-immunoprecipitation identified P2X2 and P2X6 as possible partners for generating hetero-oligomeric complexes (10), and an oocyte expression study meticulously searched for differences between singly injected P2X2 and co-injected P2X2 and P2X6 to yield P2X2/6 (16), most differences were rather modest. It was reported that, in contrast to currents through P2X2 receptors, those through P2X2/6 receptors 1) were of smaller amplitude; 2) were sometimes biphasic and occasionally showed two phases of current decay; and 3) exhibited minor differences in their agonist and antagonist sensitivities. However, a property that unequivocally distinguished the two receptors was their opposite modulation by extracellular pH. Whereas P2X2 currents were increased after acidification of the bath solution (50), P2X2/6 currents were depressed under the same conditions (16).

It is noteworthy that only some (51) and not all groups of scientists were able to detect functional homomeric P2X6 receptors in the cell membrane (52). The reason for this discrepancy might be that P2X6 receptors either do not pass the quality check of the endoplasmic reticulum (53, 54), or if they do so, only in a partially glycosylated and non-functional form (55). Further glycosylation may result in a gain of function for some of the receptors inserted into the plasma membrane. These results perfectly agree with our own findings; homomeric P2X6 receptors failed to express at the plasma membrane of HEK293 cells.

The first part of our study confirmed and extended the observations of North and colleagues (28) by co-expressing WT P2X2 or WT P2X3 with the non-functional mutant counterparts of these subunits. In addition to the P2X3 mutants K63A and K299A situated at neighboring receptor subunits, which may interfere with binding as well as gating of the channel, because their positions are adjacent to the transmembrane segments 1 and 2 forming the channel pore, two additional mutants (K176A and R281A), being less likely to interfere with gating, were also used in the present study. We found by utilizing both HEK293 cells and oocytes as expression systems that a combination of the WT P2X2 with mutated P2X3 subunits

(chosen from non-functional Ala mutants introduced in any of the four NBSs) (29) strongly inhibited or even abolished the current response to α,β -meATP, whereas the opposite combination of WT P2X3 with mutated P2X2 subunits had very little effect. Consistent with data published previously (28) these results clearly demonstrate a $(P2X2)_1/(P2X3)_2$ stoichiometry of heteromeric P2X2/3 channels, as illustrated in Fig 6Ca. As a correlate of the cationic fluxes induced by P2X2/3 receptor activation, $[Ca^{2+}]_i$ transients were also measured and yielded similar data. Further, we asked ourselves whether this observation might be true only when the P2X3-selective α,β -meATP is used (28), which occupies the agonist binding pouches between the P2X3/P2X3 and P2X2/P2X3 subunits but most probably not that one lying at the interface of the P2X2/P2X2 subunit (Fig. 6 Ca). For this purpose we applied also 2-MeSATP, which is an agonist both at homomeric P2X2 and P2X3 receptors and therefore occupies the binding sites of any of the participating receptor subunits. Thereby, it was possible to confirm that the observed phenomenon is agonist-independent.

In the second part of our study, we attempted to strengthen the hypothesis that the P2X6 subunit as a constituent of the P2X2/6 receptor complex is able to modify the original P2X characteristics, despite not being able to form a functional homomeric receptor by itself. In a mammalian cell line, the ratio of the P2X2 and P2X6 protein in P2X2/6 was either 4.1:1 or 1:2.5, depending on the ratio of the P2X2 and P2X6 plasmid cDNAs used for transfection (1:1 and 1:4) (56). However, there were no functional measurements accompanying this biochemical and atomic force microscopy investigation. We varied the plasmid cDNA ratios of the P2X2 and P2X6 subunits in the transfection reagent between 1:2 and 1:4 (the maximum ratio tested by Barrera *et al.*) (56). Indication of the formation of P2X2/6 heteromeric receptors with characteristics clearly different from those of P2X2 homomeric receptors (lower maximum current amplitude, no run-down of the current response during a 2-s application period, marked dependence of the current amplitude on the external pH) was found only at the higher transfection ratio of 1:4. A combination of the WT P2X2 subunit with P2X6 subunits mutated at sites homologous to those proven to yield non-functional P2X2 and P2X3 receptors did not alter the current response to 2-MeSATP, whereas the opposite combination of WT P2X6 with mutant P2X2 subunits resulted in non-functional receptors. Of course it cannot be excluded that at still higher transfection ratios than used by us (1:>4), P2X2/6 receptor channels with the reverse stoichiometry are formed; however, the functionality of these channels still awaits confirmation (56). In the present experiments, only P2X2/6 channels containing a minimum of two unmutated ATP binding sites were functional (Fig. 6Cb), as was the case also with the P2X2/3 heteromer (Fig. 6Ca). Therefore, a $(P2X2)_2/(P2X6)_1$ stoichiometry is the most likely one to occur.

The measurement of $[Ca^{2+}]_i$ transients caused by 2-MeSATP fully confirmed these results. In addition, our two-electrode voltage clamp data generated in *X. laevis* oocytes expressing P2X2/6 were almost identical to those obtained in the HEK293 system; the only difference was the opposite pH sensitivity of the P2X2/6 heteromer.

Subunit Stoichiometry of P2X Receptors

To exclude the possibility that the non-functional phenotype of the alanine replacement mutants within the ATP binding site originates from deficits in trimeric assembly or cell surface trafficking rather than a change in agonist action, biochemical analysis of oocytes expressing the corresponding WT and mutant P2X receptor channels was performed. Our results show that all mutants were capable of proper trimeric assembly and displayed unaltered plasma membrane trafficking. This view is further supported by the Strep-Tactin co-purification assay, which showed that all of the mutants were able to interact physically with the respective reciprocal WT subunit. Because His-P2X6-StrepII subunits reached the plasma membrane only as integral parts of the P2X2/6 heteromer (Fig. 6, A and B, *bottom*), affinity purification via the P2X6-StrepII subunit as bait (and non-Strep-tagged P2X2 as the prey) enabled us to isolate exclusively the P2X2/6 heteromer. Quantification of the relative abundance of the plasma membrane form of P2X2 and P2X6 subunits in SDS-PAGE analysis yielded a 2:1 ratio, thus also suggesting a $(P2X2)_2/(P2X6)_1$ stoichiometry.

The null hypothesis predicts that at a 1:1 protein expression ratio after transfection with two different subunits, the channel ratios for P2XA and P2XB should be 1:3:3:1 for $(P2XA)_3$, $(P2XA)_2/(P2XB)_1$, $(P2XA)_1/(P2XB)_2$, and $(P2XB)_3$; these ratios change to 1:6:12:8 and to 1:12:48:64, when the protein expression ratios are modified to 1:2 (P2X2-P2X3) and 1:4 (P2X2-P2X6), respectively. Although we did not determine the actual expression of the three receptor proteins, for P2X2/3 the subunit composition generated under the conditions of the present experiments will be by the highest likelihood $(P2X2)_1/(P2X3)_2$. Both the electrophysiological and biochemical measurements supported the existence of this preferential subunit composition in the cell membrane and its ability to respond to P2X agonists; the other possible heteromer was apparently not expressed. However, P2X2 assembled with P2X6 according to a stoichiometry of 2:1, which was not compatible with a random process of association. Nevertheless, the only subunit combination observed in the plasma membrane was $(P2X2)_2/(P2X6)_1$, which was also supported by electrophysiological measurements. Hence, recognition sites between P2X2 and its partners rather than random association may govern the subunit composition of the receptor trimers. In conclusion, P2X2 was a dominant subunit in the P2X2/6 heteromer only, and already two binding sites of the three possible ones were sufficient to allow P2X2/3 and P2X2/6 to react with their agonists (also see Refs. 32, 57, and 58).

Acknowledgments—We are most grateful to Professor Richard A. North for critically reading a previous version of the manuscript. The expert methodological support of Maria Kowalski, Nick Helms, and Gregor Pagel is gratefully acknowledged.

REFERENCES

- Griffon, N., Büttner, C., Nicke, A., Kuhse, J., Schmalzing, G., and Betz, H. (1999) Molecular determinants of glycine receptor subunit assembly. *EMBO J.* **18**, 4711–4721
- Klausberger, T., Sarto, I., Ehya, N., Fuchs, K., Furtmüller, R., Mayer, B., Huck, S., and Sieghart, W. (2001) Alternate use of distinct intersubunit contacts controls GABA_A receptor assembly and stoichiometry. *J. Neurosci.* **21**, 9124–9133
- Zhou, Y., Nelson, M. E., Kuryatov, A., Choi, C., Cooper, J., and Lindstrom, J. (2003) Human $\alpha 4\beta 2$ acetylcholine receptors formed from linked subunits. *J. Neurosci.* **23**, 9004–9015
- Mansour, M., Nagarajan, N., Nehring, R. B., Clements, J. D., and Rosenmund, C. (2001) Heteromeric AMPA receptors assemble with a preferred subunit stoichiometry and spatial arrangement. *Neuron* **32**, 841–853
- Schüler, T., Mesic, I., Madry, C., Bartholomäus, I., and Laube, B. (2008) Formation of NR1/NR2 and NR1/NR3 heterodimers constitutes the initial step in *N*-methyl-D-aspartate receptor assembly. *J. Biol. Chem.* **283**, 37–46
- North, R. A. (2002) Molecular physiology of P2X receptors. *Physiol. Rev.* **82**, 1013–1067
- Egan, T. M., Cox, J. A., and Voigt, M. M. (2004) Molecular structure of P2X receptors. *Curr. Top. Med. Chem.* **4**, 821–829
- Roberts, J. A., Vial, C., Digby, H. R., Agboh, K. C., Wen, H., Atterbury-Thomas, A., and Evans, R. J. (2006) Molecular properties of P2X receptors. *Pflugers Arch.* **452**, 486–500
- Köles, L., Fürst, S., and Illes, P. (2007) Purine ionotropic (P2X) receptors. *Curr. Pharm. Des.* **13**, 2368–2384
- Torres, G. E., Egan, T. M., and Voigt, M. M. (1999) Hetero-oligomeric assembly of P2X receptor subunits. Specificities exist with regard to possible partners. *J. Biol. Chem.* **274**, 6653–6659
- Haines, W. R., Torres, G. E., Voigt, M. M., and Egan, T. M. (1999) Properties of the novel ATP-gated ionotropic receptor composed of the P2X1 and P2X5 isoforms. *Mol. Pharmacol.* **56**, 720–727
- Aschrafi, A., Sadtler, S., Niculescu, C., Rettinger, J., and Schmalzing, G. (2004) Trimeric architecture of homomeric P2X2 and heteromeric P2X1+2 receptor subtypes. *J. Mol. Biol.* **342**, 333–343
- Nicke, A., Kerschensteiner, D., and Soto, F. (2005) Biochemical and functional evidence for heteromeric assembly of P2X1 and P2X4 subunits. *J. Neurochem.* **92**, 925–933
- Torres, G. E., Haines, W. R., Egan, T. M., and Voigt, M. M. (1998) Co-expression of P2X1 and P2X5 receptor subunits reveals a novel ATP-gated ion channel. *Mol. Pharmacol.* **54**, 989–993
- Lewis, C., Neidhart, S., Holy, C., North, R. A., Buell, G., and Surprenant, A. (1995) Coexpression of P2X2 and P2X3 receptor subunits can account for ATP-gated currents in sensory neurons. *Nature* **377**, 432–435
- King, B. F., Townsend-Nicholson, A., Wildman, S. S., Thomas, T., Spyer, K. M., and Burnstock, G. (2000) Coexpression of rat P2X2 and P2X6 subunits in *Xenopus* oocytes. *J. Neurosci.* **20**, 4871–4877
- Lê, K. T., Babinski, K., and Séguéla, P. (1998) Central P2X4 and P2X6 channel subunits coassemble into a novel heteromeric ATP receptor. *J. Neurosci.* **18**, 7152–7159
- Nörenberg, W., and Illes, P. (2000) Neuronal P2X receptors. Localization and functional properties. *Naunyn-Schmiedeberg's Arch. Pharmacol.* **362**, 324–339
- Browne, L. E., Jiang, L. H., and North, R. A. (2010) New structure enlivens interest in P2X receptors. *Trends Pharmacol. Sci.* **31**, 229–237
- Coddou, C., Yan, Z., Obsil, T., Huidobro-Toro, J. P., and Stojilkovic, S. S. (2011) Activation and regulation of purinergic P2X receptor channels. *Pharmacol. Rev.* **63**, 641–683
- Burnstock, G. (2006) Purinergic P2 receptors as targets for novel analgesics. *Pharmacol. Ther.* **110**, 433–454
- Wirkner, K., Sperlagh, B., and Illes, P. (2007) P2X3 receptor involvement in pain states. *Mol. Neurobiol.* **36**, 165–183
- Lalo, U., Pankratov, Y., Wichert, S. P., Rossner, M. J., North, R. A., Kirchhoff, F., and Verkhratsky, A. (2008) P2X1 and P2X5 subunits form the functional P2X receptor in mouse cortical astrocytes. *J. Neurosci.* **28**, 5473–5480
- Palygin, O., Lalo, U., Verkhratsky, A., and Pankratov, Y. (2010) Ionotropic NMDA and P2X1/5 receptors mediate synaptically induced Ca^{2+} signaling in cortical astrocytes. *Cell Calcium* **48**, 225–231
- Majumder, P., Trujillo, C. A., Lopes, C. G., Resende, R. R., Gomes, K. N., Yuahasi, K. K., Britto, L. R., and Ulrich, H. (2007) New insights into purinergic receptor signaling in neuronal differentiation, neuroprotection, and brain disorders. *Purinergic Signal.* **3**, 317–331
- Schwindt, T. T., Trujillo, C. A., Negraes, P. D., Lameu, C., and Ulrich, H. (2011) Directed differentiation of neural progenitors into neurons is ac-

- accompanied by altered expression of P2X purinergic receptors. *J. Mol. Neurosci.* **44**, 141–146
27. Jiang, L. H., Kim, M., Spelta, V., Bo, X., Surprenant, A., and North, R. A. (2003) Subunit arrangement in P2X receptors. *J. Neurosci.* **23**, 8903–8910
 28. Wilkinson, W. J., Jiang, L. H., Surprenant, A., and North, R. A. (2006) Role of ectodomain lysines in the subunits of the heteromeric P2X2/3 receptor. *Mol. Pharmacol.* **70**, 1159–1163
 29. Mager, P. P., Weber, A., and Illes, P. (2004) Bridging the gap between structural bioinformatics and receptor research. The membrane-embedded, ligand-gated, P2X glycoprotein receptor. *Curr. Top. Med. Chem.* **4**, 1657–1705
 30. Bodnar, M., Wang, H., Riedel, T., Hintze, S., Kato, E., Fallah, G., Gröger-Arndt, H., Giniatullin, R., Grohmann, M., Hausmann, R., Schmalzing, G., Illes, P., and Rubini, P. (2011) Amino acid residues constituting the agonist binding site of the human P2X3 receptor. *J. Biol. Chem.* **286**, 2739–2749
 31. Kawate, T., Michel, J. C., Birdsong, W. T., and Gouaux, E. (2009) Crystal structure of the ATP-gated P2X4 ion channel in the closed state. *Nature* **460**, 592–598
 32. Sokolova, E., Skorinkin, A., Moiseev, I., Agrachev, A., Nistri, A., and Giniatullin, R. (2006) Experimental and modeling studies of desensitization of P2X3 receptors. *Mol. Pharmacol.* **70**, 373–382
 33. Gerevich, Z., Zadori, Z., Müller, C., Wirkner, K., Schröder, W., Rubini, P., and Illes, P. (2007) Metabotropic P2Y receptors inhibit P2X3 receptor-channels via G protein-dependent facilitation of their desensitization. *Br. J. Pharmacol.* **151**, 226–236
 34. Jarvis, M. F., and Khakh, B. S. (2009) ATP-gated P2X cation channels. *Neuropharmacology* **56**, 208–215
 35. Fischer, W., Wirkner, K., Weber, M., Eberts, C., Köles, L., Reinhardt, R., Franke, H., Allgaier, C., Gillen, C., and Illes, P. (2003) Characterization of P2X3, P2Y1, and P2Y4 receptors in cultured HEK293-hP2X3 cells and their inhibition by ethanol and trichloroethanol. *J. Neurochem.* **85**, 779–790
 36. von Kügelgen, I., and Harden, T. K. (2011) Molecular pharmacology, physiology, and structure of the P2Y receptors. *Adv. Pharmacol.* **61**, 373–415
 37. Hausmann, R., Rettinger, J., Gerevich, Z., Meis, S., Kassack, M. U., Illes, P., Lambrecht, G., and Schmalzing, G. (2006) The suramin analog 4,4',4''-(carbonylbis(imino-5,1,3-benzenetriylbis (carbonylimino)))tetra-kis-benzenesulfonic acid (NF110) potently blocks P2X3 receptors. Subtype selectivity is determined by location of sulfonic acid groups. *Mol. Pharmacol.* **69**, 2058–2067
 38. Becker, D., Woltersdorf, R., Boldt, W., Schmitz, S., Braam, U., Schmalzing, G., and Markwardt, F. (2008) The P2X7 carboxyl tail is a regulatory module of P2X7 receptor channel activity. *J. Biol. Chem.* **283**, 25725–25734
 39. Nicke, A., Bäumert, H. G., Rettinger, J., Eichele, A., Lambrecht, G., Mutschler, E., and Schmalzing, G. (1998) P2X1 and P2X3 receptors form stable trimers. A novel structural motif of ligand-gated ion channels. *EMBO J.* **17**, 3016–3028
 40. Fallah, G., Romer, T., Detro-Dassen, S., Braam, U., Markwardt, F., and Schmalzing, G. (2011) TMEM16A(a)/anoctamin-1 shares a homodimeric architecture with CLC chloride channels. *Mol. Cell. Proteomics* **10**, M110.004697
 41. Fiser, A., and Sali, A. (2003) Modeller. Generation and refinement of homology-based protein structure models. *Methods Enzymol.* **374**, 461–491
 42. Humphrey, W., Dalke, A., and Schulten, K. (1996) VMD. Visual molecular dynamics. *J. Mol. Graph.* **14**, 33–38
 43. Evans, R. J. (2010) Structural interpretation of P2X receptor mutagenesis studies on drug action. *Br. J. Pharmacol.* **161**, 961–971
 44. Stojilkovic, S. S., Yan, Z., Obsil, T., and Zemkova, H. (2010) Structural insights into the function of P2X4. An ATP-gated cation channel of neuroendocrine cells. *Cell Mol. Neurobiol.* **30**, 1251–1258
 45. Guo, C., Masin, M., Qureshi, O. S., and Murrell-Lagnado, R. D. (2007) Evidence for functional P2X4/P2X7 heteromeric receptors. *Mol. Pharmacol.* **72**, 1447–1456
 46. Nicke, A. (2008) Homotrimeric complexes are the dominant assembly state of native P2X7 subunits. *Biochem. Biophys. Res. Commun.* **377**, 803–808
 47. King, B. F., Liu, M., Pintor, J., Gualix, J., Miras-Portugal, M. T., and Burnstock, G. (1999) Diinosine pentaphosphate (IP5I) is a potent antagonist at recombinant rat P2X1 receptors. *Br. J. Pharmacol.* **128**, 981–988
 48. Khakh, B. S., Burnstock, G., Kennedy, C., King, B. F., North, R. A., Séguéla, P., Voigt, M., and Humphrey, P. P. (2001) International union of pharmacology. XXIV. Current status of the nomenclature and properties of P2X receptors and their subunits. *Pharmacol. Rev.* **53**, 107–118
 49. Chizh, B. A., and Illes, P. (2001) P2X receptors and nociception. *Pharmacol. Rev.* **53**, 553–568
 50. King, B. F., Wildman, S. S., Ziganshina, L. E., Pintor, J., and Burnstock, G. (1997) Effects of extracellular pH on agonism and antagonism at a recombinant P2X2 receptor. *Br. J. Pharmacol.* **121**, 1445–1453
 51. Collo, G., North, R. A., Kawashima, E., Merlo-Pich, E., Neidhart, S., Surprenant, A., and Buell, G. (1996) Cloning of P2X5 and P2X6 receptors and the distribution and properties of an extended family of ATP-gated ion channels. *J. Neurosci.* **16**, 2495–2507
 52. Soto, F., Garcia-Guzman, M., Karschin, C., and Stühmer, W. (1996) Cloning and tissue distribution of a novel P2X receptor from rat brain. *Biochem. Biophys. Res. Commun.* **223**, 456–460
 53. Barrera, N. P., Ormond, S. J., Henderson, R. M., Murrell-Lagnado, R. D., and Edwardson, J. M. (2005) Atomic force microscopy imaging demonstrates that P2X2 receptors are trimers but that P2X6 receptor subunits do not oligomerize. *J. Biol. Chem.* **280**, 10759–10765
 54. Ormond, S. J., Barrera, N. P., Qureshi, O. S., Henderson, R. M., Edwardson, J. M., and Murrell-Lagnado, R. D. (2006) An uncharged region within the N terminus of the P2X6 receptor inhibits its assembly and exit from the endoplasmic reticulum. *Mol. Pharmacol.* **69**, 1692–1700
 55. Jones, C. A., Vial, C., Sellers, L. A., Humphrey, P. P., Evans, R. J., and Chessell, I. P. (2004) Functional regulation of P2X6 receptors by N-linked glycosylation. Identification of a novel α,β -methylene ATP-sensitive phenotype. *Mol. Pharmacol.* **65**, 979–985
 56. Barrera, N. P., Henderson, R. M., Murrell-Lagnado, R. D., and Edwardson, J. M. (2007) The stoichiometry of P2X2/6 receptor heteromers depends on relative subunit expression levels. *Biophys. J.* **93**, 505–512
 57. Ding, S., and Sachs, F. (1999) Single channel properties of P2X2 purinoceptors. *J. Gen. Physiol.* **113**, 695–720
 58. Karoly, R., Mike, A., Illes, P., and Gerevich, Z. (2008) The unusual state-dependent affinity of P2X3 receptors can be explained by an allosteric two-open state model. *Mol. Pharmacol.* **73**, 224–234

IV. Summary and conclusions (“Zusammenfassung der Arbeit”)

Dissertation zur Erlangung des akademischen Grades Dr. rer. med.

Titel: Amino acid residues constituting the agonist binding site of the human P2X3 receptor and subunit stoichiometry of heteromeric P2X2/3 and P2X2/6 receptors

Eingereicht von: Prof. Dr. med. Haihong Wang

Angefertigt am: Rudolf-Boehm-Institut für Pharmakologie und Toxikologie

Betreut von: Prof. Dr. Peter Illes

Monat und Jahr der Einreichung: 15. Juni 2012

Bodnar M*, **Wang H***, Riedel T, Hintze S, Kato E, Fallah G, Gröger-Arndt H, Giniatullin R, Grohmann M, Hausmann R, Schmalzing G, Illes P, Rubini P (2011) **Amino acid residues constituting the agonist binding site of the human P2X3 receptor. J Biol Chem 286:2739-2749.**

*Both authors contributed equally to this work.

Although mutagenesis studies at P2X1, P2X2 and P2X4 have identified several AA residues, which are indispensable for agonist binding, similar information for P2X3 receptors is rare. In the present study, we prepared cDNA-plasmids encoding enhanced green fluorescent protein-coupled hP2X3 subunits and transfected them into HEK293 cells. The cells carrying P2X3 receptors were visually identified by means of a differential interference contrast microscope provided with epifluorescent optics. These cells were whole-cell patch-clamped and the currents generated in response to rapid local applications of α,β -meATP were recorded as a measure of the agonist effect. In another series of experiments, changes in the intracellular concentration of free calcium ($[Ca^{2+}]_i$) were determined by a Ca^{2+} -imaging setup. The increase of $[Ca^{2+}]_i$ caused by α,β -meATP was due to the influx of this cation through the P2X3 receptor-channel. Additionally, *Xenopus laevis* oocytes were injected with cRNA for hP2X3. Current responses were again induced by α,β -meATP but recording was with a two-electrode voltage-clamp system. We constructed concentration-response curves for α,β -meATP in each of the expression system and compared the E_{max} (maximum effect) and the EC_{50} values (the agonist concentration causing 50% of E_{max}). Eventually, we measured the desensitization rate constants (τ_{off}) of the current responses both in HEK293 cells and *X. laevis* oocytes in order to obtain information on the potentially altered desensitization rate of mutant receptors

in comparison with their wild-type (wt)-counterparts. Results obtained in the two expression systems with the three techniques used yielded basically identical results. Because a number of mutants failed to react to α,β -meATP, biochemical methods (protein labelling, purification and polyacrylamide gel chromatography) were used to confirm the membrane expression and trimeric structure of P2X3 receptor mutants. These methods proved that the failure of α,β -meATP to act at some of the mutants is due to a change in agonist potency rather than the missing expression of the mutant in the plasma membrane.

Mutants were generated by consecutively replacing all conserved AAs and a few non-conserved ones within the four NBSs of the hP2X3 subunits by the neutral Ala. In the first place, we confirmed our previous results relating to the critical importance of a few positively charged AAs (K63A, K65A, K176A, R281A, R295A, K299A). Then the involvement of a range of further AAs in agonist binding was also documented. However, we report in addition three key findings: (1) Unequivocal, although sometimes minor changes occurred in the amplitude of the current and/or intracellular Ca^{2+} response, when further conserved (F171, L297) or non-conserved (T62, F174, K284, F301) AAs were replaced by Ala, or Ala itself at the position 283 was substituted by Asp or Arg. (2) The agonist potency decrease was additive when two adjacent AAs were replaced simultaneously by Ala (K65/G66, F171/T172, N279/F280; F280/R281) but not altered after Ala substitution of non-adjacent AAs of the same NBS (F171/N177). (3) The decreased current amplitude was accompanied in many cases by a pronounced decrease in the activation and/or desensitization rate of the receptor mutants (K65A, G66A, N279A). (4) All data are in complete agreement with the homology model of the hP2X3 receptor established on the basis of the crystal structure of the zebrafish P2X4 mutant.

The experimental and modelling data as a whole indicate that the NBSs shown to be involved in agonist binding were situated at opposite sites of the same subunit and were therefore able to form a binding pocket only at the interface of two adjacent subunits. Of the conserved residues investigated many were oriented toward the groove of the pocket, indicating that they may bind ATP directly (K63, K65, K176, N279, R281, R295, K299). Our experiments confirm that Ala substitution of these AA residues causes marked changes in the amplitude and/or gating and possibly desensitization kinetics of the current responses. In contrast, some of the conserved AA residues, such as T172, N177 and F280 were oriented away from the groove,

although their replacement with Ala caused pronounced changes, suggesting that they may participate in transducing conformational information changes from the binding pocket to the ion channel. The computer simulation of the agonist-induced currents on some of the receptor mutants by means of a hidden Markov model allowed to discriminate between modifications of binding or gating.

In conclusion, polypeptide clusters organized in NBSs, rather than individual AAs, might be responsible for agonist binding, gating and desensitization of P2X3 receptors.

Hausmann R, Bodnar M, Woltersdorf R, **Wang H**, Fuchs M, Messemer N, Qin Y, Gunther J, Riedel T, Grohmann M, Nieber K, Schmalzing G, Rubini P, Illes P (2012) **ATP binding site mutagenesis reveals different subunit stoichiometry of functional P2X2/3 and P2X2/6 receptors.** J Biol Chem 287:13930-13943.

The present experiments were designed to investigate the subunit composition of two neuronal heteromeric P2X receptors, consisting of P2X2 and another partner (P2X3 or P2X6). As mentioned earlier, native P2X2/3 receptors occur in sensory ganglia, while P2X2/6 receptors were found in neural stem cells in certain phases of their development. We used a similar approach to that already described in our first publication, with the exception that EGFP-coupled P2X2 subunits were co-transfected with Ds-Red-coupled P2X3 or P2X6 subunits. Co-transfected cells were identified by their mixed green-red fluorescence. The cDNA and cRNA ratios were kept at 1:2 for P2X2/3 and 1:4 for P2X2/6 during transfection into HEK293 cells or during injection into *X. laevis* oocytes, respectively.

In this study, we used a series of non-functional P2X2 and P2X3 subunit mutants, which failed to respond or only slightly responded to ATP or its structural analogues, when expressed either in HEK293 cells or in *X. laevis* oocytes. Individual, positively charged AAs were replaced sequentially in NBS1-4 by Ala (K63A, K176A, R281A, K299A; P2X3 numbering); homologous Ala-mutants were prepared also for P2X2 and P2X6. In the first part of our study, we co-expressed wt-P2X2 or wt-P2X3 with the non-functional mutant counterparts of these subunits and found that the combination P2X2-wt/P2X3-mut was non-functional, whereas the combination P2X2-mut/ P2X3-wt was fully active. These results could be confirmed, when instead of

α,β -meATP, 2-methylthio ATP (2-MeSATP; a non-selective P2X/P2Y receptor agonist) was applied. In order to achieve channel opening, at least two binding sites out of the three possible ones at P2X receptors have to be occupied by agonist molecules; therefore, we concluded that in P2X2/3 receptors 1 P2X2 subunit is associated with 2 P2X3 subunits. It has to be kept in mind that although α,β -meATP activates P2X3 and P2X2/3 receptors, only the former ones show a pronounced desensitization. Thus, already the agonist profile and the current pattern observed allows an unequivocal differentiation between P2X2 (no response to α,β -meATP, slow desensitization to ATP), P2X3 (α,β -meATP-sensitive, rapid desensitization to ATP) and P2X2/3 receptors (α,β -meATP-sensitive, slow desensitization to ATP). The chances to differentiate P2X2, P2X3 and P2X2/3 receptors from each other by using 2-MeSATP are more restricted, because this agonist activates the three above receptor-types equally well.

However, 2-MeSATP had to be utilized as an agonist for P2X2, P2X6 and P2X2/6 receptors, which are insensitive to α,β -meATP. Initially we demonstrated that P2X2/6 receptors differ in their properties from P2X2 receptors, in that they have lower maximum current amplitude, show no run-down of the current response during prolonged agonist application, and exhibit a much stronger facilitation of the current amplitudes after lowering the external pH. A combination of wt-P2X2 and mut-P2X6 subunits did not alter the effect of 2-MeSATP, whereas the opposite combination of wt-P2X6 with mut-P2X2 resulted in non-functional receptors. Thus, we concluded that in contrast to the stoichiometry of P2X2/3 in P2X2/6 2 subunits of P2X2 associate with 1 subunit of P2X6.

To exclude that the non-functional phenotype of the Ala replacement mutants within the ATP binding site originates from deficits in trimeric assembly or cell surface trafficking rather than of a change in agonist action, biochemical analysis of oocytes expressing the corresponding wt and mutant P2X receptor channels was performed. Our results show that all mutants were capable of proper trimeric assembly and displayed unaltered plasma membrane trafficking.

In conclusion, electrophysiological, biochemical and homology modelling data unequivocally suggest that the subunit combination observed in the plasma membrane was (P2X2)₁/(P2X3)₂ on the one hand and (P2X2)₂/(P2X6)₁ on the other. Hence recognition sites between P2X2 and its partners rather than random association may govern the subunit composition of the receptor trimers.

Erklärung über die eigenständige Abfassung der Arbeit

Hiermit erkläre ich, dass ich die vorliegende Arbeit selbständig und ohne unzulässige Hilfe oder Benutzung anderer als der angegebenen Hilfsmittel angefertigt habe. Ich versichere, dass Dritte von mir weder unmittelbar noch mittelbar geldwerte Leistungen für Arbeiten erhalten haben, die im Zusammenhang mit dem Inhalt der vorgelegten Dissertation stehen, und dass die vorgelegte Arbeit weder im Inland noch im Ausland in gleicher oder ähnlicher Form einer anderen Prüfungsbehörde zum Zweck einer Promotion oder eines anderen Prüfungsverfahrens vorgelegt wurde. Alles aus anderen Quellen und von anderen Personen übernommene Material, das in der Arbeit verwendet wurde oder auf das direkt Bezug genommen wird, wurde als solches kenntlich gemacht. Insbesondere wurden alle Personen genannt, die direkt an der Entstehung der vorliegenden Arbeit beteiligt waren.

Der Inhalt dieser Erklärung wurde mir in das Englische übersetzt und ich bestätige deren Richtigkeit.

Shanghai, 15. Juni 2012

A handwritten signature in cursive script, reading 'Wang Haihong'.

Prof. Dr. med. Haihong Wang

Curriculum Vitae

Name: HaiHong WANG

Gender: Male

Date & Place of Birth: August 18, 1962 in Jiang Su, China

Citizenship: Chinese

Marital status: Married with one daughter

Institute address:

Department of Physiology
School of Medicine
Tongji University
1239, Siping Road
Shanghai 200092
PR China

Home Address:

Apt. 503, 2/669 Ping Xing Guan Road
Shanghai 200072
PR China
Tel.(86-21) 56380337

Tel.(86-21) 65985448

Mobile phone: (86)136-2166-9056

e-mail: iamhhwang@yahoo.com

Education

1987-1990 Shanghai Medical University, Shanghai, China

M.Sc. Neurobiology

1980-1987 Shanghai Medical University(Now it's merged with Fudan University),
Shanghai, China

B.S. Medicine

Professional Experience

Nov 2001-present Associate professor & Director, Department of Physiology,
School of Medicine, Tongji University

Jul 1990-Oct 2001 Assistant, Lecturer, Associate professor, Department of
Physiology , Shanghai Second Medical University, Shanghai,
China

Stays abroad

Oct 1993-Nov1993 one month, IBRO workshop, Department of Pharmacology,
Chinese University of Hong Kong, Hong Kong

Oct 2003-Dec 2001 six months, visiting scholar, Department of Pharmacology and
Toxicology, Medical Faculty, University of Leipzig, Germany

Nov 2008-Nov 2009 one year, sabbatical leave, Department of Pharmacology and
Toxicology, Medical Faculty, University of Leipzig, Germany

Dec 2011-Feb 2012 three months, DAAD visiting scientist scholarship, Department
of Pharmacology and Toxicology, Medical Faculty, University of
Leipzig, Germany

Awards

2007 Award for the Best Teaching Lecturer(1st class) of Tongji University

Membership of Associations

1991- Chinese Association for Physiologic Sciences (CAPS), Member

1993- Society of Physiologic Science in Shanghai, Council member

Publications:

1. Hausmann R, Bodnar M, Woltersdorf R, Wang HH, Fuchs M, Messemer N, Qin Y, Günther J, Riedel T, Grohmann M, Nieber K, Schmalzing G, Rubini P, and Illes P. ATP Binding Site Mutagenesis Reveals Different Subunit Stoichiometry of Functional P2X2/3 and P2X2/6 Receptors. *J. Biol. Chem.*. 2012. 287: 13930-13943.
2. Bodnar M, Wang HH, Kato E, Hausmann R, Hintze S, Fallah G, Riedel T, Gröger-Arndt H, Grohmann M, Schmalzing G, Illes P, and Rubini P. Amino acid residues constituting the agonist binding site of the human P2X3 receptor. *J. Biol. Chem.*. 2011. 286: 2739-2749. (co-first author)
3. D-P Xie, X Yang, C-Y Cao, H-H Wang, Y-X Li, Y Qin, J-P Zhang, X-W Chang . Exogenous oxytocin reverses the decrease of colonic smooth muscle contraction in antenatal maternal hypoxia mice via ganglia. *Regulatory Peptides - REGUL PEPTIDES* , .2011. 172(1): 30-34.
4. C Wolf, C Rosefort, G Fallah, MU Kassack, A Hamacher, M Bodnar, HH Wang, P Illes, A Kless, G Bahrenberg, G Schmalzing, R Hausmann. Molecular Determinants of Potent P2X2 Antagonism Identified by Functional Analysis, Mutagenesis and Homology Docking. *Mol. Pharmacology* .2011. 79(4): 649-661.
5. CY Cao, XM Li, BG Zhu, HH Wang, YY Li. High frequency stimulation to subthalamic nucleus inhibits the expression of serotonin in dorsal raphe nucleus of rats. 2009 *Chinese Journal of Neuroanatomy*. 25(4):412-416.
6. Y.X. Li, L.B. Chen, Z.L.Xia, J.P. Zhang, H.H. Wang. Expression of BCL-2, Bax and Ultrastructural Changes in Hippocampus After Blockage of Cervical Lymphatic Draining of Rats. 2007. *Chinese Journal of Neuroanatomy*, 23(3):267-271
7. X.Y. Qi, Y.Q. Xu, W.B. Shi, H.H. Wang, Z.X. Zhang. A study on the electrophysiological heterogeneity of rabbit ventricular myocytes the effect of ischemia on action potentials and potassium currents. 2000. *Acta Physiologica Sinica*, 52(5):260-264
8. H.H. Wang, Y.H. Zhu, S.F. Xu. The potentiating effect of haloperidol on the binding of etorphine to brain membranes in acupuncture analgesia. 1994. *Acta Physiologica Sinica*, 46(4):313-319

Acknowledgements

I am most grateful for all of those who have supported my work in Leipzig. In the first line I thank to Prof. Peter Illes, who supplied me with the subject of my thesis, raised the money to cover my personal and scientific expenses and was a perfect head of the lab in all respects. I am also most grateful to Prof. Michael Schaefer, the director of the Rudolf-Boehm-Institute for Pharmacology and Toxicology for kindly accepting me as a “Dr. rer. med.” student.

Out of the lab co-workers I am deeply grateful to Dr. Mandy Bodnar and Dr. Thomas Riedel, with whom I interacted on a day-to-day basis, when I had methodological or scientific problem. Without their invaluable advice this thesis could not have been written.

Eventually I thank to my wife Jiang Na and my parents who tolerated my long-lasting stay abroad. Their encouragement during the compilement of this thesis was essential for eventually finishing it.